AD_____

Award Number: W81XWH-04-1-0300

TITLE: Interaction of the MUC1 Tumor Antigen and the Adenomatous Polyposis Coli Tumor Suppressor in Human Breast Cancer

PRINCIPAL INVESTIGATOR: Christine L. Hattrup
                                   Sandra J. Gendler, Ph.D.
                                   Gunnar C. Hansson, M.D., Ph.D.

CONTRACTING ORGANIZATION: Mayo Clinic
                                       Scottsdale, AZ 85259

REPORT DATE: March 2006

TYPE OF REPORT: Annual Summary

 PREPARED FOR: U.S. Army Medical Research and Materiel Command
                       Fort Detrick, Maryland 21702-5012

REPORT DOCUMENTATION PAGE

Form Approved
OMB No. 0704-0188

1. REPORT DATE	2. REPORT TYPE	3. DATES COVERED
01-03-2006	Annual Summary	23 Feb 2005 – 22 Feb 2006

4. TITLE AND SUBTITLE

Interaction of the MUC1 Tumor Antigen and the Adenomatous Polyposis Coli Tumor Suppressor in Human Breast Cancer

5a. CONTRACT NUMBER

5b. GRANT NUMBER
W81XWH-04-1-0300

5c. PROGRAM ELEMENT NUMBER

6. AUTHOR(S)
Christine L. Hattrup

Sandra J. Gendler, Ph.D.
Gunnar C. Hansson, M.D., Ph.D.

5d. PROJECT NUMBER

5e. TASK NUMBER

5f. WORK UNIT NUMBER

7. PERFORMING ORGANIZATION NAME(S) AND ADDRESS(ES)

Mayo Clinic
Scottsdale, AZ 85259

8. PERFORMING ORGANIZATION REPORT NUMBER

9. SPONSORING / MONITORING AGENCY NAME(S) AND ADDRESS(ES)
U.S. Army Medical Research and Materiel Command
Fort Detrick, Maryland 21702-5012

10. SPONSOR/MONITOR'S ACRONYM(S)

11. SPONSOR/MONITOR'S REPORT NUMBER(S)

12. DISTRIBUTION / AVAILABILITY STATEMENT
Approved for Public Release; Distribution Unlimited

13. SUPPLEMENTARY NOTES
Original contains colored plates: ALL DTIC reproductions will be in black and white.

14. ABSTRACT

This project was designed to analyze the effect of MUC1 and APC on two important signaling pathways in breast cancer, those mediated by β-catenin and the ErbB kinases. We present herein results indicating that loss of MUC1 corresponds to decreased total β-catenin levels in breast cancer cells; as this is accompanied by a reduction in the amount of β-catenin that lacks GSK3β-mediated phosphorylation, the destabilization of β-catenin after MUC1 loss occurs at least in part through the APC/GSK3β destruction complex. We also show that another APC-dependent pathway involving p53 might participate as well, since MUC1 loss correlates to increased p53 levels. Finally, we show that loss of MUC1 alters β-catenin dependent transcription, as well as demonstrating a novel link between expression of MUC1 and transcription of members of the ERK pathway downstream of the ErbB kinases. These transcriptional changes are correlated to alterations in oncogenic events, further supporting the idea that MUC1 and APC are integral factors in regulation of signaling in breast cancer. These findings add to the growing understanding of how the oncoprotein MUC1 alters breast cancer signaling, specifically in relationship to the APC tumor suppressor.

15. SUBJECT TERMS
metastasis, protein interactions, cell signaling, MUC1 tumor antigen, APC tumor suppressor 15. Number of Pages (count all pages including appendices) 66 Beta-catenin, ErbB kinases

16. SECURITY CLASSIFICATION OF:

a. REPORT	b. ABSTRACT	c. THIS PAGE	18. NUMBER OF PAGES	19a. NAME OF RESPONSIBLE PERSON USAMRMC
U	U	U		

17. LIMITATION OF ABSTRACT: UU

18. NUMBER OF PAGES: 66

19b. TELEPHONE NUMBER *(include area code)*

Standard Form 298 (Rev. 8-98)
Prescribed by ANSI Std. Z39.18
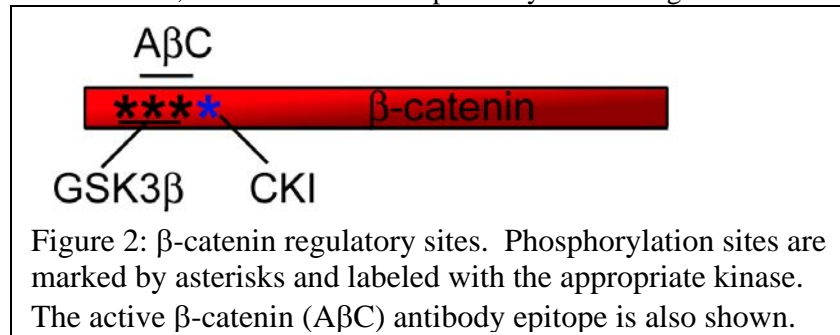
Table of Contents

Introduction

This project was designed to study the interaction between the MUC1 oncoprotein and the adenomatous polyposis coli (APC) tumor suppressor in human breast cancer. MUC1 has long been known to play an important role in breast cancer, first as a tumor antigen overexpressed on more than 90% of human breast tumors and metastases, then as a signaling molecule capable of interacting with a variety of pathways implicated in cancer, and finally as an oncogene in its own right, driving mammary tumorigenesis.[1-3] In particular, the MUC1 cytoplasmic tail (MUC1-CT, Figure 1) can associate with members of the Wnt pathway (β-catenin,[4] glycogen synthase kinase 3β (GSK3β),[5] and APC[6]) and

Figure 1: MUC1 domain sequences: transmembrane (TM) and cytoplasmic tail (CT), with known binding sites underlined and tyrosines highlighted.

with all four ErbB receptor tyrosine kinases,[7] resulting in effects such as anchorage-independent growth,[2] recruitment of β-catenin away from E-cadherin at the adherens junctions,[8] and stimulation of the extracellular signal regulated kinase (ERK1/2) pathway.[7] Interestingly, recent reports have shown that the MUC1-CT can be found in the nucleus, and that it plays a role in transcriptional regulation. These indicate that MUC1 expression can activate β-catenin oncogenic transcription,[9] dampen p53-mediated apoptotic transcription after genotoxic stress,[10] increase FOXO3a pro-survival transcription after oxidative stress,[11] and stabilize estrogen receptor α transcription in breast cancer.[12]

The current model of how MUC1 acts as an oncoprotein involves its ability to serve a scaffolding role, bringing signal transducers together to facilitate oncogenic signaling. For example, in the polyomavirus middle T antigen-induced mouse mammary tumor model, MUC1 expression enhances association of one of the main effectors of the T antigen, c-src, with one of its substrates, the p85 regulatory subunit of phosphatidyl inositol-3 kinase.[13] The model of MUC1-induced tumorigenesis proposes that MUC1 overexpression in the mammary epithelium stimulates association of oncogenic signaling proteins, while disrupting the normal regulation of its binding partners. The latter function is best-described for β-catenin, which MUC1 can recruit away from its normal adhesive function as a component of the adherens junctions; this results in diminished association of β-catenin with E-cadherin, leading to disruption of cellular adhesion.[8] Recently, MUC1 has been shown to directly stabilize β-catenin protein by inhibiting its destruction by a complex of proteins containing APC, GSK3β, and axin.[14]

This complex acts by binding cytoplasmic β-catenin, phosphorylating it on N-terminal regulatory residues, and ubiquitinating it, leading to proteasomal degradation. The key proteins involved include: APC and axin, both of which serve primarily scaffolding functions to stabilize the complex; casein kinase

Figure 2: β-catenin regulatory sites. Phosphorylation sites are marked by asterisks and labeled with the appropriate kinase. The active β-catenin (AβC) antibody epitope is also shown.

I (CKI), which "primes" β-catenin by phosphorylating it on serine 45 (Figure 2); GSK3β, which recognizes pSer45 and sequentially phosphorylates β-catenin on three additional sites (threonine 41, serine 37, and serine 33); and βTrCP, an E3 ubiquitin ligase that targets β-catenin once phosphorylated at Ser37 and Ser33. When not properly regulated, β-catenin can accumulate in the cytoplasm and enter the nucleus to activate transcription in concert with the T-cell factor / lymphocyte enhancing factor family of

transcription factors.[15,16] Although APC is a key player in the regulation of β-catenin, it has been implicated in a number of additional cellular events, all of which could contribute to its importance as a tumor suppressor. These events include regulation of adhesion and migration through links to the actin cytoskeleton and microtubules, maintenance of proper chromosome segregation during mitosis, and involvement in both cell cycle progression and apoptosis.[17] Interestingly, MUC1 has been linked to several of these functions in cancer.[1,18]

There are indications that signaling through β-catenin, APC, the ErbB family, and MUC1 may be co-regulated in breast cancer. For example, ErbB1 and ErbB2 form tumor-specific complexes with β-catenin in human breast cancer specimens. Interestingly, the association between ErbB2 and β-catenin is stronger in lymph node metastases than in the primary breast tumors; this pattern exactly mirrors those seen with MUC1-β-catenin and MUC1-APC associations in human breast cancer, suggesting coordinate regulation of the interactions of these proteins. In addition, ErbB1 is a β-catenin target gene; this is particularly interesting in light of the fact that MUC1 and APC have opposing functions in regulating β-catenin-mediated transcription, as it reaffirms the idea that MUC1 antagonizes the tumor suppressive capacity of APC. This is supported by a recent report showing that siRNA-mediated decrease in MUC1 expression results in downregulation of ErbB1 and decreased proliferation.

Interestingly, though, the relationship between MUC1 and oncogenic signaling is not as simple as it might appear. Two independent reports seem to contradict the clear-cut model of MUC1 as a purely oncogenic model. In one, MUC1 expression is correlated to heightened apoptosis; the mechanism behind this effect was the stimulation of trafficking of Fas receptor, resulting in increased levels of this death receptor on the cell surface.[19] The other report describes tumor-specific downregulation of *Muc1* transcription in c-neu-induced mammary tumors, suggesting that the presence of Muc1 has an unknown, detrimental effect on erbB-mediated tumorigenesis.[20] These data indicate that the simplified model of MUC1 as a purely oncogenic molecule likely needs refinement and expansion; work described in this report corroborates this need for a re-examination of the model of MUC1 oncogenesis.

The primary hypothesis of this project is that <u>the interaction of MUC1 and APC affects β-catenin and ErbB signaling in the mammary gland and has a significant impact on mammary carcinogenesis and metastasis.</u> The studies reported in this annual summary pertain largely to the third aim of this project, namely understanding the physiological relevance of MUC1 and APC in human breast cancer, particularly in light of β-catenin and ErbB signaling.

Body

The focus of the studies in this report is again on Specific Aim 3 (Task 4 of the Statement of Work), the relevance of the MUC1-APC interaction in β-catenin and ErbB signaling. Due to the poor quality of APC reagents (as has been published in the literature[21-23]), we have pursued a promising line of study as described in our annual summary of 2005: using small interfering RNA (siRNA) technology to decrease the levels of MUC1 in breast cancer cells, in order to understand its effects on β-catenin and ErbB signaling. We report that loss of MUC1 expression in breast cancer cells results in decreased levels of total and active β-catenin, indicating that MUC1 antagonizes GSK3β-mediated degradation of β-catenin. We also present the finding that decreased MUC1 expression results in increased p53 in a breast cancer cell line, suggesting that MUC1 may influence an alternative pathway for β-catenin degradation involving p53, APC, and the Siah E3 ubiquitin ligase. Finally, we discuss the effects of MUC1 siRNA on transcription and oncogenic events such as proliferation, apoptosis, and invasion, with particular emphasis on the alterations seen in β-catenin target genes and members of the ErbB family. These last form the basis for the publication included as Appendix I to this report.

As reported in the 2005 annual summary, we had also intended to address the questions posed in Specific Aims 1 and 2 (the nature and regulation of MUC1-APC interaction, and the proteins associated with the MUC1-APC complex, respectively), using the constructs developed for tandem affinity purification (TAP) and fluorescence resonance energy transfer (FRET) analysis. However, technical difficulties arose which necessitated changing the experimental strategy. Specifically, we were unable to achieve adequate transient expression of tagged APC and MUC1 constructs for our analyses. These problems were not entirely unexpected, as APC transfection is notoriously difficult (only one stable, APC-transfected cell line has ever been established,[24] since APC overexpression induces apoptosis[25]), and the addition of epitope tags onto two large proteins is known to complicate studies. We had hoped to circumvent these concerns by using the readily-transfected, easily-manipulated cell lines COS-1, COS-7, CHO, and BHK. Lines such as these are frequently employed in mechanistic studies, as they are far more amenable to expression of exogenous proteins than most other established cells, including the breast cancer cell lines we had previously used to study MUC1-APC co-immunoprecipitation. However, despite numerous attempts to optimize transfection conditions, the sole construct which expressed efficiently was the "SYM" fusion of YFP at the N-terminus of MUC1. Though a useful positive control for transfection, SYM is not feasible for FRET analysis of MUC1-APC interaction: it places the fluorescent protein in the extracellular portion of MUC1, a domain which extends several hundred nanometers from the cell surface, much too far away from the cytoplasmic APC protein to undergo a FRET energy transfer.

For these reasons, and because we felt that analyzing MUC1 and APC in an artificial system (such as overexpression of both in lines that normally make minimal amounts of these proteins) would not be as likely to reveal findings that are physiologically relevant to human breast cancer, we re-focused on another aspect of our studies that was also reported in our 2005 annual summary. Specifically, we reported an association between decreased MUC1 expression after siRNA treatment and reduction in the levels of active (unphosphorylated) β-catenin in MDA-MB-468 breast cancer cells. As seen in Figure 3, transient transfection of increasing concentrations (10, 50, 100 nM) of MUC1 siRNA (Dharmacon, "smartpool" of 4 oligonucleotides) results in decreased levels of both MUC1 and active β-catenin as compared to mock transfected cells, analyzed 48 hr post-transfection. The active β-catenin antibody

Figure 3: SiRNA knocks down MUC1 and results in decreased active β-catenin (AβC) in MDA-MB-468 cells.

measures the amount of β-catenin protein that lacks phosphorylation at two key residues, serine 37 and threonine 41 (Figure 2); as these sites can be phosphorylated by GSK3β to stimulate β-catenin degradation, lack of phosphorylation is seen on β-catenin molecules that have not been regulated by the APC/GSK3β/axin destruction complex and thus may be transcriptionally active. In addition, we have
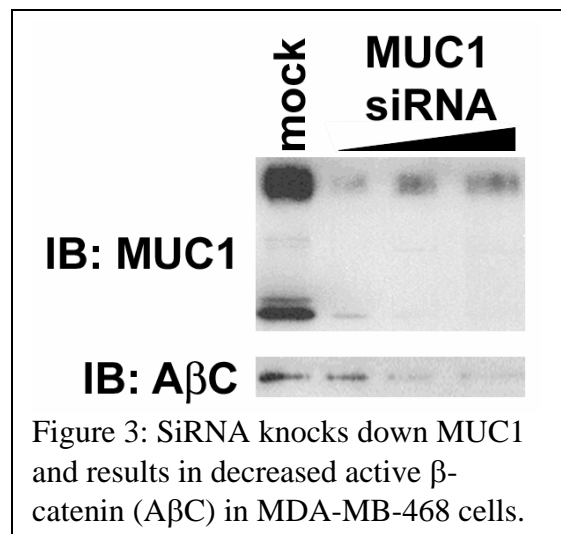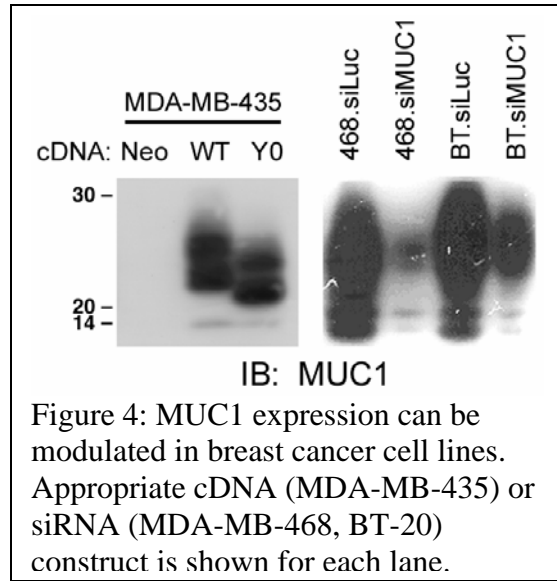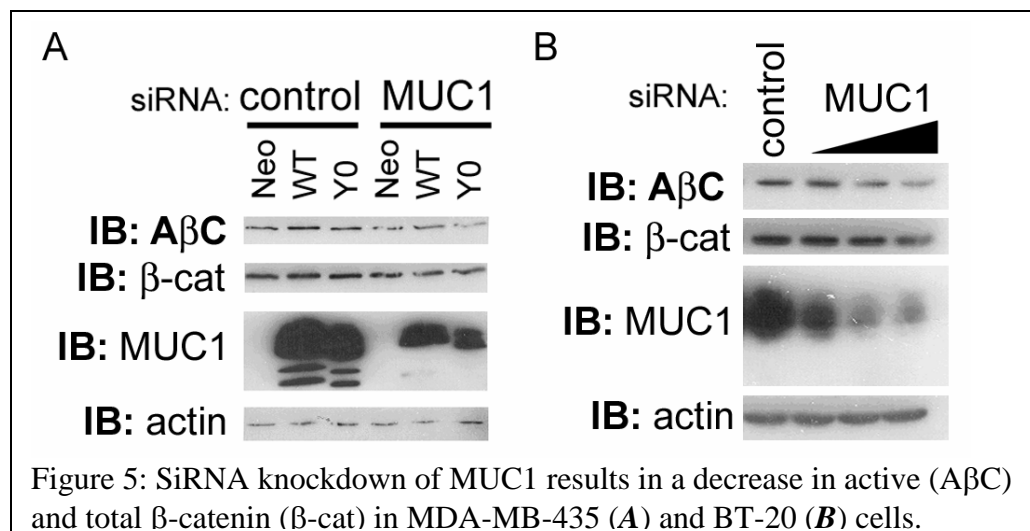
seen that total β-catenin levels decrease as active β-catenin levels decline, likely due to proteasomal degradation stimulated by GSK3β phosphorylation.

Figure 4: MUC1 expression can be modulated in breast cancer cell lines. Appropriate cDNA (MDA-MB-435) or siRNA (MDA-MB-468, BT-20) construct is shown for each lane.

We extended these findings to two additional established breast cancer cell lines, BT-20 and MDA-MB-435. BT-20, like MDA-MB-468, express endogenous MUC1 at high levels, while MDA-MB-435 normally produce very little MUC1 protein. The MDA-MB-435 lines used for these studies were stably infected with retroviral constructs in the pLNCX.1 vector expressing only the neomycin resistance gene for selection (435.Neo), or the Neo gene plus either full-length wildtype MUC1 (435.MUC1 WT) or a full-length MUC1 construct with all seven of the cytoplasmic tail tyrosine residues mutated to phenylalanine (435.MUC1 Y0). The constructs are described in detail in Appendix II. MUC1 levels in MDA-MB-435 after infection, as well as in BT-20 and MDA-MB-468 after siRNA transfection, are shown in Figure 4. Note that the lack of tyrosine residues affects electrophoretic mobility of the MUC1 Y0 construct; on reducing polyacrylamide gels, the

MUC1 Y0 cytoplasmic tail runs with a lower apparent weight than does the MUC1 WT construct, likely reflecting the loss of phosphorylation from the MUC1-CT (Figure 4). MDA-MB-468 and BT-20 cells were transfected transiently with siRNA at concentrations ranging from 10-100 nM to determine optimal experimental conditions (100 nM concentration is used for subsequent experiments, except where noted), and MUC1 knockdown was observed as early as 24 hr post-transfection lasting to 96 hr post-transfection (data not shown). Except where noted, experiments were performed at 48 hr post-transfection, as this timepoint showed optimal knockdown of MUC1; all experiments were completed within 96 hr of transfection. MDA-MB-468 cells display very effective siRNA-mediated knockdown of MUC1, with levels <25% of control, while BT-20 are somewhat less efficient in reducing MUC1 expression, which is approximately 50% in MUC1 siRNA-treated as compared to control (quantitation from flow cytometry staining, data not shown). Luciferase siRNA was used as a control for MUC1 siRNA in the MDA-MB-468 and BT-20 lines.

As expected, based on indications that MUC1 expression and active β-catenin levels are directly correlated (Figure 3), 435.MUC1 WT and 435.MUC1 Y0 cells show increased active β-catenin as compared to 435.Neo (Figure 5A, lanes 2 and 3 compared to lane 1); this is abrogated by MUC1 siRNA (lanes 4-6), resulting in lower active β-catenin levels in MUC1 siRNA-treated 435.MUC1 WT and 435.MUC1 Y0 (lanes 5 and 6) as compared to both 435.Neo controls (lanes 1 and 4) and to luciferase siRNA-treatment of the same lines (lanes 2 and 3). The decrease in active β-catenin seen in 435.Neo cells after MUC1 siRNA (lane 4 as compared to lane 1) is likely due to knockdown of the small amount of

Figure 5: SiRNA knockdown of MUC1 results in a decrease in active (AβC) and total β-catenin (ß-cat) in MDA-MB-435 (*A*) and BT-20 (*B*) cells.

endogenous MUC1 found in this cell line, which can be seen with long exposure of blots (data not shown). As seen in Figure 5B, BT-20 cells show a decrease in active and total β-catenin after MUC1 siRNA similar to that seen with knockdown of endogenous MUC1 in MDA-MB-468 cells (Figure 3). The siRNA oligonucleotide used in this figure[26] is independent from the siRNA pool used in Figures 1 and 4; both the pool and the independent oligonucleotide have been used in multiple experiments to ensure that these results are not artifacts of a particular siRNA construct.
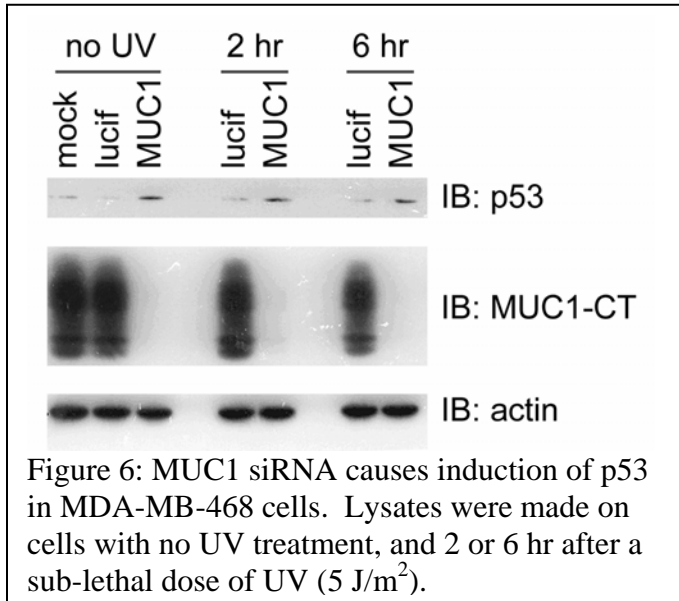

Figure 6: MUC1 siRNA causes induction of p53 in MDA-MB-468 cells. Lysates were made on cells with no UV treatment, and 2 or 6 hr after a sub-lethal dose of UV (5 J/m^2).

The active β-catenin antibody recognizes β-catenin that lacks GSK3β-mediated phosphorylation, i.e., it only gives information regarding the standard, APC/GSK3β/axin destruction complex. As there are other mechanisms by which β-catenin can be degraded, we also examined an alternative pathway for regulation of β-catenin that links p53 to APC via the Siah E3 ligase.[27] Intriguingly, Siah has been found in our lab to interact with MUC1 in a yeast two-hybrid screen and in GST pulldowns,[28] suggesting that this association might also be regulated by MUC1. The study of Siah, as with APC, is plagued by the existence of very few antibodies of poor quality, making direct observation of the endogenous protein difficult. Because of this, we examined whether MUC1 siRNA could alter p53 levels as a starting point for analyzing potential effects on β-catenin via this pathway. As seen in Figure 6, MUC1 siRNA appears to slightly raise the level of p53 in MDA-MB-468 cells, opening up the possibility that the APC-dependent, p53—Siah pathway for degradation of β-catenin may be affected by MUC1 expression. However, as p53 is mutated[29] and largely non-functional in these cells (note the lack of induction upon ultraviolet radiation), they are not a good line for studying the effect of MUC1 on this pathway. The other two cell lines, BT-20 and MDA-MB-435, also have mutated, non-functional p53, indicating that another model system is needed to further explore this avenue of the MUC1-APC interaction.

Shortly after we observed the association between MUC1 expression and active β-catenin levels, a manuscript from another lab was published describing much the same effect.[14] Their results showed decreased phosphorylation of β-catenin regulatory residues and increased active (unphosphorylated) β-catenin after MUC1 transfection; this effect was traced to MUC1 inhibition of GSK3β-mediated degradation of β-catenin. As a result of this, we focused our efforts on exploring the implications of the influence of MUC1 on β-catenin from another angle, namely transcriptional regulation. Both our studies (Figure 7) and existing literature[9,30] provide evidence that MUC1 can regulate β-catenin-mediated transcription. Figure 7 shows the results of a luciferase assay
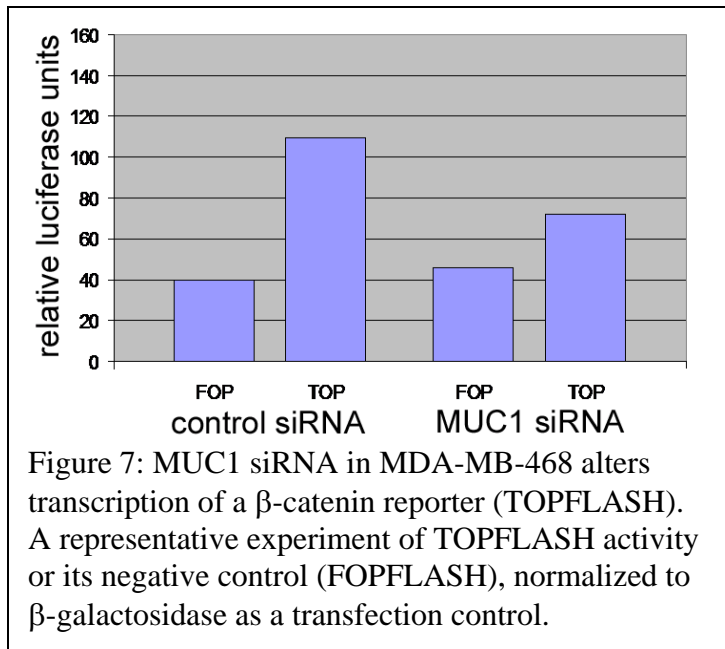

Figure 7: MUC1 siRNA in MDA-MB-468 alters transcription of a β-catenin reporter (TOPFLASH). A representative experiment of TOPFLASH activity or its negative control (FOPFLASH), normalized to β-galactosidase as a transfection control.

using an optimized β-catenin/TCF reporter construct (TOPFLASH) in siRNA-treated cells. Cells were

first transfected with siRNA, allowed to recover for 48 hr, and then transfected again with the TOPFLASH reporter construct or its negative control containing scrambled TCF recognition sites (FOPFLASH). A β-galactosidase construct was also included as a control for transfection efficiency; all luciferase results are shown normalized to β-galactosidase. Luciferase activity was measured 48 hr after the second transfection, i.e., 96 hr post-siRNA. MUC1 siRNA-treated cells display approximately 40% lower levels of β-catenin transcription than do control siRNA cells, as is expected given the role of MUC1 in stabilizing β-catenin and facilitating transcription of its target genes.

Beyond looking at optimized reporter constructs, we were interested in studying the effects of MUC1 siRNA on transcription of endogenous β-catenin target genes, as well as other genes implicated in cancer. For this, we extracted total RNA from siRNA-transfected MDA-MB-468 and BT-20 cells 48 hr post-transfection. Total RNA (1 µg) was reversed transcribed into cDNA, and analyzed by real-time PCR using SuperArray Cancer PathwayFinder arrays. These arrays are set up in a 96-well format and analyze levels of 84 different genes that have been implicated in cancer. The genes are organized into pathways, including cell cycle and DNA repair (analyzing genes such as cyclins and cyclin-dependent kinases, *CHEK1* and *ATM*), apoptosis and cell senescence (including BCL family members, *TERT*, and TNF receptors), signal transduction molecules and transcription factors (members of the MAPK, PI3K, NF-κB and similar networks), adhesion (integrins and related genes), angiogenesis (largely secreted factors such as angiopoietins, *PDGFA/B*, *TNF*, and *VEGF*), and finally invasion and metastasis (primarily proteases and related genes, such as *MMP*s and *TIMP*s). The arrays also have five housekeeping genes (*18srRNA*, *HPRT1*, *RPL13A*, *GAPD*, and *ACTB*) for normalizing the results of each array, a dilution series to ensure accurate pipetting, and control wells with non-reverse-transcribed RNA or no template to check for DNA or other contamination. All array products were also analyzed by agarose gel to confirm the presence of only a single band for each PCR reaction, with no primer dimers or other contaminants that might cloud the real-time results.

Transcription of several genes was found to be altered in one or both of the cell lines studied (Figure 8); results are shown as fold change of MUC1 siRNA versus control (i.e., fold change of 0.5 means there was half as much mRNA for that gene in MUC1 siRNA-treated cells. This figure displays all genes in the array that were significantly altered, not a selected group. An extensive commentary on these genes and their implications in MUC1 signaling and breast cancer can be found in the discussion section of Appendix I. Notably, the results include a number of β-catenin target genes, providing further evidence of a role for MUC1 in regulating transcription by β-catenin and other transcription factors. Genes that were altered after MUC1 siRNA and have been described as β-catenin target genes include: *MYC* (encoding c-Myc), *JUN* (encoding c-Jun), and *VEGF* (encoding vascular endothelial growth factor) and *MMP2* (encoding matrix metalloproteinase-

Figure 8: Transcription changes after MUC1 siRNA. Fold change is shown in parentheses behind each gene.

2), which is increased in Wnt-induced mammary tumors.[31] Though the β-catenin target genes *JUN* and *VEGF* displayed decreased transcription after MUC1 siRNA (as would be expected, given that MUC1
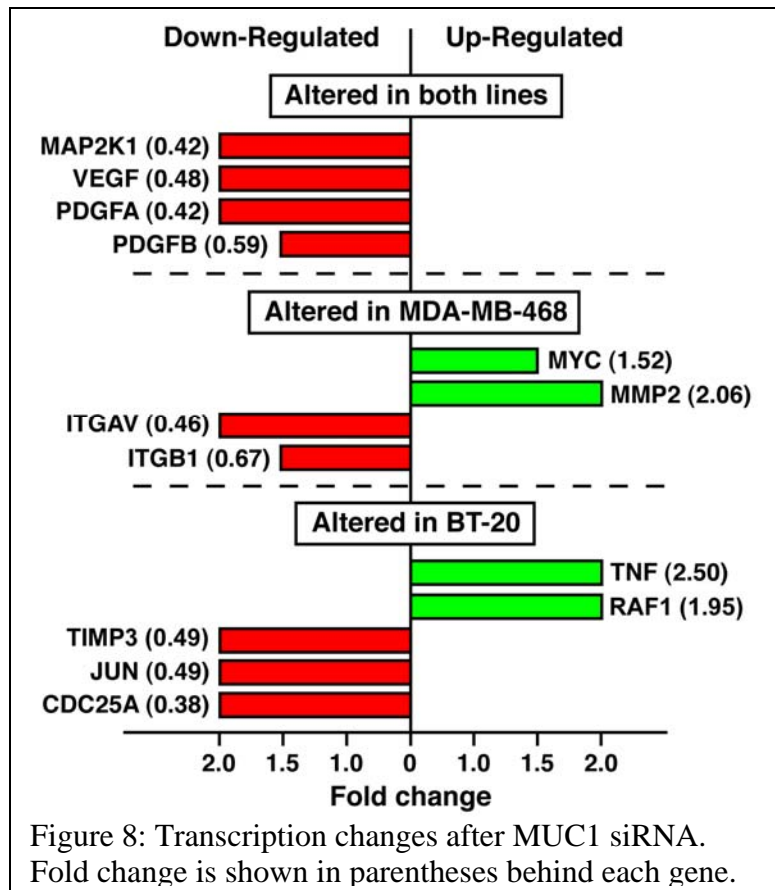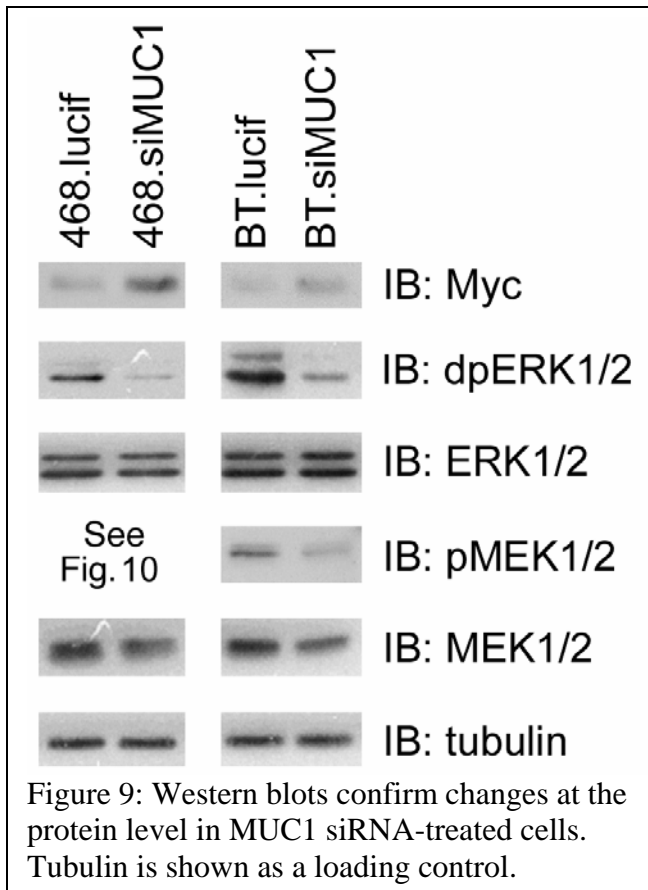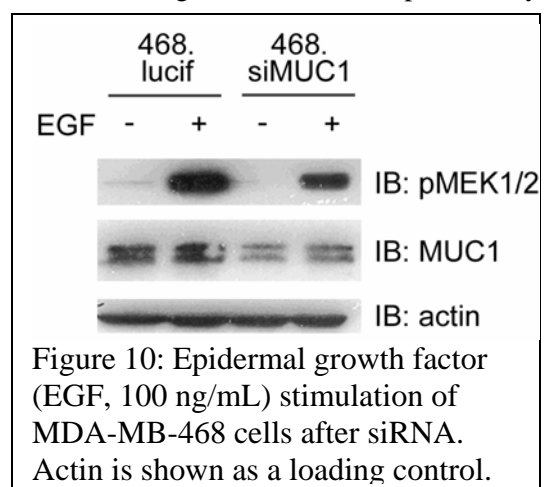
9

Figure 9: Western blots confirm changes at the protein level in MUC1 siRNA-treated cells. Tubulin is shown as a loading control.

can stabilize β-catenin and strengthen its transcriptional activity), intriguingly, some genes showed increased transcription in MUC1 siRNA-treated cells. *MMP2* transcription was increased after MUC1 siRNA; as MMP-2 expression is confined to stromal cells in Wnt-induced mammary tumors,[31] this may reflect a shift towards a mesenchymal phenotype following loss of the epithelium-specific MUC1. In addition, *MYC* transcription was increased by 1.5-fold in MDA-MB-468; though not a significant increase in transcription, this was confirmed by western blot in both cell lines (Figure 9), and may reflect modulation of Myc by MUC1 at multiple levels, as the increase in Myc protein seen in 468.siMUC1 cells appears greater than what would be expected for a 1.5-fold increase. We also examined another important β-catenin target, COX-2 (cyclooxygenase-2) by western blot to see if its expression was affected by MUC1 siRNA; however, no change in COX-2 level was seen in either MDA-MB-468 or BT-20 with loss of MUC1 (data not shown).

In addition to β-catenin targets, several genes related to the ErbB pathway were differentially regulated after MUC1 siRNA. Notably, transcription of *MAP2K1*, the gene encoding MEK1, was decreased significantly in both MDA-MB-468 and BT-20 cells after MUC1 siRNA. MEK1 is one of the primary links in the Ras pathway that is activated downstream of ErbB and other growth factor receptor tyrosine kinase signaling; the most common cascade involves sequential activation of Ras, Raf, MEK1/2, and ERK1/2 to regulate transcription by AP-1 (a dimer consisting of c-Fos and c-Jun) and other transcription factors.[32] Reduction of MEK1 was confirmed at the protein level in both cell lines (Figure 9), though the change in total MEK1/2 is actually not as striking as the decrease in active (phosphorylated) MEK1/2 levels, whether basal (BT-20, Figure 9) or following epidermal growth factor stimulation (MDA-MB-468, Figure 10). MDA-MB-468 overexpress ErbB1, making them quite sensitive to EGF. Loss of MUC1 disrupts the MAPK cascade downstream of MEK1/2 as well, as levels of active ERK1/2 (dpERK1/2, Figure 9) are decreased in both lines following MUC1 siRNA, though total ERK1/2 levels remain unchanged. Interestingly, BT-20 cells also showed significant alterations in transcription of two other members of this MAPK cascade, namely *RAF1* and *JUN* (Figure 8). What is particularly striking is that, despite decreased transcription of MAP2K1 and JUN in BT.siMUC1, RAF1 transcription is actually increased. Given that Raf is the primary activator of MEK, it is not clear why they show opposite directions of transcriptional alteration after MUC1 siRNA. However, it is important to note that there are two MEK proteins (MEK1 and MEK2) and three mammalian Raf proteins; the distinctions in regulation and signaling between the various isoforms remain largely unknown. Therefore, the effects of transcriptional alteration of one isoform may well be clouded by differences in level or activation of the other isoforms. Regardless, these data present a novel mechanism by which MUC1 can regulate the ErbB – ERK signaling network: modulation of the transcription of several integral pathway members.

Figure 10: Epidermal growth factor (EGF, 100 ng/mL) stimulation of MDA-MB-468 cells after siRNA. Actin is shown as a loading control.

10

We next wanted to determine whether these transcriptional alterations would correlate with effects at the cellular level. As APC and β-catenin have been linked to regulating the cell cycle, apoptosis, and invasion, we chose these three phenomena as endpoints for our study of MUC1 siRNA in breast cancer cell lines. As an oncogene, MUC1 would be expected to stimulate proliferation, inhibit apoptosis, and enhance cellular invasion. Our hypothesis was therefore that MUC1 siRNA would cause the opposite effects in breast cancer cell lines. Interestingly, although MDA-MB-468 cells fit our hypothesis exactly, BT-20 cells showed a very different phenotype after MUC1 siRNA, suggesting that MUC1 function in breast cancer may be considerably more complex than has been previously realized.

As seen in Figure 11, MDA-MB-468 transfected with MUC1 siRNA show a statistically significant decrease in proliferation as compared to control siRNA; intriguingly, BT-20 show a significant increase in proliferation after MUC1 siRNA. This assay measures incorporation of radiolabeled thymidine nucleotide into cells: siRNA-transfected cells were re-plated
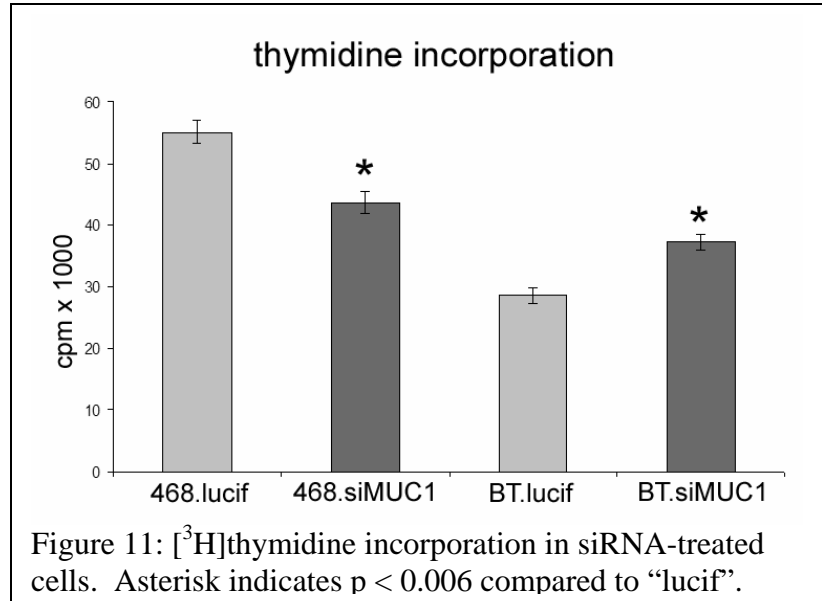
Figure 11: [^{3}H]thymidine incorporation in siRNA-treated cells. Asterisk indicates $p < 0.006$ compared to "lucif".

into 96-well plates 24 hr post-transfection, at a count of 15,000 cells per well. [^{3}H]thymidine was added simultaneously, and cells were analyzed 24 hr later for incorporation of radiolabel (i.e., 48 hr post-transfection. Proliferation was also measured 72 hr post-siRNA by re-plating the cells with radiolabeled thymidine at 48 hr post-transfection. These results were confirmed with another assay, BrdU incorporation, which does not require trypsinization of cells prior to analysis (discussed below). Cells were given BrdU in fresh medium for 1.5 hr, 48 hr post-transfection. After incubation, BrdU was washed off and cells were harvested for analysis by flow cytometry. Again, 468.siMUC1 cells showed decreased incorporation as compared to control, but BT.siMUC1 increased this measure of proliferation as compared to control cells (data not shown).

Analysis of apoptosis added to these findings. Though basal levels of apoptosis in both lines were unaffected by MUC1 siRNA as compared to control (data not shown), trypsinization 24 hr post-transfection results in increased apoptosis in the 468.siMUC1 cells (Figure 12). This figure shows representative flow cytometry staining for annexin V and propidium iodide on siRNA-treated cells that were trypsinized 24 hr post-transfection and re-plated at 200,000 cells per well on 6-well plates. The cells were then
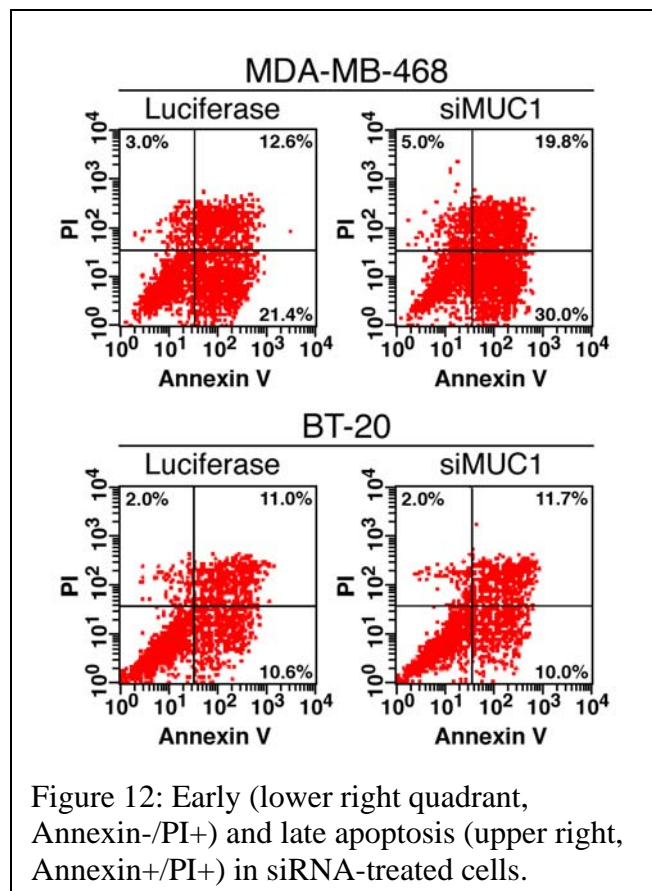
Figure 12: Early (lower right quadrant, Annexin-/PI+) and late apoptosis (upper right, Annexin+/PI+) in siRNA-treated cells.

harvested at 24 hr intervals (48 and 72 hr post-transfection) for analysis of apoptosis. Early (annexin V+ / PI-) and late (annexin V+ / PI+) apoptosis are increased in 468.siMUC1 cells as compared to 468.lucif (30.0% early and 19.8% late vs. 21.4% early and 12.6% late for MUC1 siRNA and luciferase siRNA, respectively). No change in the level of apoptosis was seen in BT-20 cells regardless of the siRNA used. We determined that this effect was part of a general stress response in the MDA-MB-468 line that appears to depend upon MUC1 expression, as treatment with a panel of stress-inducing agents (heat shock, H_2O_2, G418, trypsin, celecoxib) caused greater cell death in 468.siMUC1 cells as compared to controls, while BT-20 cells were again unaffected by loss of MUC1 (data not shown). These differences could reflect the striking disparity in levels of active (pAKT) and total AKT between the two cell lines (Figure 13), as BT-20 have considerably more pAKT than do MDA-MB-468, despite having less total AKT. The exposures shown in Figure 13 are the same in

Figure 13: BT-20 cells have more active AKT (pAKT) than do MDA-MB-468, despite lower levels of total AKT. Tubulin is shown as a loading control.

both cell lines for each antibody. The remarkably strong activation of the pro-survival AKT pathway in BT-20 cells may well account for their insensitivity to the increase in apoptosis this is expected with MUC1 siRNA.
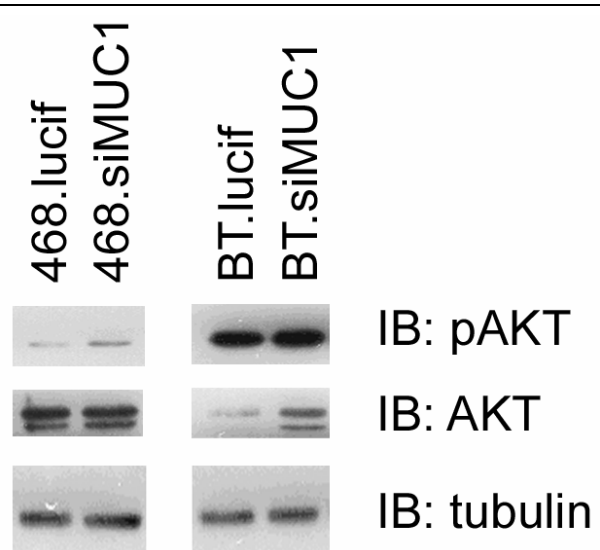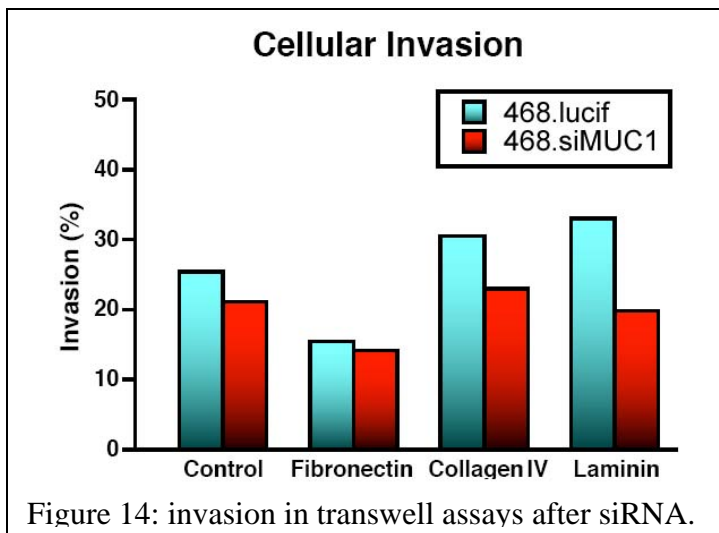
Figure 14: invasion in transwell assays after siRNA.

Since MUC1 is known to modulate adhesion, we also investigated whether siRNA would affect the invasive capacity of these cells. Transwell assays were used to examine MDA-MB-468 invasion across a panel of extracellular matrix proteins (Figure 14). Assays were conducted by serum starving siRNA-treated cells beginning 24 hr post-transfection. The next day (48 hr post-siRNA) cells were trypsinized and re-plated in serum-free medium in the top well of a transwell insert. Serum-containing medium was placed in the bottom to attract the cells, which would have to cross a matrix-coated membrane in traveling towards the serum. Invasion was measured by fixing and staining the cells with crystal violet after 24-48 hr invasion (i.e., 72 or 96 hr post-transfection). "Sample" wells had the cells swabbed from the top prior to staining (leaving only cells that had successfully invaded); "control" wells were not swabbed, leaving behind cells which had not invaded into the matrix. Cells were then counted manually on the membrane or destained and read in a 96-well plate format, and invasion was determined as the percentage of sample over control. As seen in Figure 14, 468.siMUC1 cells invade less readily than control cells across laminin, fibronectin, collagen IV, and the no-matrix control, indicating that loss of MUC1 is detrimental to the migratory capacity of breast cancer cells. BT-20 cells were not studied on this panel of extracellular matrices, as preliminary experiments indicated that this line does not invade particularly well (data not shown).

In summary, these data indicate that loss of MUC1 expression in these two breast cancer cell lines results in some effects, such as destabilization of β-catenin and decreased transcription of certain genes, are conserved across both lines. Intriguingly, there are other effects, such as levels of proliferation and apoptosis, that are greatly disparate between MDA-MB-468 and BT-20. This could suggest that MUC1 is not strictly oncogenic in breast cancer, as is currently thought; the increased proliferation in BT-20 after MUC1 siRNA could reflect the removal of an unknown, growth inhibitory effect of MUC1 expression. This might be related to the findings in previous reports that MUC1 expression can actually stimulate Fas-induced apoptosis,[19] and that Muc1 is specifically downregulated in c-neu-induced mouse mammary tumors.[20] However, it is vital to always bear in mind the fact that these studies are conducted on established cell lines in two-dimensional culture. A recent paper from the Bissell group[33] highlights the importance of cellular context in understanding protein function: the report outlines an anti-metastatic effect for the well-characterized oncogene AKT, and emphasizes that understanding a complex network of cellular signaling events is essential in drawing conclusions about the role of any one protein in the process of oncogenesis. Therefore, it is quite likely that these results largely reflect cell-specific differences between the cell lines used, as MUC1 has been characterized as an oncogene by its overexpression in the mouse mammary gland.

Alternatively, the results in the BT-20 line could indicate that there is a balance between MUC1 overexpression and its ability to stimulate oncogenic events, which could be a reflection of the scaffolding function of MUC1.[13] As a scaffold, the function of MUC1 is to stimulate association of individual signaling proteins into a complex for efficient signal transduction. Increased expression of MUC1 would therefore enhance this activity, as there would be a greater number of MUC1 molecules available to play this scaffolding role. However, if MUC1 levels increase far beyond the levels of its binding partners, it could actually result in a dilution of the necessary signaling proteins, thus weakening the potency of MUC1-induced oncogenesis. As BT-20 cells show less knockdown of MUC1 than MDA-MB-468 (Figure 3, 50% vs. >75%, respectively) it is possible that MUC1 levels were reduced sufficiently to abrogate this dilution effect, but not so far as to interfere with the ability of MUC1 to stimulate proliferation.

This report describes results pertaining to Task 4 of the approved Statement of Work: "To clarify the functional significance of the [MUC1-APC] interaction in relation to β-catenin and ErbB signaling". We have shown that MUC1 siRNA results in decreased levels of active (unphosphorylated) and total β-catenin in breast cancer cell lines. As the active β-catenin antibody only addresses GSK3β-mediated degradation of β-catenin, we also examined whether another pathway involving p53, APC, and Siah might be involved in the reduction of total β-catenin. Levels of p53 were found to be increased after MUC1 siRNA, perhaps indicating that MUC1 expression destabilizes p53. However, as these cells lack functional p53, a better model system must be found to further examine the role of MUC1 in β-catenin degradation as mediated by p53, APC, and Siah. Transcription of known β-catenin target genes was significantly altered after MUC1 siRNA, as was transcription of several members of the ErbB signaling pathway. These links between MUC1 expression and regulatory control over both β-catenin- and ErbB-mediated signaling events suggests that the MUC1-APC interaction is yet another means by which MUC1 can affect these two signaling pathways in breast cancer.

Key Research Accomplishments

- Endogenous MUC1 has been consistently and significantly knocked down in human breast cancer cell lines, notably MDA-MB-468 and BT-20, which showed >75% and approximately 50% decrease in MUC1 expression after siRNA transfection, respectively. Given the extreme difficulty inherent in transfecting breast cancer cells, it is remarkable that this degree of MUC1 knockdown can be reliably achieved. In addition, MDA-MB-435 cells infected with expression constructs for full-length MUC1 (wildtype or tyrosine mutated) also show downregulation of MUC1 after siRNA treatment.

- Loss of MUC1 in breast cancer cell lines (MDA-MB-468, BT-20, and MDA-MB-435) results in decreased amounts of active (unphosphorylated) β-catenin. This antibody gives information on GSK3β-mediated degradation of β-catenin, which was reported this year to be inhibited by MUC1 expression.[14]

- MUC1 may also regulate the β-catenin degradation pathway that is mediated by APC, Siah, and p53, as it interacts with Siah, and as p53 levels increase with MUC1 siRNA. A better model system than the above-mentioned cell lines must be employed for further study of this phenomenon, as all three lines express mutant p53 and therefore lack proper p53 function.

- Levels of MUC1 affect β-catenin mediated transcription, both of an artificial, optimized luciferase reporter construct (TOPFLASH) and of endogenous genes as seen by RT-PCR array. Target genes of β-catenin that were altered after MUC1 siRNA include: *MYC*, *JUN*, and *VEGF*, as were *TNF* and *MMP2* (both closely related to known β-catenin target genes) Increased expression of c-Myc was confirmed by western blot, but levels of another β-catenin target, COX-2, were unchanged after MUC1 siRNA.

- Transcription of *MAP2K1* (encoding MEK1) and *JUN* were decreased in human breast cancer cells after MUC1 siRNA, while *RAF1* transcription was increased, providing a novel mechanism by which MUC1 can affect ErbB signaling in breast cancer: transcriptional regulation of members of the MAPK pathway.

- MUC1 siRNA in MDA-MB-468 cells resulted in significantly decreased proliferation, increased apoptosis in response to stress, and lowered invasion across several extracellular matrix proteins. These findings were in agreement with our hypothesis that MUC1, as an oncogene capable of regulating β-catenin activity in breast cancer cells, would be required for these events.

- In BT-20 cells, MUC1 siRNA did not affect apoptosis or invasion, and actually increased proliferation of cells, suggesting that the role of MUC1 in breast cancer may be more complex than was previously thought, and that understanding the cell-specific environment is essential to proper interpretation of MUC1 function.

- The difference in phenotype between MDA-MB-468 and BT-20 cells after MUC1 siRNA may be related to the substantially larger level of active AKT relative to total AKT in the BT-20 line. MUC1 and β-catenin are both linked to the AKT pathway and its regulation of GSK3β.

Reportable Outcomes

- <u>Hattrup, C.L.</u>, and Gendler, S.J. "MUC1 alters oncogenic events and transcription in human breast cancer cells." Manuscript in preparation for submission and appended to this report (Appendix I).

- Thompson, E.J., Shanmugam, K., <u>Hattrup, C.L.</u>, Kotlarczyk, K.L., Bradley, J.M., Gutierrez, A., Mukherjee, P., and Gendler, S.J. "Tyrosines in the MUC1 cytoplasmic tail modulate transcription via the ERK1/2 and NF-κB pathways." Manuscript submitted (*Mol Cancer Res*) and appended to this report (Appendix II).

- Basu, G., Tinder, T.L., Bradley, J.M., Tu, T., <u>Hattrup, C.L.</u>, Pockaj, B.A., and Mukherjee, P. "Cyclooxygenase 2 inhibitor enhances the efficacy of a breast cancer vaccine: Role of indoleamine 2,3, dioxygenase." Manuscript accepted for publication (*J. Immunol*). As I was not a main author on this manuscript, it is not appended to this report.

- Attendance at the 2005 Era of Hope conference for the Department of Defense Breast Cancer Research Program, June, 2005. A poster was presented, entitled "Characterization of the interaction of MUC1 and the adenomatous polyposis coli tumor suppressor in breast cancer."

- Presentation of a poster at the American Association for Cancer Research (AACR) annual conference, April 1-5, 2006, entitled: "Functional studies of the MUC1 oncoprotein in human breast cancer".

- Quarterly presentation of publications from high-impact journals as part of the "Current Events in Tumor Biology" journal club that is videoconferenced between Mayo Clinic sites in Rochester, MN, Scottsdale, AZ, and Jacksonville, FL. This journal club is attended by graduate students, postdoctoral fellows, and principle investigators and takes place weekly.

- Frequent presentations (every 6-8 weeks) of publications as part of a laboratory journal club. This journal club occurs every other week and is attended by members of Dr. Sandra Gendler's and Dr. Pinku Mukherjee's research groups.

- Frequent presentation (every 2-3 months) of my own research in lab meeting, which occurs every other week and is attended by members of Dr. Sandra Gendler's and Dr. Pinku Mukherjee's research groups.

- Yearly presentation of my work as part of "Research Project Update" and "Tumor Biology Interest Group". Research Project Update is the forum of biomedical research at Mayo Clinic Arizona; presentations are attended by all members of the research labs, including technologists, students, fellows, and principle investigators. Tumor Biology Interest Group is a similar forum encompassing all students, postdoctoral fellows, and principle investigators participating in the Tumor Biology training program at all three Mayo Clinic sites. Yearly presentation in both Research Project Update and the Tumor Biology Interest Group is required of all students and fellows, and encouraged for principle investigators.

- Acceptance as a postdoctoral fellow (pending completion of the Ph.D., scheduled for April, 2006) in the Clinical Chemistry Training Program of the Department of Lab Medicine and Pathology, Mayo Clinic Rochester. This program is one of the best in the country for training residents and fellows in the field of clinical chemistry; only 2 candidates per year are accepted into the program.

Conclusions

The work presented here addresses the physiological relevance of MUC1 and APC in breast cancer, in particular the β-catenin and ErbB signaling networks. Technical difficulties in analyzing APC directly have steered our work largely towards a very interesting avenue of study that was first presented as preliminary data in the previous year's annual summary. This line of work is the analysis of β-catenin and ErbB signaling after siRNA-mediated knockdown of MUC1 expression in breast cancer cell lines.

We report that loss of MUC1 results in decreased levels of total and active (unphosphorylated) β-catenin in breast cancer cells. Three lines were used for these analyses: MDA-MB-435, MDA-MB-468, and BT-20. The first of these, MDA-MB-435, has minimal endogenous MUC1 and was therefore infected with stable constructs expressing full-length MUC1, either wild-type or the Y0 mutant lacking the seven tyrosines in the cytoplasmic tail. The latter two lines express ample endogenous MUC1 and were selected from a panel of breast cancer cell lines for their high-level, consistent knockdown of MUC1 upon transient siRNA transfection. As the active β-catenin antibody only measures regulation via the standard APC/GSK3β/axin-containing destruction complex, it is clear that the loss of active β-catenin after MUC1 siRNA reflects activation of this pathway of β-catenin degradation. We also have indications that an alternative mechanism for β-catenin destruction may be involved; this pathway requires p53, APC, and the Siah E3 ligase. We show that MUC1 siRNA also results in increased levels of p53, indicating that MUC1 expression may destabilize p53. However, as the p53 in these cells is mutated and non-functional, a better model system must be found to explore this possibility further.

In both MDA-MB-468 and BT-20, MUC1 siRNA causes alterations in transcription of β-catenin target genes, notably *MYC*, *JUN*, and *VEGF*, adding to the growing body of evidence describing an essential role for MUC1 in β-catenin-mediated oncogenesis. We also describe a novel role for MUC1 in regulating the transcription of members of the ERK1/2 MAPK pathway that is downstream of the ErbB kinases. Though it is already known that MUC1 expression stimulates this pathway, our results regarding transcription of *MAP2K1*, *RAF1*, and *JUN* provide a new mechanism by which MUC1 can affect MAPK signaling.

The changes in transcription seen with MUC1 siRNA are correlated with alterations in oncogenic events such as proliferation, apoptosis, and invasion. Interestingly, MDA-MB-468 and BT-20 show very different responses to MUC1 siRNA. MDA-MB-468 fit the pattern expected for cells experiencing the loss of an oncogene: decreased proliferation, increased apoptosis in response to stress, and decreased invasion. In contrast, BT-20 cells show no alterations in apoptosis or invasion and actually increase proliferation after loss of MUC1. These data suggest that the mechanism of MUC1 oncogenic function—which has been largely elucidated in cultured cells—needs to be clarified with further work, with particular emphasis on analyzing MUC1 in the context of cell-specific signaling environments.

References

1. Gendler, S.J. MUC1, the renaissance molecule. *J Mammary Gland Biol Neoplasia* **6**, 339-53. (2001).
2. Li, Y., Liu, D., Chen, D., Kharbanda, S. & Kufe, D. Human DF3/MUC1 carcinoma-associated protein functions as an oncogene. *Oncogene* **22**, 6107-10 (2003).
3. Schroeder, J.A. et al. MUC1 overexpression results in mammary gland tumorigenesis and prolonged alveolar differentiation. *Oncogene* **23**, 5739-47 (2004).
4. Yamamoto, M., Bharti, A., Li, Y. & Kufe, D. Interaction of the DF3/MUC1 breast carcinoma-associated antigen and beta-catenin in cell adhesion. *J Biol Chem* **272**, 12492-4 (1997).
5. Li, Y., Bharti, A., Chen, D., Gong, J. & Kufe, D. Interaction of glycogen synthase kinase 3beta with the DF3/MUC1 carcinoma-associated antigen and beta-catenin. *Mol Cell Biol* **18**, 7216-24 (1998).
6. Hattrup, C.L., Fernandez-Rodriguez, J., Schroeder, J.A., Hansson, G.C., Gendler, S.J. MUC1 can interact with adenomatous polyposis coli in breast cancer. *Biochem Biophys Res Commun* **316**, 364-369 (2004).
7. Schroeder, J.A., Thompson, M.C., Gardner, M.M. & Gendler, S.J. Transgenic MUC1 interacts with epidermal growth factor receptor and correlates with mitogen-activated protein kinase activation in the mouse mammary gland. *J Biol Chem* **276**, 13057-64. (2001).
8. Ren, J., Li, Y. & Kufe, D. Protein kinase C delta regulates function of the DF3/MUC1 carcinoma antigen in beta-catenin signaling. *J Biol Chem* **277**, 17616-22 (2002).
9. Huang, L. et al. MUC1 cytoplasmic domain coactivates Wnt target gene transcription and confers transformation. *Cancer Biol Ther* **2**, 702-6 (2003).
10. Wei, X., Xu, H. & Kufe, D. Human MUC1 oncoprotein regulates p53-responsive gene transcription in the genotoxic stress response. *Cancer Cell* **7**, 167-78 (2005).
11. Yin, L., Huang, L. & Kufe, D. MUC1 oncoprotein activates the FOXO3a transcription factor in a survival response to oxidative stress. *J Biol Chem* **279**, 45721-7 (2004).
12. Wei, X., Xu, H. & Kufe, D. MUC1 oncoprotein stabilizes and activates estrogen receptor alpha. *Mol Cell* **21**, 295-305 (2006).
13. Al Masri, A. & Gendler, S.J. Muc1 affects c-Src signaling in PyV MT-induced mammary tumorigenesis. *Oncogene* **24**, 5799-808 (2005).
14. Huang, L. et al. MUC1 oncoprotein blocks glycogen synthase kinase 3beta-mediated phosphorylation and degradation of beta-catenin. *Cancer Res* **65**, 10413-22 (2005).
15. Giles, R.H., van Es, J.H. & Clevers, H. Caught up in a Wnt storm: Wnt signaling in cancer. *Biochim Biophys Acta* **1653**, 1-24 (2003).
16. Behrens, J. The role of the Wnt signalling pathway in colorectal tumorigenesis. *Biochem Soc Trans* **33**, 672-5 (2005).
17. Hanson, C.A. & Miller, J.R. Non-traditional roles for the Adenomatous Polyposis Coli (APC) tumor suppressor protein. *Gene* **361**, 1-12 (2005).
18. Carraway, K.L., 3rd, Ramsauer, V.P., Carothers Carraway, C.A. Glycoprotein contributions to mammary gland and mammary tumor structure and function: roles of adherens junctions, ErbBs and membrane MUCs. *J Cell Biochem* **96**, 914-926 (2005).
19. Chaturvedi, R. et al. Augmentation of Fas ligand-induced apoptosis by MUC1 mucin. *Int J Oncol* **26**, 1169-76 (2005).
20. Adriance, M.C. & Gendler, S.J. Downregulation of Muc1 in MMTV-c-Neu tumors. *Oncogene* **23**, 697-705 (2004).
21. Roberts, G.T., Davies, M.L. & Wakeman, J.A. Interaction between Ku80 protein and a widely used antibody to adenomatous polyposis coli. *Br J Cancer* **88**, 202-5 (2003).
22. Brocardo, M., Nathke, I.S. & Henderson, B.R. Redefining the subcellular location and transport of APC: new insights using a panel of antibodies. *EMBO Rep* **6**, 184-90 (2005).

23. Mogensen, M.M., Tucker, J.B., Mackie, J.B., Prescott, A.R. & Nathke, I.S. The adenomatous polyposis coli protein unambiguously localizes to microtubule plus ends and is involved in establishing parallel arrays of microtubule bundles in highly polarized epithelial cells. *J Cell Biol* **157**, 1041-8 (2002).

24. Faux, M.C. et al. Restoration of full-length adenomatous polyposis coli (APC) protein in a colon cancer cell line enhances cell adhesion. *J Cell Sci* **117**, 427-39 (2004).

25. Fearnhead, N.S., Britton, M.P. & Bodmer, W.F. The ABC of APC. *Hum Mol Genet* **10**, 721-33. (2001).

26. Mukherjee, P., Tinder, T.L., Basu, G.D. & Gendler, S.J. MUC1 (CD227) interacts with lck tyrosine kinase in Jurkat lymphoma cells and normal T cells. *J Leukoc Biol* **77**, 90-9 (2005).

27. Liu, J., Stevens, J., Rote, C.A., Yost, H.J., Hu, Y., Neufeld, K.L., White, R.L., Matsunami, N. Siah-1 mediates a novel beta-catenin degradation pathway linking p53 to the adenomatous polyposis coli protein. *Mol Cell* **7**, 927-936 (2001).

28. Gendler, S.J., et al. unpublished data.

29. Do, T.N. et al. Preferential induction of necrosis in human breast cancer cells by a p53 peptide derived from the MDM2 binding site. *Oncogene* **22**, 1431-44 (2003).

30. Wen, Y., Caffrey, T.C., Wheelock, M.J., Johnson, K.R. & Hollingsworth, M.A. Nuclear association of the cytoplasmic tail of MUC1 and beta-catenin. *J Biol Chem* **278**, 38029-39 (2003).

31. Blavier, L., Lazaryev, A., Dorey, F., Shackleford, G.M., DeClerck, Y.A. Matrix metalloproteinases play an active role in Wnt1-induced mammary tumorigenesis. *Cancer Res* **66**, 2691-2699 (2006).

32. Johnson, G.L., Lapadat, R. Mitogen-activated protein kinase pathways mediated by ERK, JNK, and p38 protein kinases. *Science* **298**, 1911-1912 (2002).

33. Liu, H., Radisky, D.C., Nelson, C.M., Zhang, H., Fata, J.E., Roth, R.A., Bissell, M.J. Mechanism of Akt1 inhibition of breast cancer cell invasion reveals a protumorigenic role for TSC2. *Proc Natl Acad Sci* **103**, 4134-4139 (2006).

APPENDIX I

MUC1 alters oncogenic events and transcription in human breast cancer cells

Christine L. Hattrup and Sandra J. Gendler*
Mayo Clinic College of Medicine, Mayo Clinic Arizona, Scottsdale, AZ 85260

e-mail addresses: hattrup.christine@mayo.edu and gendler.sandra@mayo.edu

To whom correspondence should be addressed:
Sandra J. Gendler
Mayo Clinic Arizona
13400 E. Shea Boulevard,
Scottsdale, AZ 85260
e-mail: gendler.sandra@mayo.edu
phone: (480) 301-7062
fax: (480) 301-7017

Abstract

INTRODUCTION: MUC1 is an oncoprotein whose expression has been correlated with aggressiveness of tumors and poor survival of cancer patients. Much of the ability of MUC1 to foster oncogenesis is believed to occur through its cytoplasmic tail, which regulates cellular signaling events. As expected for a protein with oncogenic functions, MUC1 has been linked to proliferation, apoptosis, invasion, and regulation of transcription. METHODS: In order to clarify the role of MUC1 in cancer, we transfected two established breast cancer cell lines (MDA-MB-468 and BT-20) with siRNA directed against MUC1, and analyzed transcriptional responses and oncogenic events, namely proliferation, apoptosis and invasion. RESULTS: Transcription of several genes was significantly altered after MUC1 siRNA, including decreased *MAP2K1* (encoding MEK1), *JUN*, *PDGFA* (encoding platelet derived growth factor α) *CDC25A*, *VEGF* and *ITGAV* (encoding integrin α_v) transcription, and increased *TNF*, *RAF1*, and *MMP2* transcription. Additional changes were seen at the protein level, such as increased expression of c-Myc, heightened phosphorylation of AKT, and decreased levels of active MEK1/2 and ERK1/2. These were correlated to cellular events, as MUC1 siRNA in the MDA-MB-468 line decreased proliferation and invasion, and increased stress-induced apoptosis. Intriguingly, BT-20 cells displayed similar levels of apoptosis regardless of siRNA, and actually increased proliferation after MUC1 siRNA. CONCLUSIONS: These results further the growing knowledge of MUC1 regulation of transcription, and suggest that the regulation of MUC1 in breast cancer may be more complex than previously appreciated. The differences between these two cell lines emphasize the importance of understanding the context of cell-specific signaling events when analyzing the oncogenic functions of MUC1, and caution against generalizing the results of individual cell lines without adequate confirmation in intact biological systems.

Introduction

MUC1 is the founding member of the mucin family, a group of glycoproteins characterized by heavy O-glycosylation centering around the "mucin domain": a variable number of tandem repeats that are rich in serine and threonine residues [1]. The mature form of MUC1 is a transmembrane heterodimer with one subunit solely extracellular (MUC1-EX), and the other subunit comprised of a short extracellular stem, a single transmembrane domain, and the 72-amino acid cytoplasmic tail (together called the MUC1-CT). Initially described as a tumor antigen highly overexpressed in >90% of breast cancers, MUC1 is now known as an oncogene with roles in both tumor formation and progression, and is a useful therapeutic target [2, 3]. MUC1 possesses both pro- and anti-adhesive capacities, as the MUC1-EX provides binding sites for a variety of mammalian (e.g., ICAM-1 [4]) and prokaryotic (e.g., flagellin [5]) proteins, while its enormous size and extended structure prevents cell-cell adhesion via steric hindrance [6].

Mouse studies have been integral to the current understanding of MUC1 in cancer. The mouse Muc1 knockout (Muc1$^{-/-}$, MUC1 is human; Muc1 is mouse) has no noticeable phenotype when maintained in pathogen-free conditions [7]. However, once crossed onto tumor models, Muc1$^{-/-}$ mice show a reduction in oncogenic phenotype. For example, Muc1$^{-/-}$ x MMTV-Wnt-1 mice (Wnt-1 oncogene driven by the mouse mammary tumor virus promoter) [8] have delayed mammary tumors onset compared to Muc1$^{+/+}$ [9]; similarly, Muc1$^{-/-}$ x MMTV-PyV MT [10] (polyomavirus middle T antigen) mice display slowed tumor growth and a trend towards decreased metastasis [7]. In complementary studies, human MUC1 overexpression in the mammary gland drives tumor formation by itself [11], indicating that MUC1 is a true oncogene.

Much of the oncogenic ability of MUC1 is believed to stem from the interactions of its cytoplasmic tail. The MUC1-CT contains numerous binding sites for proteins implicated in cancer formation and progression, including c-Src [12, 13], the epidermal growth factor receptor (EGFR) family [14, 15], glycogen synthase kinase 3β [16], and β-catenin [12, 17, 18]. MUC1 expression stimulates mitogen activated protein kinase (MAPK) signaling through the extracellular signal regulated kinases (ERK1/2) [14, 19]; this can occur through activation of the Ras pathway by binding of the MUC1-CT to Grb-2 and son of sevenless [20]. The most common route by which ERK1/2 signaling is activated is the Ras—Raf—MEK1/2 cascade, which stimulates transcription via several factors including the activator protein-1 complex containing c-Fos and c-Jun; this pathway is normally activated by mitogens, including growth factor receptors such as EGFR [21]. Interestingly, loss of MUC1 can result in reduced proliferation and decreased EGFR expression [22], providing another means of affecting MAPK signaling. Our results describe a novel mechanism by which MUC1 can regulate the ERK1/2 MAPK pathway: modulating transcription of the genes encoding MEK1, Raf-1, and c-Jun.

In cell lines, MUC1 expression has been correlated with increased survival in response to cytotoxic or oxidative agents [23-26], and MUC1 can activate the phosphatidyl inositol-3 kinase – AKT pathway as part of an anti-apoptotic response [23]. MUC1 has also recently been linked to transcription: the MUC1-CT localizes to the nucleus [27] and can affect potent transcription factors such as β-catenin [27, 28], FOXO-3 [26], p53 [29], and estrogen receptor α [30]. Interestingly, though, there are indications that the role of MUC1 in oncogenesis is regulated by cell type and signaling context: e.g., MUC1 can stimulate Fas-mediated apoptosis [31], and Muc1 expression is specifically downregulated in c-neu-induced mammary tumors [32]. This report emphasizes the complexity of MUC1 signaling in breast cancer by contrasting results from two established breast cancer cell lines.

In order to understand MUC1 function in the context of cells with high endogenous expression, i.e., cells likely to have evolved with active MUC1 signaling, we studied the effects of small interfering RNA (siRNA)-mediated knockdown of MUC1 in MDA-MB-468 and BT-20 cells. These lines were chosen for strong MUC1 expression and amenability to transient siRNA transfection. After MUC1 siRNA, we analyzed transcription of 84 genes involved in cancer

formation and progression, as well as the effects upon cellular events linked to oncogenesis, such as apoptosis and proliferation. Interestingly, loss of MUC1 alters transcription of a variety of genes implicated in cancer, including *JUN*, *RAF1*, and *MAP2K1* (MEK1), constituting a novel link between MUC1 and transcriptional regulation of the ERK1/2 MAPK pathway. The two cell lines show very different responses to MUC1 siRNA: MDA-MB-468 proliferate more slowly, die more readily, and invade less ably, while BT-20 proliferate more rapidly after loss of MUC1. This last may reflect the striking amount of active AKT in the BT-20 line; AKT activity is increased in both cell lines after MUC1 siRNA, which disagrees with the findings of previous work in 3Y1 fibroblasts [23]. Recent studies have emphasized the complex and context-specific regulation of even such classical oncogenes as AKT [33]. The differences between the two breast cancer cell lines in this study suggest that MUC1 oncogenic functions are also subject to cell-specific regulation, and stress the need for understanding the cellular signaling context when interpreting results.

Materials and Methods

Cell culture and siRNA transfection – MDA-MB-468 and BT-20 cells (American Type Culture Collection) were cultured in Dulbecco's Modified Eagle's Medium (Invitrogen) plus 10% fetal calf serum, 1% Glutamax (Invitrogen) and 1% penicillin/streptomycin. Stable cell lines (468.Neo and 468.MUC1Δ8) were also given 0.5 mg/mL G418 for selection. For EGF stimulation, MDA-MB-468 cells were serum-starved overnight and treated for 10 min at 37°C with 100 ng/mL EGF prior to lysis. Transient siRNA transfection was performed with Lipofectamine2000 (Invitrogen) and 100 nM siRNA oligonucleotides. The commercially available siRNA constructs (all from Dharmacon) were scrambled (siCONTROL non-targeting siRNA #1), or directed against firefly luciferase (siCONTROL non-targeting siRNA #2) or MUC1 (siGENOME smartpool). The independent oligonucleotides designed in our laboratory target sequences beginning at MUC1 codons 882 and 956, and have been described previously [34].

Cloning of MUC1 WT vector and stable transfection – Two silent mutations (G891A and T894C) were introduced into the MUC1 cDNA to make it resistant to the 882 siRNA oligonucleotide that hybridizes to that region of the mRNA. The mutant cDNA was cloned into the neomycin resistance gene-containing pLNCX.1 vector (gift of Joseph Loftus, Mayo Clinic Arizona). Stable transfection was performed with Lipofectamine2000; cells were selected continuously from 24 hr post-transfection and maintained as a polyclonal population.

Western blots, immunoprecipitations, and antibodies - Cells were lysed in pH 7.6 lysis buffer (20 mM HEPES, 150 mM sodium chloride, 1% Triton X-100, 2 mM EDTA) with a commercial protease inhibitor (Complete inhibitor cocktail, Roche) and phosphatase inhibitors (10 mM sodium fluoride, 2 mM sodium vanadate, 50 μM ammonium molybdate). Protein concentration was determined by BCA assay (Pierce); 25 - 50 μg of lysate were loaded on SDS-PAGE gels. Non-commercial antibodies used were: BC2, a mouse monoclonal to the MUC1-EX (gift of Dr. McGuckin, Queensland University), and CT2, an Armenian hamster monoclonal to the MUC1-CT developed in our lab [14]. Antibodies to pMEK1/2, MEK1/2, ERK1/2, Myc, pAKT, AKT, β-tubulin (all Cell Signaling), β-actin and dpERK1/2 (both Sigma) were used according to manufacturer's recommendations. All antibodies except β-actin (1:2500) and dpERK1/2 (1:10,000) were used at 1:1000 dilution for western blots. Flow cytometric analysis of MUC1 expression was done with HMPV-FITC, which recognizes the core peptide of the MUC1-EX tandem repeats (Pharmingen). BrdU staining was performed with a fluorescently conjugated antibody to BrdU (BrdU-PE, BD Biosciences) as described below.

Transwell invasion assays – SiRNA-transfected cells were serum-starved beginning 24 hr post-transfection. Cells were re-plated (serum-free) 48 hr post-transfection at 50,000 cells per insert (sized for 24-well plates), with serum-free medium in the top well and serum-containing medium

in the bottom as an attractant. Transwell chambers (BD Biosciences) pre-coated with laminin, fibronectin, collagen IV, or control (no matrix) were used, and cells were permitted to invade for 48 hr. At this point (96 hr post-transfection), non-invaded cells were swabbed from the tops of half of the wells ("samples", containing only invaded cells), and retained in the others ("controls", containing all cells). All wells were stained 10 min with 0.5% crystal violet in 20% methanol and washed extensively with water. Membranes were then cut from the wells and destained 10 min in 10% acetic acid in a 96-well plate; membranes were removed and absorbance was read at 570 nm. Percent invasion is defined as (absorbance of samples / absorbance of controls) * 100.

[^{3}H]thymidine incorporation assays – SiRNA-transfected cells were trypsinized 24 hr post-transfection and re-plated in quadruplicate at 15,000 cells/well (96-well plate), with 1 μCi [^{3}H]thymidine added to each well. Cells were incubated in normal conditions for 24 hr. At this time (48 hr post-siRNA transfection) excess radioactivity was washed off and the cells were harvested to a filter plate, which was then read on a TopCount plate reader. Statistical analysis was performed using JMP 5.1.2 software (SAS Institute, Inc.); the student's t-test was used to determine p values and significance was confirmed with Wilcoxon rank sum and Pearson chi squared analyses.

BrdU incorporation – BrdU (50 μM) was given to cells in fresh medium 48 hr post-siRNA transfection, and permitted to incorporate for 1.5 hr after addition. At this time, cells were washed with PBS, trypsinized, and washed again to remove trypsin. BrdU staining was performed according to an adaptation of the manufacturer's protocol, as follows. Cells were re-suspended in PBS, mixed 1:1 with -20°C neat ethanol, and incubated at -20°C for 1 hr. Fixed cells were then washed gently with PBS, denatured in 2 M HCl for 20 min at room temperature, and washed again. Following 2 min incubation with 0.1 M Tris to neutralize the acid, cells were re-suspended in FACS buffer (0.5% fetal calf serum in PBS) and stained with PE-conjugated anti-BrdU according to the manufacturer's protocol (20 μL antibody per 100 μL cells) for flow cytometry analysis on a FACScan instrument.

Apoptosis and trypan blue staining – Apoptosis was measured using a kit (BD Biosciences) containing FITC-conjugated annexin V and propidium iodide (PI). Cells were stained according to the manufacturer's protocol and the level of apoptosis determined by flow cytometry. Quadrants are: early apoptosis (annexin V^+/PI^-), late apoptosis (annexin V^+/PI^+), and necrosis (annexin V^-/PI^+). Treatments for the stress panel were as follows: no treatment (control); DMSO as a control for celecoxib, 1.9 μL per 10 mL medium (DMSO); 100 mM celecoxib, brand name Celebrex™ (celecoxib dissolved in DMSO, 1.9 μL per 10 mL medium) [35]; 0.2 mM H_2O_2 in medium (peroxide) [36]; or 1 mg/mL G418 in medium (G418).

Real-time PCR arrays – Transcriptional analysis used Cancer PathwayFinder RT^2 profiler PCR arrays (SuperArray) following the manufacturer's protocol. Briefly, total RNA was isolated using an RNeasy RNA extraction kit (Qiagen); 1 μg of RNA was reverse transcribed to cDNA with the cDNA synthesis kit (SuperArray) and cDNA was subjected to real-time PCR using SYBR green to detect product. Arrays were performed independently at least twice for each cell line; all PCR products were checked on agarose gels to rule out the presence of contaminants. Values were obtained for cycle threshold (Ct) for each gene and normalized using the average of four housekeeping genes on the same array (*HPRT1*, *RPL13A*, *GAPD*, *ACTB*). The Ct values for housekeeping genes and a dilution series of *ACTB* were also monitored for consistency between arrays. Change (ΔCt) between MUC1 siRNA and control siRNA was found by: $\Delta Ct = Ct_{MUC1 \ siRNA} - Ct_{control \ siRNA}$ and fold change by: fold change = 2^(-ΔCt). Values are given as fold change; 2-fold or greater change was defined as significant. Both luciferase and scrambled siRNA controls were used in BT-20; only genes showing consistent alteration with both controls were included in the results reported here. The scrambled siRNA could be not used in MDA-MB-468 as this line decreases MUC1 expression in response to this construct.

Results

Transfection of siRNA oligonucleotides transiently decreases MUC1 expression in breast cancer cell lines. Two human breast cancer cell lines, MDA-MB-468 and BT-20, were transiently transfected with a pool of four siRNA oligonucleotides directed against the MUC1 mRNA (468.siMUC1 and BT.siMUC1), or a control oligonucleotide directed against luciferase (468.siLuc and BT.siLuc). Both of these cell lines express high endogenous levels of MUC1, making them promising targets for this sort of analysis. Western blots (Figure 1A) show successful knockdown of both the extracellular domain and cytoplasmic tail fragments of MUC1 48 hr post-transfection. 468.siMUC1 show a substantial decrease in the amount of MUC1-CT, while BT.siMUC1 show slightly less knockdown of MUC1-CT. Both MDA-MB-468 and BT-20 display a less dramatic decrease of MUC1 extracellular domain as compared to MUC1-CT (Figure 1A); this likely represents protein existing prior to siRNA transfection, and may reflect differences in the turnover rates of the two subunits. Alternatively, as the MUC1 extracellular domain antibody recognizes multiple epitopes within the tandem repeat region, any alteration of glycosylation that may occur with siRNA could potentially reveal or occlude epitopes, which would complicate determination of protein level.

Analysis of the MUC1 extracellular domain by flow cytometry confirms that a substantial fraction of cells in both lines decrease MUC1 expression after siRNA (Figure 1B). In three independent transfections, 468.siMUC1 averaged 75% knockdown of MUC1 compared to 468.siLuc; BT.siMUC1 averaged 50% knockdown relative to BT.siLuc. These effects could be titrated with increasing concentrations of siRNA, were seen as early as 24 hr post-transfection (data not shown) and lasted to at least 96 hr post-transfection (Figure 1B). All experiments were conducted within 48 - 96 hr after siRNA transfection. Similar results were obtained using two independent oligonucleotides designed in our lab (data not shown), designated "882" and "956" for the initial codon recognized by each. In addition, we analyzed a second, "scrambled" siRNA control; though in BT-20 cells this control resulted in levels of MUC1 similar to both untransfected cells and BT.siLuc, the scrambled siRNA resulted in decreased MUC1 expression only in MDA-MB-468 and was therefore not used in analysis of this line (data not shown).

Transcriptional changes are seen after MUC1 siRNA. Recent work has indicated that MUC1 may affect transcription both directly via interaction with transcription factors and indirectly (e.g., through modulating signaling). In order to study the effects of MUC1 knockdown in breast cancer cell lines, we analyzed transcription of 84 genes implicated in cancer formation and progression via RT-PCR array. The arrays include genes involved in a variety of cellular pathways, including cell cycle control, survival/apoptosis, invasion, and angiogenesis. For this analysis, genes with greater than two-fold change were considered significant.

Three genes (*MAP2K1*, *VEGF*, *PDGFA*) were found to be significantly altered after MUC1 siRNA in both MDA-MB-468 and BT-20 cells (Figure 2), two genes (*ITGAV*, *MMP2*) were significantly changed only in 468.siMUC1, and five genes (*TIMP3*, *RAF1*, *JUN*, *TNF*, *CDC25A*) only in BT.siMUC1. This list represents all of the genes that were found to be significantly altered after MUC1 siRNA, rather than a select group. In addition, three genes whose transcription was changed by less than two-fold are shown in Figure 2. Two of these, *PDGFB* and *ITGB1*, are listed because they relate closely to significantly altered genes (*PDGFA* and *ITGAV*, respectively). The third, *MYC*, is included because western blot results confirm a substantial change at the protein level (Figure 3A) that may reflect both transcriptional and post-transcriptional regulation. An extensive discussion of these genes and their implications in breast cancer and MUC1-mediated oncogenesis can be found in the next section.

Interestingly, transcription of *MAP2K1* was significantly decreased in both cell lines after MUC1 siRNA. This gene encodes MEK1, one of the primary regulators of the ERK1/2 MAPK pathway [37], a network which has been linked several times to MUC1 in cancer [14, 38-40]. We

examined MEK1 and MEK2 levels by western blot to confirm decreased protein in MUC1 siRNA-treated cells, and found that not only were total MEK1/2 levels in 468.siMUC1 and BT.siMUC1 lower as compared to their respective controls, but so were the basal amounts of active (phosphorylated) MEK1/2 in BT.siMUC1 (Figure 3, IB: MEK1/2 and IB: pMEK1/2). Basal pMEK1/2 levels were too low to be detected in MDA-MB-468 cells (see next paragraph). Both 468.siMUC1 and BT.siMUC1 also show reduced activation of ERK1/2 (Figure 3A, dpERK1/2), as would be expected with diminished signaling through MEK1/2; total ERK1/2 levels remain unchanged (Figure 3A, ERK1/2).

As basal levels of pMEK1/2 were too low for ready detection in the MDA-MB-468 line, siRNA-transfected cells were treated with epidermal growth factor (EGF); both of these lines have high levels of EGFR and thus activate the MEK—ERK cascade intensely when stimulated with EGF [41]. Notably, MUC1 siRNA impairs this important oncogenic pathway in MDA-MB-468 cells, as 468.siMUC1 display less pMEK1/2 in response to EGF than do 468.siLuc (Figure 3B). Interestingly, EGF treatment of BT-20 cells results in increased pMEK1/2 levels in BT.siMUC1 as compared to BT.siLuc. Though this result seems paradoxical in light of the decreased *MAP2K1* transcription in BT.siMUC1, it is likely the result of differences in the functions of Raf isoforms in combination with increased *RAF1* transcription. Specifically, B-Raf is considered to be the main activator of MEK1/2; Raf-1 has several other known substrates though it does activate MEK1/2, especially in response to stimulus [42]. Thus, it appears that basal pMEK1/2 levels are not greatly affected by Raf-1 overexpression in BT.siMUC1 cells, likely because it is regulated primarily by B-Raf under normal growth conditions. In contrast, when the cells are stimulated with EGF, the increase in Raf-1 levels in BT.siMUC1 leads to heightened activation of MEK1/2, as seen in Figure 3B.

MUC1 siRNA increases apoptosis in MDA-MB-468 cells but not BT-20. Based on these results, we examined whether MUC1 knockdown and its associated transcriptional alterations would affect overall cellular events. As several of the genes altered are important in regulating proliferation and survival, and because of the recently-described role of MUC1 in modulating apoptosis in response to cellular stresses [25, 26, 29], we first analyzed whether MUC1 siRNA would alter apoptosis in these lines. Although there was no change in basal apoptosis in either line (Figure 4A), we observed that cells responded differently when trypsinized for re-plating 24 hr after transfection (Figure 4B). Interestingly, 468.siMUC1 cells show greater apoptosis after trypsinization than do 468.siLuc (49.8% vs 34.0%, respectively), while BT-20 cells from both siRNA treatments display similar levels of apoptosis (approximately 22%).

To examine whether this phenomenon is specific to trypsin treatment, or part of a general stress response involving MUC1, we subjected cells to a panel of stresses and measured apoptosis. In agreement with the patterns seen with trypsinization, BT.siLuc and BT.siMUC1 respond similarly to all treatments (data not shown), while 468.siMUC1 show more apoptosis than 468.siLuc in response to trypsin, G418, or hydrogen peroxide (Figure 4C). Similar results were also obtained with celecoxib, a chemotherapeutic that targets the COX-2 pathway; apoptosis data were confirmed with two independent siRNA oligonucleotides directed against MUC1 to exclude the possibility that these effects are artifacts of the reagents used (data not shown).

Like the MAPK pathway, AKT signaling has also been linked to MUC1 in cancer. Although transcription of *AKT* was not significantly altered in MUC1 siRNA-treated cells, the results of our apoptosis studies prompted us to investigate levels of AKT further. As expected, total AKT protein level is not greatly changed after MUC1 siRNA in either cell line; however, the active, phosphorylated form of the protein (pAKT) is increased in both 468.siMUC1 and BT.siMUC1 compared to controls (Figure 3A). This result disagrees with the activation of the AKT pathway by MUC1 expression in rat 3Y1 cells [23], and may reflect regulation more appropriate to breast cancer cells than 3Y1 fibroblasts. In addition, there is a striking difference in the relative amounts of AKT and pAKT in the two cell lines (Figure 4D). When the BT-20 and MDA-MB-

468 lysates are exposed to film for the same length of time (though overexposure masks the differences between BT.siLuc and BT.siMUC1 that are apparent in Figure 3A), it is apparent that the level of pAKT in BT-20 cells is considerably higher than in MDA-MB-468, despite substantially lower total AKT expression. This difference in AKT activation between the two cell lines very likely contributes to the disparity in their sensitivity to the increase in apoptosis that would be expected with loss of MUC1.

MUC1 siRNA alters proliferation and invasion. As MUC1 expression is involved in regulating cell death, we next analyzed its effects on proliferation. BrdU incorporation, [^{3}H]thymidine incorporation, and growth curves were used to analyze proliferation after MUC1 siRNA. 468.siMUC1 cells show a significant decrease in [^{3}H]thymidine incorporation compared to 468.siLuc, while intriguingly, BT.siMUC1 cells show a significant increase in nucleotide incorporation (Figure 5A). Growth curves mirror these results, as do experiments with the two independent MUC1 siRNA oligonucleotides (data not shown). Note that these assays require re-plating cells 24 hr after transfection to control for cell number; therefore the results seen in the MDA-MB-468 line could stem from the changes in apoptosis described in the previous section, rather than a true effect on proliferation. To control for this, we incubated non-trypsinized, siRNA-transfected cells at similar confluence with bromodeoxyuridine (BrdU) and analyzed by flow cytometry to measure incorporation. The "clumped" profile of cells in this assay (contrast to Figure 4B) is likely a result of the HCl denaturation step, as it occurs uniformly in these experiments. BrdU incorporation (Figure 5B) confirms that the [^{3}H]thymidine results are not solely due to altered apoptosis, as 468.siMUC1 cells display decreased BrdU incorporation compared to 468.siLuc; once again, BT.siMUC1 cells show increased proliferation over BT.siLuc.

Given the role of MUC1 in adhesion, we also examined whether MUC1 siRNA would affect cellular invasion. In transwell assays, BT-20 cells invaded poorly, regardless of the siRNA used (data not shown). However, MDA-MB-468 cells invade more readily, and were analyzed on a panel of three different extracellular matrix proteins. Interestingly, 468.siMUC1 cells display a trend towards decreased invasion on collagen IV, laminin, and fibronectin matrices, and on a no-matrix control (Figure 5C).

Transfection of MUC1 rescues the 468.siMUC1 phenotype. In order to determine whether the effects described above are specific to MUC1 knockdown, we created stable transfectants of the MDA-MB-468 line using an empty vector control (468.Neo) or a full-length MUC1 construct (468.MUC1Δ8) that is resistant to one of the independent MUC1-directed oligonucleotides designed in our lab ("882"). These cells were maintained in G418-containing medium to retain transgene selection. As expected, 468.MUC1Δ8 cells express higher basal levels of both the MUC1 extracellular domain and the MUC1-CT than do 468.Neo (Figure 6A). Note that 468.Neo express comparable levels of MUC1 to wildtype MDA-MB-468 (data not shown); the exposures in Figure 6A is considerably lighter than those in Figure 1A, in order to clearly show the relative levels of MUC1 in the stably transfected cells. After MUC1 siRNA, 468.MUC1Δ8 lose some MUC1 (likely endogenous protein, which is not siRNA-resistant) but retain high-level expression, while 468.Neo show a decrease in MUC1 levels similar to parental 468.siMUC1 cells (Figure 6B).

BrdU incorporation (Figure 6C) indicates that 468.Neo show a decrease in nucleotide incorporation after MUC1 siRNA as compared to luciferase siRNA (3.3% vs. 25.0%, respectively); this is not seen in 468.MUC1Δ8 cells, which show similar levels of BrdU incorporation regardless of the siRNA used (21.5% for luciferase siRNA and 23.9% for MUC1 siRNA). The MUC1 siRNA-transfected 468.Neo cells display a more dramatic decrease in BrdU than what is seen in parental 468.siMUC1 cells; this may reflect the additional stress on

the cells from being maintained in G418-containing medium.

Similarly, analysis of apoptosis in trypsinized cells indicates that the increased apoptosis seen in parental 468.siMUC1 cells is also present in the 468.Neo line after MUC1 siRNA (Figure 6D, 43.6% vs. 59.6% for luciferase and MUC1 siRNAs, respectively). However, in 468.MUC1Δ8 cells, the level of apoptosis after luciferase siRNA (34.1%) is lower than that in 468.Neo cells; MUC1 siRNA increases the amount of apoptosis slightly (42.8%), restoring it to a level similar to that seen in luciferase siRNA-treated 468.Neo cells. Together, these studies suggest that the above-described results are specific to MUC1, as stable transfection of an siRNA-resistant MUC1 rescues the phenotype seen in 468.siMUC1 cells.

Discussion

This report describes both the transcriptional alterations seen after MUC1 siRNA in human breast cancer cells and the effects on events such as apoptosis and proliferation. These studies analyzed MUC1 function in the context of cell lines with endogenous expression, rather than introducing exogenous protein into MUC1-null cells. The two cell lines (MDA-MB-468 and BT-20) were chosen for high expression of MUC1 and a substantial (50-75%), consistent decrease in MUC1 expression after siRNA. Both lines are epithelial in morphology, form tumors slowly in nude mice, express EGFR, have mutant p53, and lack ERα. One striking difference between these lines, however, is their response to MUC1 siRNA. MDA-MB-468 cells behave as would be expected with loss of an oncogene: MUC1 siRNA correlates with increased apoptosis in response to stress, decreased proliferation, and reduced invasion. In contrast, BT.siMUC1 proliferate more rapidly than BT.siLuc with little effect on apoptosis.

Much of the phenotype of MUC1 siRNA-treated cells can be understood in light of protein levels and transcriptional activity. As mentioned, both MDA-MB-468 and BT-20 display increased pAKT after MUC1 siRNA, but the ratio of active to total AKT is considerably higher in BT-20 cells, which may help these cells resist the increased apoptosis that would be expected with loss of MUC1. Levels of Myc are also higher in both cell lines after MUC1 siRNA; however, the dual ability of Myc to promote proliferation and apoptosis in different cellular contexts [43] complicates the interpretation of this finding without greater knowledge of surrounding signaling events. It may be that increased Myc levels are performing different functions in the two cell lines, or performing the same function with varying results, due to other cell-specific signaling activity.

Both cell lines show reduced transcription of *VEGF*, *PDGFA*, *PDGFB*, and *MAP2K1* (MEK1) after MUC1 siRNA. The genes encoding vascular endothelial growth factor (VEGF) and the A and B chains of platelet-derived growth factor (PDGF-A and PDGF-B) are interesting as these proteins have been heavily implicated in angiogenesis, suggesting a novel function for MUC1 in regulating this process. VEGF is perhaps the best-known angiogenic factor, and its expression in cancer is linked to tumor growth and metastasis [44, 45]. PDGF is also angiogenic, but has an additional role in breast cancer: stimulating the desmoplastic reaction that accompanies tumor development [46]. Reduced transcription of these genes after MUC1 siRNA therefore suggests that MUC1 may foster angiogenesis and stromal proliferation, although this would have to be confirmed in a more appropriate model system than cell lines in two-dimensional culture.

Decreased *MAP2K1* (MEK1) transcription after MUC1 siRNA provides a novel mechanism by which MUC1 can affect the ERK1/2 MAPK pathway. MUC1 has been linked to the Ras—Raf—MEK—ERK cascade numerous times [14, 38-40, 47], and at least two mechanisms by which MUC1 can alter MAPK signaling have been described: MUC1 interaction with and phosphorylation by the ErbB family [14, 15], and MUC1 binding to the Grb2/Sos complex that activates Ras [47]. Reduction of MEK1 levels after MUC1 siRNA agrees with the role of MUC1 in strengthening MAPK signaling, and indicates that MUC1 can regulate both transcription and activity of members of this pathway.

Two additional MAPK pathway members are altered specifically in BT.siMUC1, with no corresponding change in 468.siMUC1 cells. These genes are *RAF1*, which is increased after MUC1 siRNA, and *JUN*, which decreases with loss of MUC1. The products of these genes, Raf-1 (c-Raf) and c-Jun, are both known to function outside of the ERK1/2 MAPK pathway, which may explain the seeming paradox of increased *RAF1* transcription with simultaneous decreases in *MAP2K1* and *JUN*. Specifically, Raf-1 has been found to inhibit the apoptosis-inducing effects of ASK1 (apoptosis signal-regulated kinase 1) upstream of p38 and JNK (Jun N-terminal kinase) [42]. ASK1 is a MAP kinase kinase kinase that phosphorylates JNK in response to stress, resulting in activation of c-Jun and stimulation of apoptosis [48], indicating that the coordinate upregulation of RAF1 and downregulation of JUN may provide a potent anti-apoptotic effect in BT-20 cells, which would counter the expected increase in apoptosis after MUC1 siRNA.

Regulation of proliferation and apoptosis is a hallmark of two other genes whose transcription is altered in BT.siMUC1 cells: *CDC25A* and *TNF*. The *CDC25A* gene product is a phosphatase that stimulates cell cycle progression by removing inhibitory phosphorylation from cyclin-dependent kinases [49]. The cause for its transcriptional decrease in BT.siMUC1 is not clear, especially in light of the increased proliferation of these cells; however, the CDC25 proteins (A, B, and C) were recently shown to have greater functional overlap than was previously thought [50], suggesting that the other two isoforms may compensate for reduced CDC25A levels. *TNF* encodes tumor necrosis factor α (TNFα), a protein known for potent, cell type-specific control of life and death. In tumor cells, TNFα expression can promote proliferation in an autocrine fashion, and inhibit apoptosis through activation of AKT, nuclear factor κB, and other pro-survival regulators [51]. These results suggest that TNFα produced in BT.siMUC1 could contribute to the increased proliferation seen in these cells.

Interestingly, the increase in TNFα is accompanied by decreased transcription of *TIMP3*, encoding tissue inhibitor of metalloproteinases 3 (TIMP3). The TIMP family disrupts the function of matrix metalloproteinases (MMPs), generally resulting in decreased invasion as a consequence of blocking MMP-mediated degradation of extracellular matrix proteins [52]. TIMP3 is unique among members of the TIMP family in that it can also bind to and inhibit TNFα converting enzyme (TACE), which activates TNFα by cleaving the membrane-bound precursor peptide to release TNFα from the cell surface [51]. Reduced expression of TIMP3 would therefore foster signaling through TNFα by releasing inhibition of TACE. In agreement with this, TIMP3 can promote apoptosis [53]; thus its downregulation in BT.siMUC1 provides another mechanism by which these cells are able to resist the increased apoptosis expected with loss of MUC1.

Another TIMP target responds to MUC1 siRNA, as 468.siMUC1 cells show significantly increased expression of *MMP2* (encoding MMP-2/gelatinase A). This enzyme degrades type IV collagen, which is primarily found in the basement membrane separating epithelial cells from the underlying stroma [53]. In breast cancer, the ratio of active to latent MMP-2 increases in parallel with tumor progression; MMP-2 may facilitate both angiogenesis and metastasis [53]. Its increase after loss of MUC1 is therefore unexpected, but at least two lines of reasoning may clarify this result. First, though MMP-2 levels increase downstream of Wnt-1 in mouse mammary tumors, its expression is confined to the stroma [54], suggesting that increased *MMP2* transcription after loss of the epithelium-specific MUC1 might reflect a shift towards a more mesenchymal phenotype. Second, MMP-2 levels are increased by overexpression of erbB2 [53]; previous studies have shown that erbB2 and Muc1 expression are mutually exclusive in mammary tumors [32], implying that MMP-2 might be part of a transcriptional profile linked to low MUC1 levels.

It is intriguing that, despite increased *MMP2* transcription, invasion is decreased in 468.siMUC1 cells, even on collagen IV. This may reflect insufficient activation of MMP-2, as

the precursor protein must be cleaved for enzymatic function [53]; increased transcription alone may not bolster MMP-2 activity. Alternatively, the slowed invasion of these cells may relate to impaired adhesion resulting from decreased transcription of *ITGAV* and *ITGB1* (α_v and β_1 integrins, respectively). Integrin signaling is tied to life-or-death decisions in epithelial cells, and integrin expression is vital for processes from wound healing to metastasis [55]. Integrin $\alpha_v\beta_3$ is implicated in facilitating metastasis of breast cancer cells to bone [56]; decreased transcription of *ITGAV* after MUC1 siRNA may therefore suggest that MUC1 is involved in this lethal process as well.

MUC1 is an oncogene in the mammary gland and has been linked to apoptosis [23, 25, 31], proliferation [22], and transcription [26, 28-30]. However, the two cell lines chosen for our study display very different patterns of behavior in response to MUC1 siRNA, indicating that regulation of MUC1 in breast cancer is likely quite complex and cautioning against over-generalization of results from individual cell lines. Previous reports have suggested that, though the majority of publications outline a clearly oncogenic role for MUC1 in breast cancer, the exact details may vary depending on factors such as cell type and signaling context. For example, in CHO cells, MUC1 expression stimulates Fas-mediated apoptosis [31], quite unlike the inhibition of apoptosis seen in most other cell lines. Similarly, despite the facts that MUC1 drives mouse mammary oncogenesis in its own right [11] and facilitates tumorigenesis driven by other oncogenes [7, 9], Muc1 is selectively downregulated in c-neu induced mouse mammary tumors [32], indicating that the context of oncogenic signaling is vital to understanding the function of MUC1.

In interpreting these results, therefore, it is important to take into account the relative levels of knockdown of MUC1 in the two cell lines. BT-20 cells reduce MUC1 expression less efficiently after siRNA than do MDA-MB-468 (50% vs 75% knockdown, respectively). Though independent cell lines—originating from individuals with different genetics, disease history, and treatment—are expected to show some dissimilarities, the relative efficiency of knockdown may also contribute to the divergent phenotypes of these cell lines after MUC1 siRNA. As MUC1 is known to perform a scaffolding function [13], strong expression of MUC1 relative to its associated signaling proteins might create a dilution effect, sequestering signal transducers away from each other; this would be relieved by MUC1 siRNA. Thus, enough MUC1 expression may be retained in BT.siMUC1 cells for its oncogenic effects, while signaling complex formation would be enhanced by lowering the amount of MUC1 relative to other signaling proteins.

Conclusions

The fascinating contrast between these MDA-MB-468 and BT-20 lines in response to MUC1 siRNA serves as a reminder that simplified models such as cell lines fail to encompass the complexity of intact biological systems. This report describes transcriptional alterations seen after MUC1 knockdown: significantly decreased transcription of *MAP2K1*, *VEGF*, *PDGFA*, *ITGAV*, *TIMP3*, *CDC25A*, and *JUN*, and increased transcription of *MMP2*, *TNF*, and *RAF1*. The alterations in *MAP2K1*, *RAF1*, and *JUN* represent a novel means by which MUC1 can affect ERK1/2 signaling: transcriptional regulation of MAPK pathway members. Oncogenic events are also altered in both cell lines after MUC1 siRNA, but intriguingly, BT-20 cells do not display the expected phenotype after loss of MUC1. These results strengthen the growing ties linking MUC1 and transcriptional regulation, and suggest that the role of MUC1 in breast cancer may be more complex than a direct correlation between MUC1 level and oncogenic function.

Abbreviations used: bromodeoxyuridine (BrdU), epidermal growth factor receptor (EGFR), extracellular signal regulated kinases 1 and 2 (ERK1/2), mitogen activated protein kinase (MAPK), MAPK and ERK kinases 1 and 2 (MEK1/2), mouse mammary tumor virus (MMTV), MUC1 cytoplasmic tail (MUC1-CT), propidium iodide (PI), small interfering RNA (siRNA)

References
1. Baldus SE, Engelmann, Katja, Hanisch, Franz-Georg: **MUC1 and the MUCs: A Family of Human Mucins with Impact in Cancer Biology**. *Critical Reviews in Clinical Laboratory Sciences* 2004, **41**(2):189-231.
2. Gendler SJ: **MUC1, the renaissance molecule**. *J Mammary Gland Biol Neoplasia* 2001, **6**(3):339-353.
3. Braun DP, Crist KA, Shaheen F, Staren ED, Andrews S, Parker J: **Aromatase inhibitors increase the sensitivity of human tumor cells to monocyte-mediated, antibody-dependent cellular cytotoxicity**. *Am J Surg* 2005, **190**(4):570-571.
4. Regimbald LH, Pilarski LM, Longenecker BM, Reddish MA, Zimmermann G, Hugh JC: **The breast mucin MUC1 as a novel adhesion ligand for endothelial intercellular adhesion molecule 1 in breast cancer**. *Cancer Res* 1996, **56**(18):4244-4249.
5. Lillehoj EP, Kim BT, Kim KC: **Identification of Pseudomonas aeruginosa flagellin as an adhesin for Muc1 mucin**. *Am J Physiol Lung Cell Mol Physiol* 2002, **282**(4):L751-756.
6. Carraway KL, 3rd, Ramsauer, V.P., Carothers Carraway, C.A.: **Glycoprotein contributions to mammary gland and mammary tumor structure and function: roles of adherens junctions, ErbBs and membrane MUCs**. *J Cell Biochem* 2005, **96**:914-926.
7. Spicer AP, Rowse GJ, Lidner TK, Gendler SJ: **Delayed mammary tumor progression in Muc-1 null mice**. *J Biol Chem* 1995, **270**(50):30093-30101.
8. Li Y, Hively WP, Varmus HE: **Use of MMTV-Wnt-1 transgenic mice for studying the genetic basis of breast cancer**. *Oncogene* 2000, **19**(8):1002-1009.
9. Schroeder JA, Adriance MC, Thompson MC, Camenisch TD, Gendler SJ: **MUC1 alters beta-catenin-dependent tumor formation and promotes cellular invasion**. *Oncogene* 2003, **22**(9):1324-1332.
10. Guy CT, Cardiff RD, Muller WJ: **Induction of mammary tumors by expression of polyomavirus middle T oncogene: a transgenic mouse model for metastatic disease**. *Mol Cell Biol* 1992, **12**(3):954-961.
11. Schroeder JA, Masri AA, Adriance MC, Tessier JC, Kotlarczyk KL, Thompson MC, Gendler SJ: **MUC1 overexpression results in mammary gland tumorigenesis and prolonged alveolar differentiation**. *Oncogene* 2004, **23**(34):5739-5747.
12. Li Y, Kuwahara H, Ren J, Wen G, Kufe D: **The c-Src tyrosine kinase regulates signaling of the human DF3/MUC1 carcinoma-associated antigen with GSK3 beta and beta-catenin**. *J Biol Chem* 2001, **276**(9):6061-6064.
13. Al Masri A, Gendler SJ: **Muc1 affects c-Src signaling in PyV MT-induced mammary tumorigenesis**. *Oncogene* 2005, **24**(38):5799-5808.

14. Schroeder JA, Thompson MC, Gardner MM, Gendler SJ: **Transgenic MUC1 interacts with epidermal growth factor receptor and correlates with mitogen-activated protein kinase activation in the mouse mammary gland**. *J Biol Chem* 2001, **276**(16):13057-13064.
15. Li Y, Ren J, Yu W, Li Q, Kuwahara H, Yin L, Carraway KL, 3rd, Kufe D: **The epidermal growth factor receptor regulates interaction of the human DF3/MUC1 carcinoma antigen with c-Src and beta-catenin**. *J Biol Chem* 2001, **276**(38):35239-35242.
16. Li Y, Bharti A, Chen D, Gong J, Kufe D: **Interaction of glycogen synthase kinase 3beta with the DF3/MUC1 carcinoma-associated antigen and beta-catenin**. *Mol Cell Biol* 1998, **18**(12):7216-7224.
17. Ren J, Li Y, Kufe D: **Protein Kinase C delta Regulates Function of the DF3/MUC1 Carcinoma Antigen in beta -Catenin Signaling**. *J Biol Chem* 2002, **277**(20):17616-17622.
18. Yamamoto M, Bharti A, Li Y, Kufe D: **Interaction of the DF3/MUC1 breast carcinoma-associated antigen and beta-catenin in cell adhesion**. *J Biol Chem* 1997, **272**(19):12492-12494.
19. Meerzaman D, Shapiro PS, Kim KC: **Involvement of the MAP kinase ERK2 in MUC1 mucin signaling**. *Am J Physiol Lung Cell Mol Physiol* 2001, **281**(1):L86-91.
20. Pandey P, Kharbanda, S, Kufe, D: **Association of the DF3/MUC1 breast cancer antigen with Grb2 and the Sos/Ras exchange protein.** *Cancer Res* 1995, **55**:4000-4003.
21. Steelman LS, Pohnert, S.C., Shelton, J.G., Franklin, R.A., Bertrand, F.E., McCubrey, J.A.: **JAK/STAT, Raf/MERK/ERK, PI3K/Akt and BCR-ABL in cell cycle progression and leukemogenesis**. *Leukemia* 2004, **18**:189-218.
22. Li X, Wang, L., Nunes, D.P., Troxler, R.F., Offner, G.D.: **Suppression of MUC1 synthesis downregulates expression of the epidermal growth factor receptor**. *Cancer Biol Ther* 2005, **4**(8):e8-e13.
23. Raina D, Kharbanda S, Kufe D: **The MUC1 oncoprotein activates the anti-apoptotic phosphoinositide 3-kinase/Akt and Bcl-xL pathways in rat 3Y1 fibroblasts**. *J Biol Chem* 2004, **279**(20):20607-20612.
24. Ren J, Agata N, Chen D, Li Y, Yu WH, Huang L, Raina D, Chen W, Kharbanda S, Kufe D: **Human MUC1 carcinoma-associated protein confers resistance to genotoxic anticancer agents**. *Cancer Cell* 2004, **5**(2):163-175.
25. Yin L, Li Y, Ren J, Kuwahara H, Kufe D: **Human MUC1 carcinoma antigen regulates intracellular oxidant levels and the apoptotic response to oxidative stress**. *J Biol Chem* 2003, **278**(37):35458-35464.
26. Yin L, Huang L, Kufe D: **MUC1 oncoprotein activates the FOXO3a transcription factor in a survival response to oxidative stress**. *J Biol Chem* 2004, **279**(44):45721-45727.
27. Wen Y, Caffrey TC, Wheelock MJ, Johnson KR, Hollingsworth MA: **Nuclear association of the cytoplasmic tail of MUC1 and beta-catenin**. *J Biol Chem* 2003, **278**(39):38029-38039.
28. Huang L, Ren J, Chen D, Li Y, Kharbanda S, Kufe D: **MUC1 cytoplasmic domain coactivates Wnt target gene transcription and confers transformation**. *Cancer Biol Ther* 2003, **2**(6):702-706.
29. Wei X, Xu H, Kufe D: **Human MUC1 oncoprotein regulates p53-responsive gene transcription in the genotoxic stress response**. *Cancer Cell* 2005, **7**(2):167-178.
30. Wei X, Xu H, Kufe D: **MUC1 oncoprotein stabilizes and activates estrogen receptor alpha**. *Mol Cell* 2006, **21**(2):295-305.
31. Chaturvedi R, Srivastava RK, Hisatsune A, Shankar S, Lillehoj EP, Kim KC: **Augmentation of Fas ligand-induced apoptosis by MUC1 mucin**. *Int J Oncol* 2005, **26**(5):1169-1176.
32. Adriance MC, Gendler SJ: **Downregulation of Muc1 in MMTV-c-Neu tumors**. *Oncogene* 2004, **23**(3):697-705.
33. Liu H, Radisky, D.C., Nelson, C.M., Zhang, H., Fata, J.E., Roth, R.A., Bissell, M.J.: **Mechanism of Akt1 inhibition of breast cancer cell invasion reveals a protumorigenic role for TSC2**. *Proc Natl Acad Sci* 2006, **103**(11):4134-4139.

34. Mukherjee P, Tinder TL, Basu GD, Gendler SJ: **MUC1 (CD227) interacts with lck tyrosine kinase in Jurkat lymphoma cells and normal T cells**. *J Leukoc Biol* 2005, **77**(1):90-99.

35. Basu GD, Pathangey LB, Tinder TL, Gendler SJ, Mukherjee P: **Mechanisms underlying the growth inhibitory effects of the cyclo-oxygenase-2 inhibitor celecoxib in human breast cancer cells**. *Breast Cancer Res* 2005, **7**(4):R422-435.

36. Troyano A, Sancho P, Fernandez C, de Blas E, Bernardi P, Aller P: **The selection between apoptosis and necrosis is differentially regulated in hydrogen peroxide-treated and glutathione-depleted human promonocytic cells**. *Cell Death Differ* 2003, **10**(8):889-898.

37. Johnson GL, Lapadat, R.: **Mitogen-activated protein kinase pathways mediated by ERK, JNK, and p38 protein kinases**. *Science* 2002, **298**:1911-1912.

38. Meerzaman D, Shapiro PS, Kim KC: **Involvement of the MAP kinase ERK2 in MUC1 mucin signaling**. *Am J Physiol Lung Cell Mol Physiol* 2001, **281**(1):L86-91.

39. Wang H, Lillehoj EP, Kim KC: **MUC1 tyrosine phosphorylation activates the extracellular signal-regulated kinase**. *Biochem Biophys Res Commun* 2004, **321**(2):448-454.

40. Lillehoj EP, Kim H, Chun EY, Kim KC: **Pseudomonas aeruginosa stimulates phosphorylation of the airway epithelial membrane glycoprotein Muc1 and activates MAP kinase**. *Am J Physiol Lung Cell Mol Physiol* 2004, **287**(4):L809-815.

41. Arteaga CL, Hurd SD, Dugger TC, Winnier AR, Robertson JB: **Epidermal growth factor receptors in human breast carcinoma cells: a potential selective target for transforming growth factor alpha-Pseudomonas exotoxin 40 fusion protein**. *Cancer Res* 1994, **54**(17):4703-4709.

42. Baccarini M: **Second nature: Biological functions of the Raf-1 "kinase"**. *FEBS Lett* 2005, **579**:3271-3277.

43. Dang CV, O'Donnell, K.A., Juopperi, T.: **The great MYC escape in tumorigenesis**. *Cancer Cell* 2005, **8**(3):177-178.

44. Robinson CJ, Stringer SE: **The splice variants of vascular endothelial growth factor (VEGF) and their receptors**. *J Cell Sci* 2001, **114**(Pt 5):853-865.

45. Augustin HG: **Translating angiogenesis research into the clinic: the challenges ahead**. *Br J Radiology* 2003, **76**:S3-S10.

46. Shao ZM, Nguyen, M., Barsky, S.H.: **Human breast carcinoma desmoplasia is PDGF initiated**. *Oncogene* 2000, **19**(38):4337-4345.

47. Pandey P, Kharbanda S, Kufe D: **Association of the DF3/MUC1 breast cancer antigen with Grb2 and the Sos/Ras exchange protein**. *Cancer Res* 1995, **55**(18):4000-4003.

48. Takeda K, Matsuzawa A, Nishitoh H, Ichijo H: **Roles of MAPKKK ASK1 in stress-induced cell death**. *Cell Struct Funct* 2003, **28**(1):23-29.

49. Boutros R, Dozier, C., Ducommun, B.: **The when and wheres of CDC25 phosphatases**. *Curr Opin Cell Biol* 2006, **18**:185-191.

50. Lindqvist A, Kallstrom, H., Lundgren, A., Barsoum, E., Rosenthal, C.K.: **Cdc25B cooperates with Cdc25A to induce mitosis but has a unique role in activating cyclin B1-Cdk1 at the centrosome**. *J Cell Biol* 2005, **171**:35-45.

51. Mocellin S, Rossi, C.R., Pilati, P., Nitti, D.: **Tumor necrosis factor, cancer and anticancer therapy**. *Cytokine Growth Factor Rev* 2005, **16**:35-53.

52. Brew K, Dinakarpandian, D., Nagase, H.: **Tissue inhibitors of metalloproteinases: evolution, structure and function**. *Biochim Biophys Acta* 2000, **1477**:267-283.

53. Duffy MJ, Maguire, T.M., Hill, A., McDermott, E., O'Higgins, N.: **Metalloproteinases: role in breast carcinogenesis, invasion, and metastasis**. *Br Cancer Res* 2000, **2**:252-257.

54. Blavier L, Lazaryev, A., Dorey, F., Shackleford, G.M., DeClerck, Y.A.: **Matrix metalloproteinases play an active role in Wnt1-induced mammary tumorigenesis**. *Cancer Res* 2006, **66**(5):2691-2699.

55. van der Flier A, Sonnenberg, A.: **Function and interactions of integrins**. *Cell Tissue Res* 2001, **305**:285-298.
56. Sloan EK, Anderson, R.L.: **Genes involved in breast cancer metastasis to bone**. *Cell Mol Life Sci* 2002, **59**:1491-1502.

Figure legends

Figure 1: Small interfering RNA decreases MUC1 levels in breast cancer cells. A. western blots of the MUC1 cytoplasmic tail (MUC1-CT) and extracellular domain (MUC1 excell) in luciferase siRNA or MUC1 siRNA treated MDA-MB-468 and BT-20 cells. Actin is shown as a loading control. **B.** flow cytometry analysis of the MUC1 extracellular domain in siRNA-treated MDA-MB-468 and BT-20 lines. Cells were analyzed at 24 hr intervals beginning 48 hr post-tranfection. The black line represents isotype control, the green luciferase siRNA, and the red MUC1 siRNA.

Figure 2: Transcription of genes involved in cancer is altered in response to MUC1 siRNA. Genes whose transcription was altered by at least 2-fold in MUC1 siRNA-treated cells as compared to control siRNA are shown. The average fold change is shown in parentheses after the gene name; for genes altered in both MDA-MB-468 and BT-20, these values reflect the average from both cell lines.

Figure 3: Western blot analysis confirms changes in protein levels after MUC1 siRNA. A. whole cell lysates were analyzed for the following proteins: c-Myc, total and active MEK1/2 (MEK1/2, pMEK1/2), total and active ERK1/2 (ERK1/2, dpERK1/2), total and active AKT (AKT, pAKT), and tubulin as a loading control. Optimal exposures for comparing luciferase siRNA and MUC1 siRNA-treated cells from the same parental line are shown. **B.** lysates from EGF-stimulated MDA-MB-468 and BT-20 cells were blotted for pMEK1/2, MUC1 extracellular domain, and actin as a loading control.

Figure 4: MUC1 siRNA affects cell death in response to stress in MDA-MB-468, but not BT-20 cells. A. basal apoptosis is shown as the combined total of early (PI^-/annexin V^+) and late (PI^+/annexin V^+) apoptotic populations. Results reflect the averages of three independent experiments. **B.** apoptosis after trypsinization 24 hr post-transfection. Representative flow cytometry results are shown for MDA-MB-468 and BT-20 cells transfected with siRNA. **C.** total cell death (sum of necrosis (PI^+/annexin V^-), and early and late apoptosis) is shown for MDA-MB-468 cells in response to a panel of cellular stresses (G418, trypsin, peroxide) and controls (control, DMSO). A representative experiment is shown. **D.** western blots for total and active AKT (AKT, pAKT) and actin loading control, performed on whole cell lysates from siRNA transfected cells. The same exposure is shown for both cell lines to show the relative levels of protein between lines, rather than optimal exposure times for comparison within a single cell line (shown in Figure 3A).
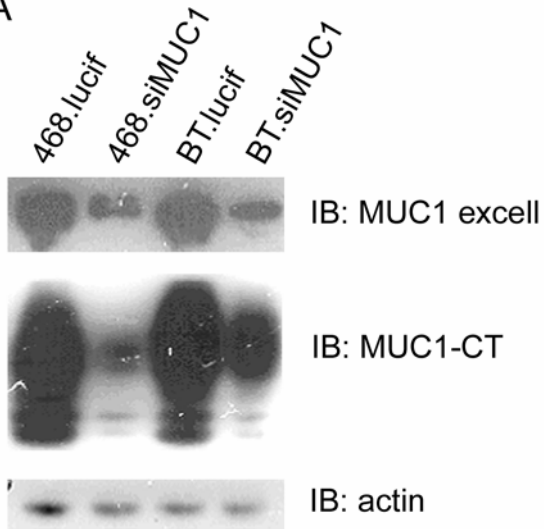
Figure 5: Proliferation is altered by MUC1 siRNA in both cell lines. A. [^{3}H]thymidine incorporation is shown by the level of radioactivity (cpm) emitted from cells after 24 hr incubation with radionucleotide. Results reflect the average of three independent experiments. *$p < 0.006$ as compared to luciferase siRNA-treated cells of the same line. **B.** flow cytometric analysis of BrdU incorporation. SiRNA-transfected cells were incubated with BrdU for 1.5 hr, and stained with a PE-conjugated antibody against BrdU. A representative experiment is shown. **C.** invasion of MDA-MB-468 cells in transwells plated with a panel of extracellular matrix proteins or no matrix (control). Representative results are shown as percent invasion, calculated

as: number of invaded cells / total number of cells * 100.

Figure 6: The MUC1 siRNA phenotype is rescued by stable transfection with MUC1. A.
MDA-MB-468 cells transfected with a full-length, siRNA-resistant MUC1 construct
(468.MUC1Δ8) or empty vector (468.Neo) were blotted for MUC1 extracellular and cytoplasmic
domains (MUC1 excell and MUC1-CT) and actin as a loading control. **B.** analysis of MUC1
levels by flow cytometry. SiRNA-transfected 468.Neo and 468.MUC1Δ8 cells were stained for
expression of the MUC1 extracellular domain 48 hr post-transfection. The black line represents
isotype control, the green luciferase siRNA, and the red MUC1 siRNA. **C.** flow cytometric
analysis of BrdU incorporation. SiRNA-transfected cells were incubated with BrdU for 1.5 hr,
and stained with a PE-conjugated antibody against BrdU. A representative experiment is shown.
D. total apoptosis is shown as the combined total of early (PI$^-$/annexin V$^+$) and late (PI$^+$/annexin
V$^+$) apoptotic populations for 468.Neo and 468.MUC1Δ8 cells trypsinized 24 hr post-
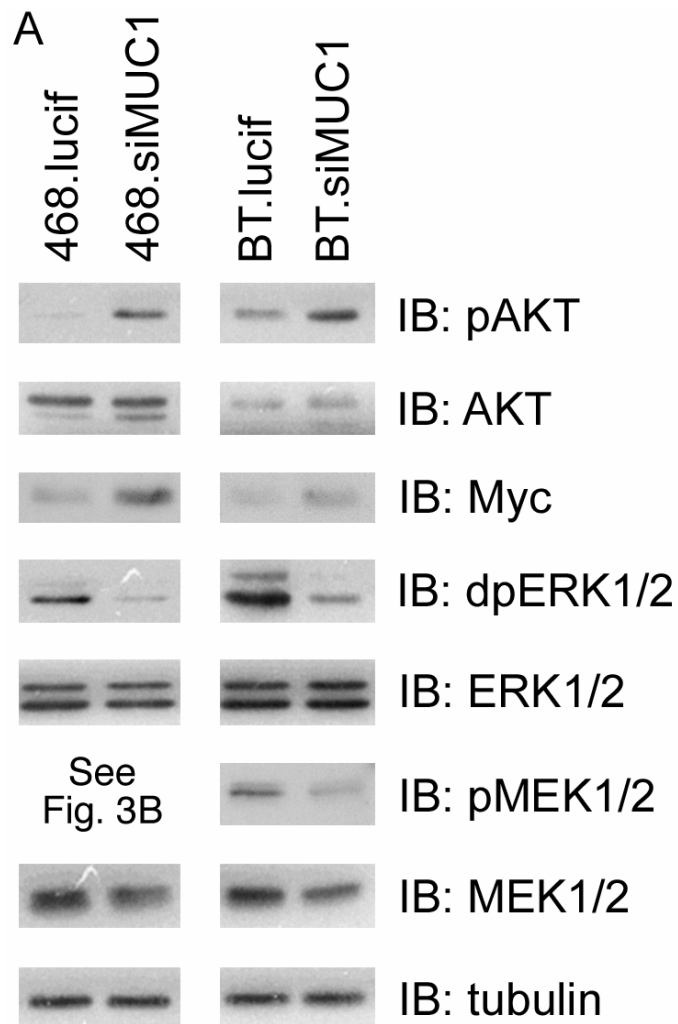transfection. A representative example is shown.

Figure 1

Figure 2

Figure 3

A

468.lucif 468.siMUC1 BT.lucif BT.siMUC1

IB: pAKT

IB: AKT

IB: Myc

IB: dpERK1/2

IB: ERK1/2

See
Fig. 3B   IB: pMEK1/2

IB: MEK1/2

IB: tubulin

B

486.
siLuc   486.
siMUC1   BT.
siLuc   BT.
siMUC1

EGF   −   +   −   +   −   +   −   +
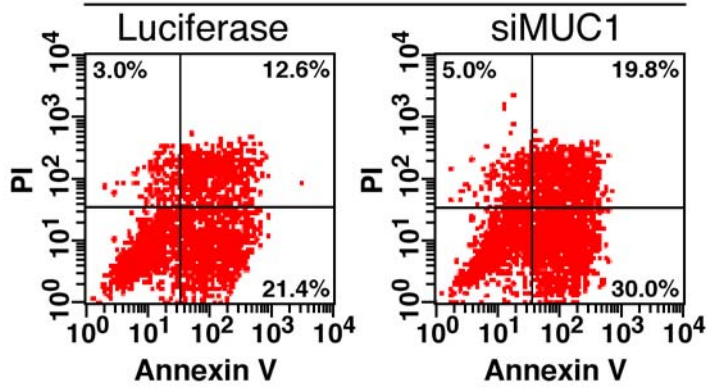
IB: pMEK 1/2

IB: MUC1

IB: β-actin
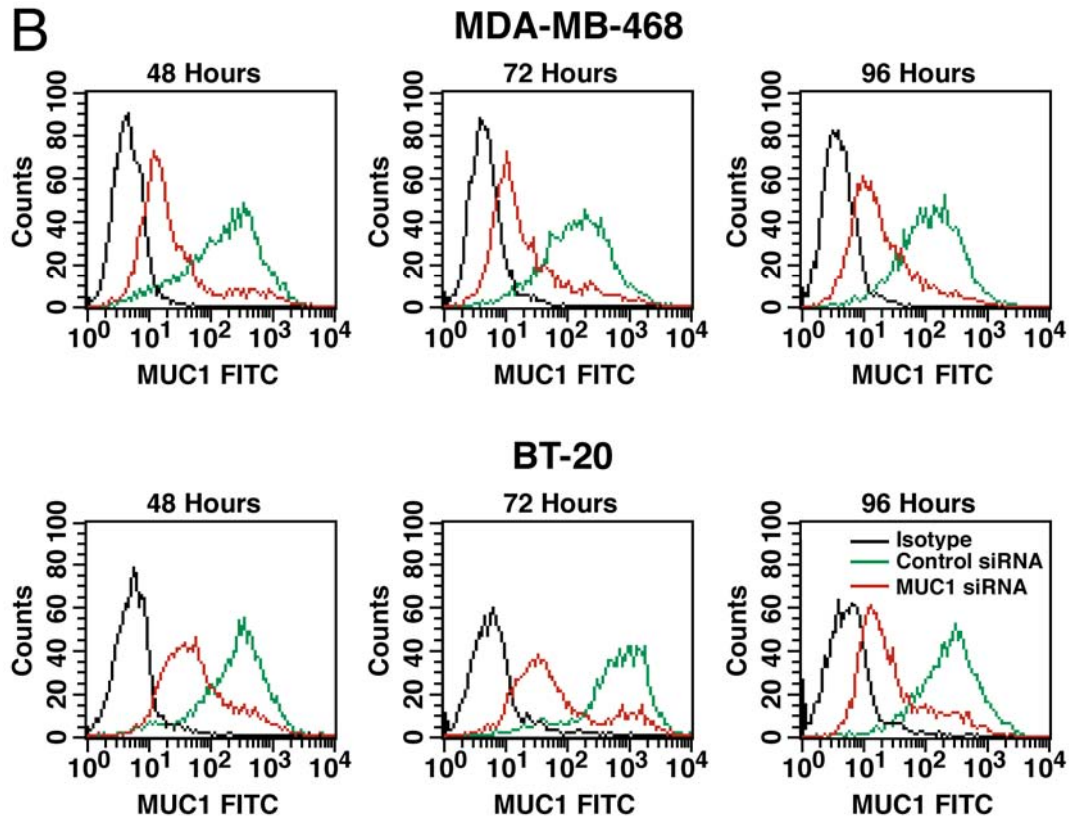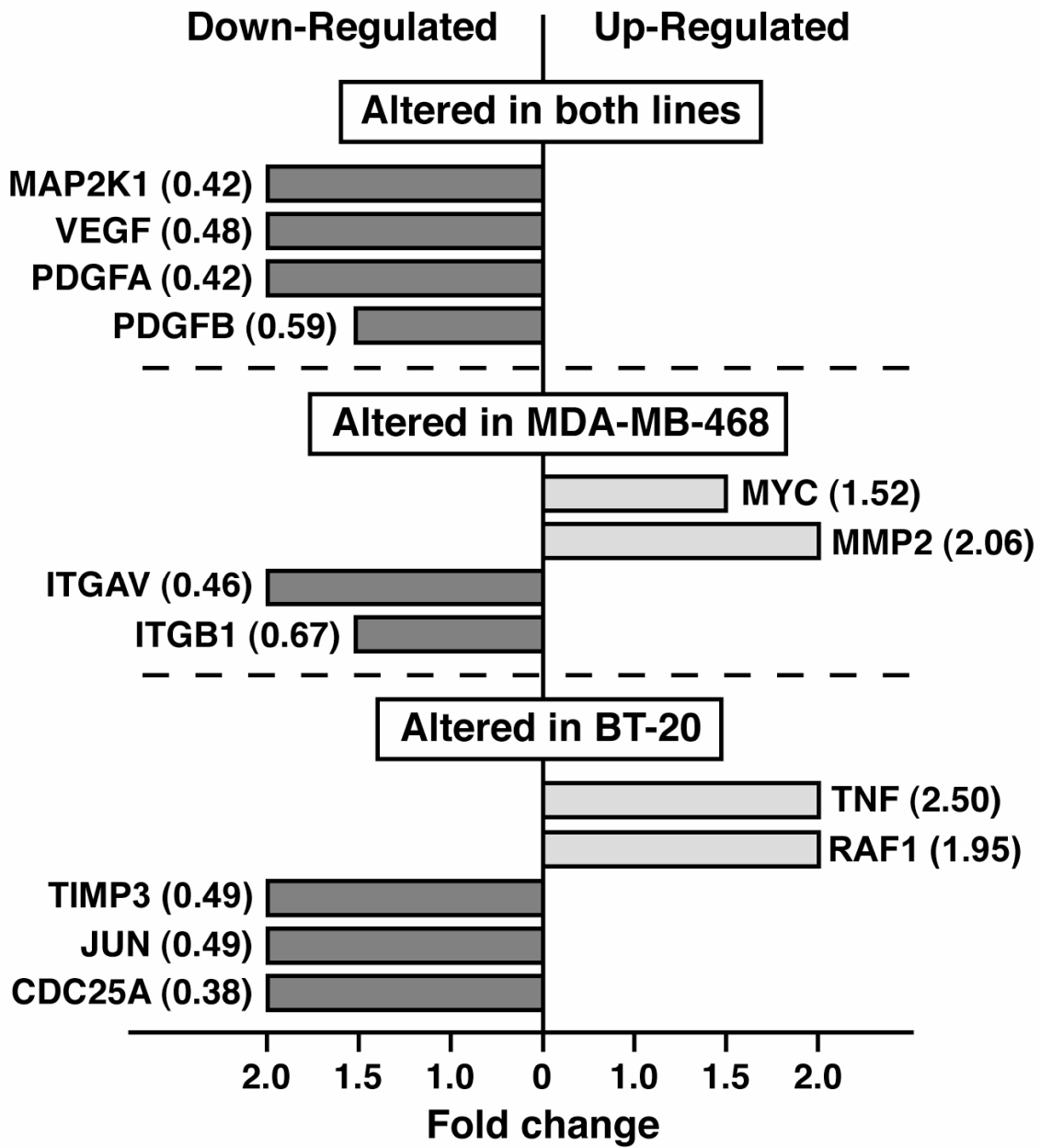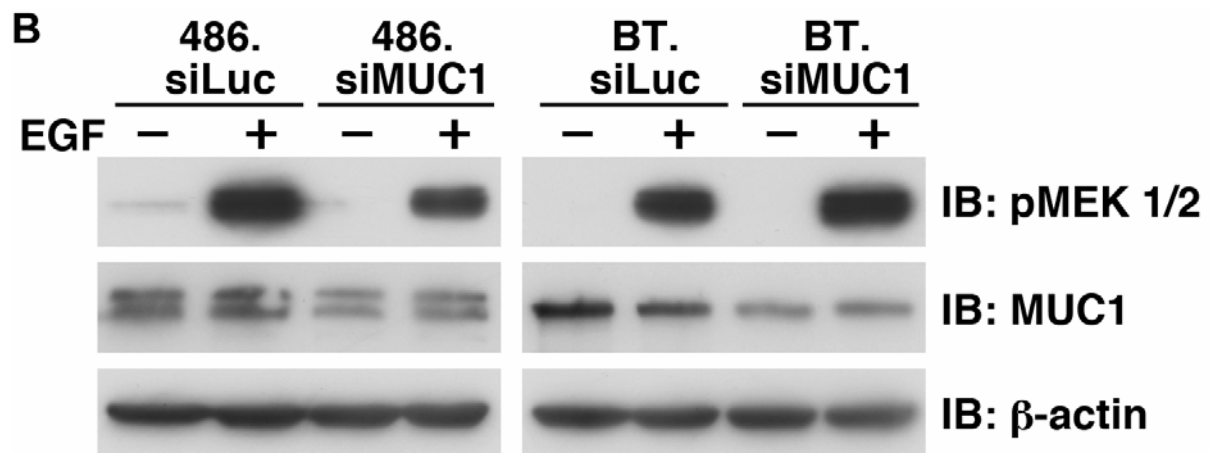
Figure 4

A

Basal apoptosis (total)
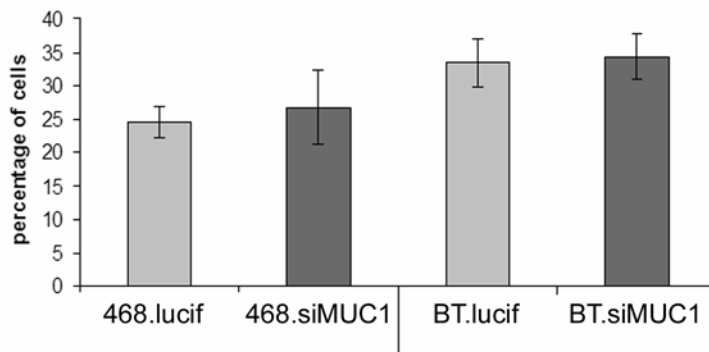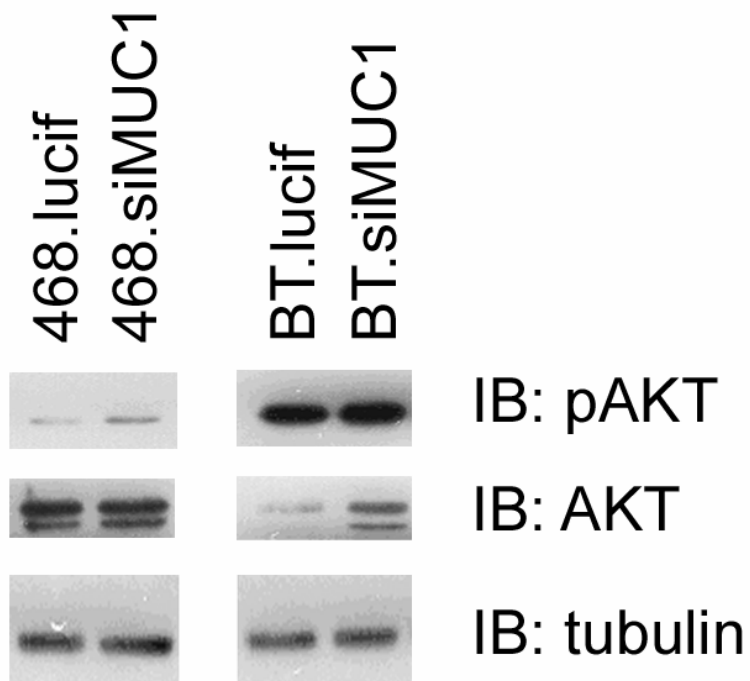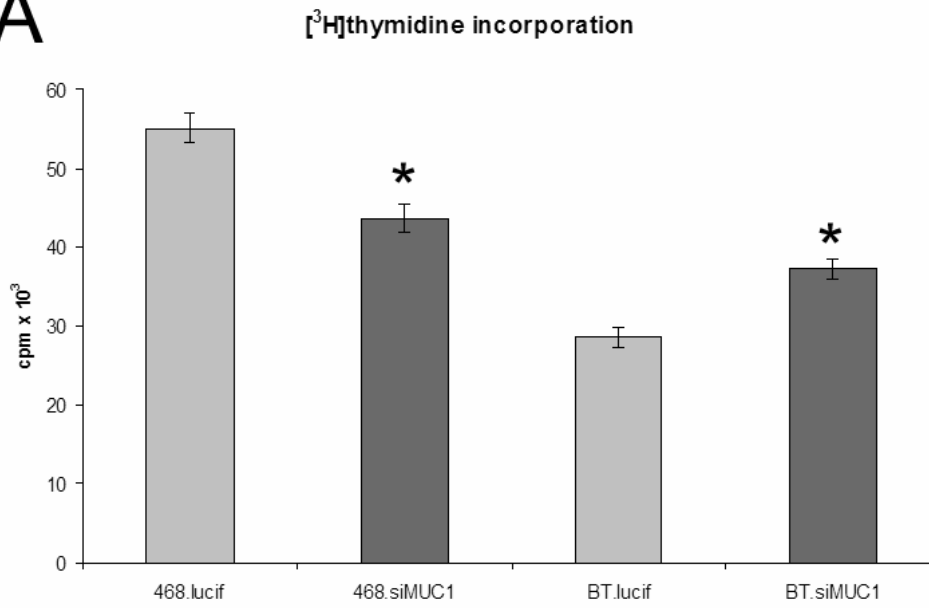

B

MDA-MB-468

BT-20

Figure 4 (cont'd)

C

Total cell death

468.lucif
468.siMUC1

D

468.lucif
468.siMUC1

BT.lucif
BT.siMUC1

IB: pAKT

IB: AKT

IB: tubulin

Figure 5

Figure 5 cont'd

B   BrdU incorporation
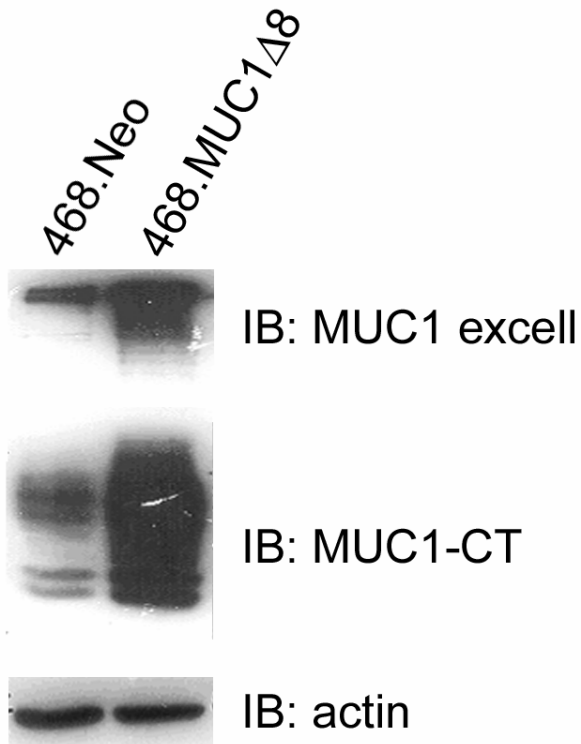

C   Cellular Invasion

Figure 6

A

IB: MUC1 excell
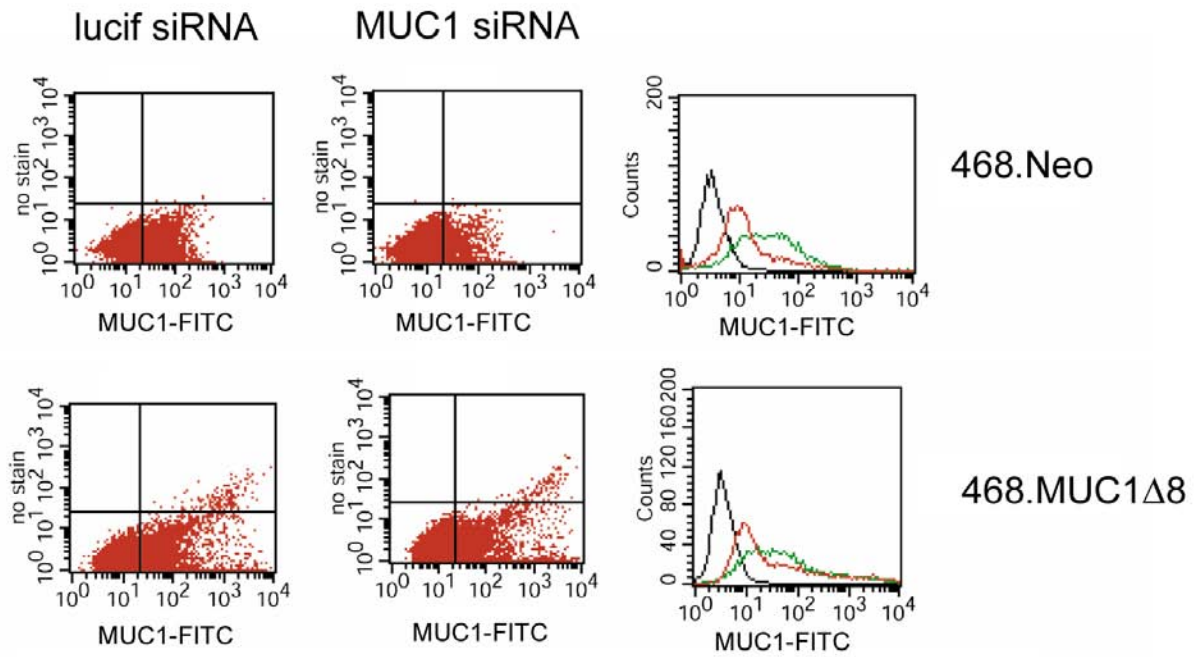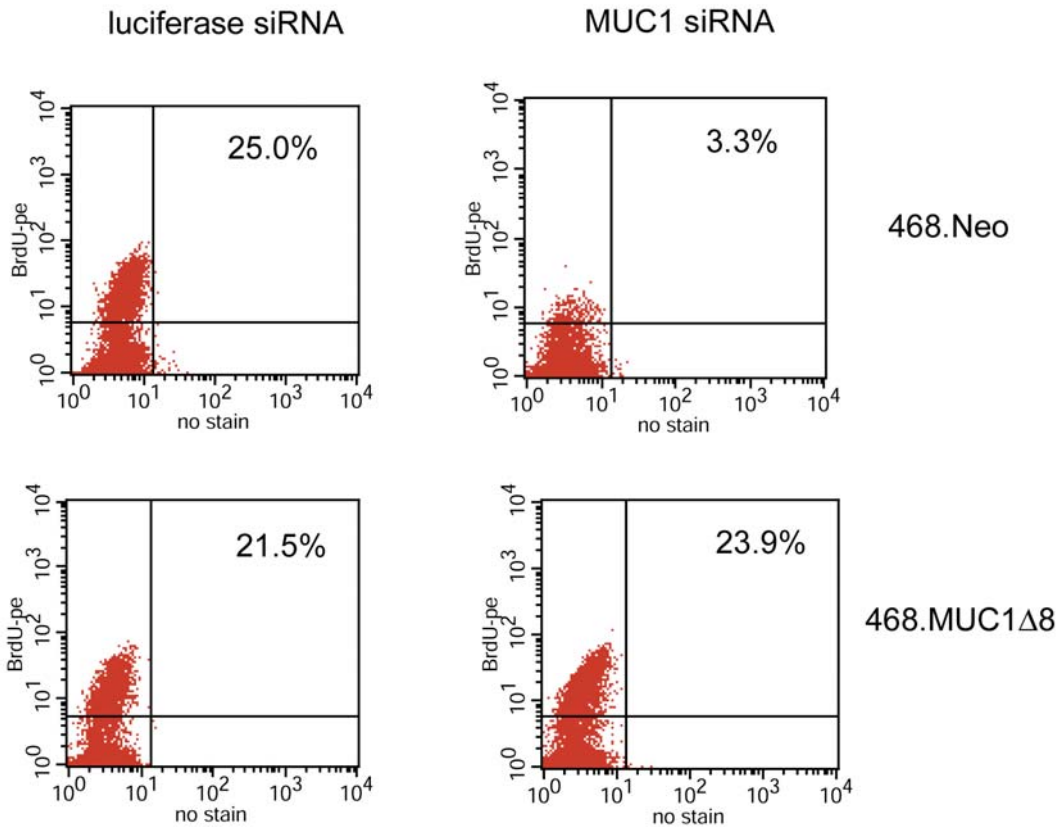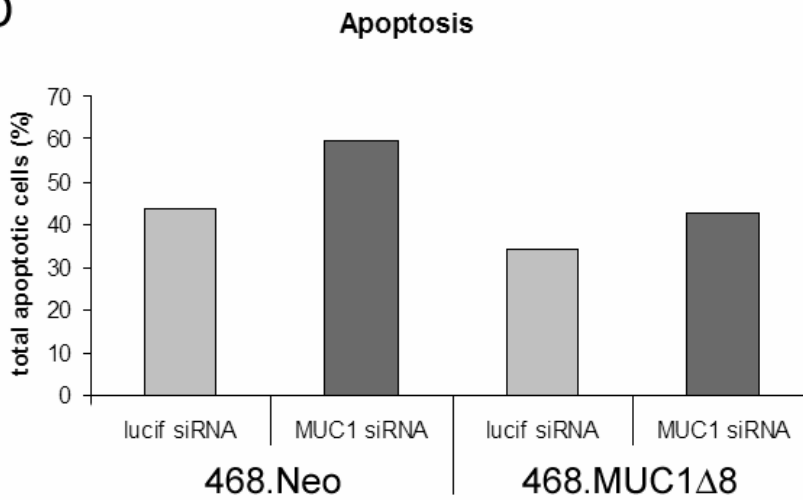
IB: MUC1-CT

IB: actin
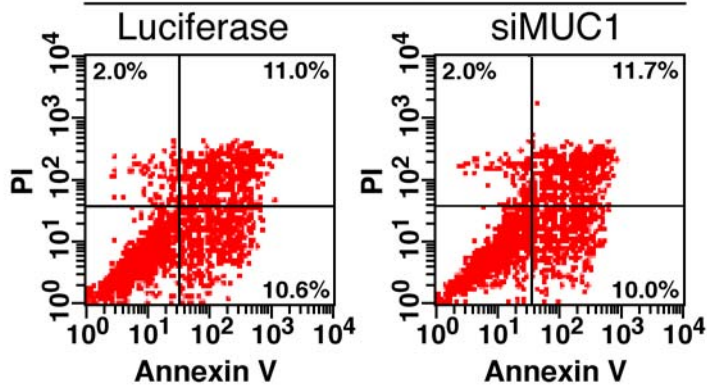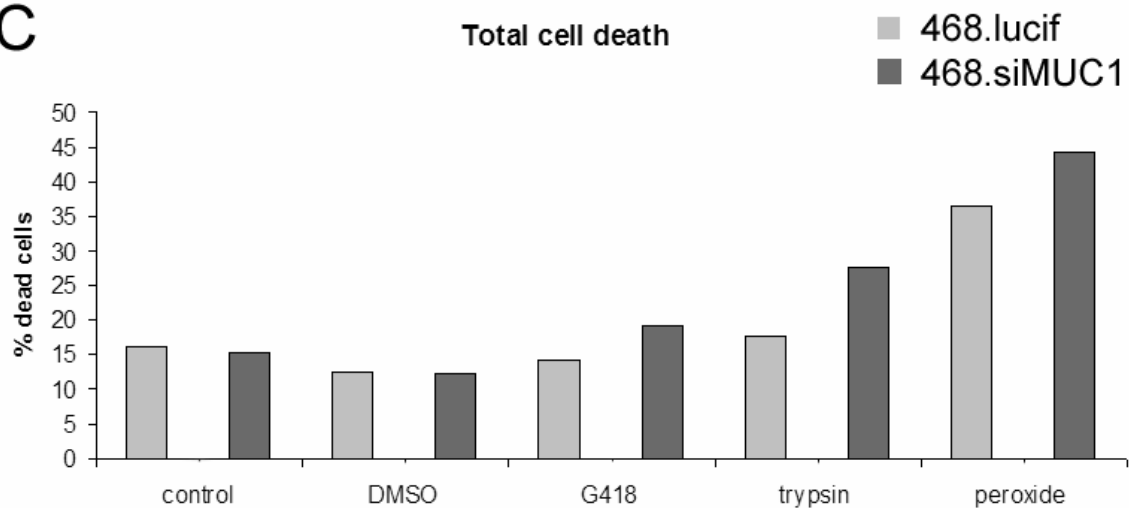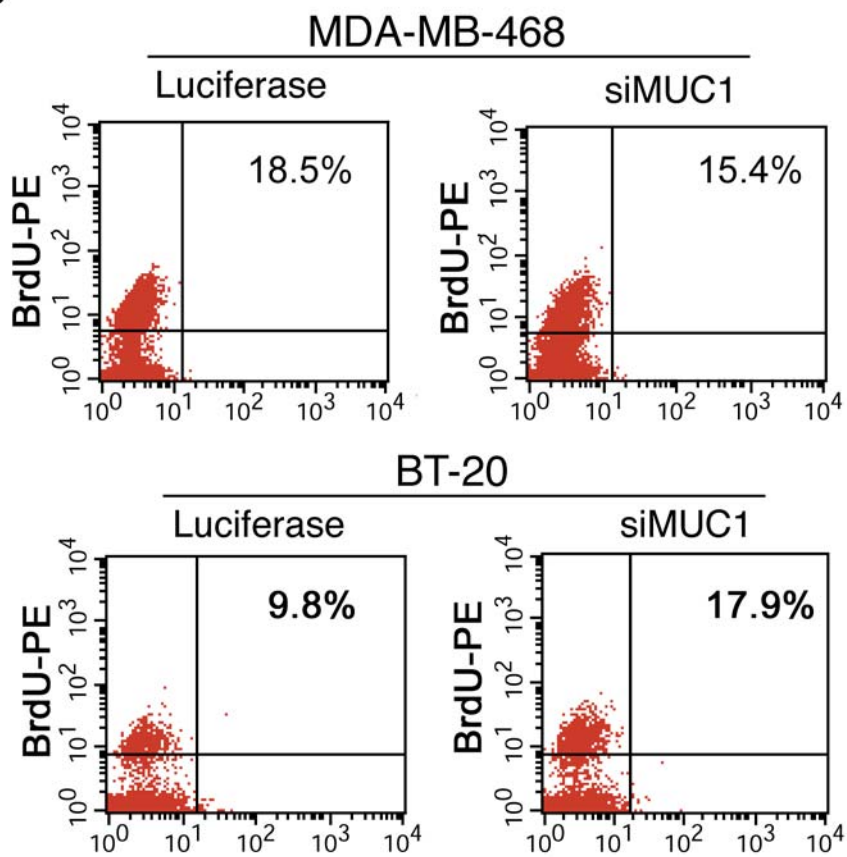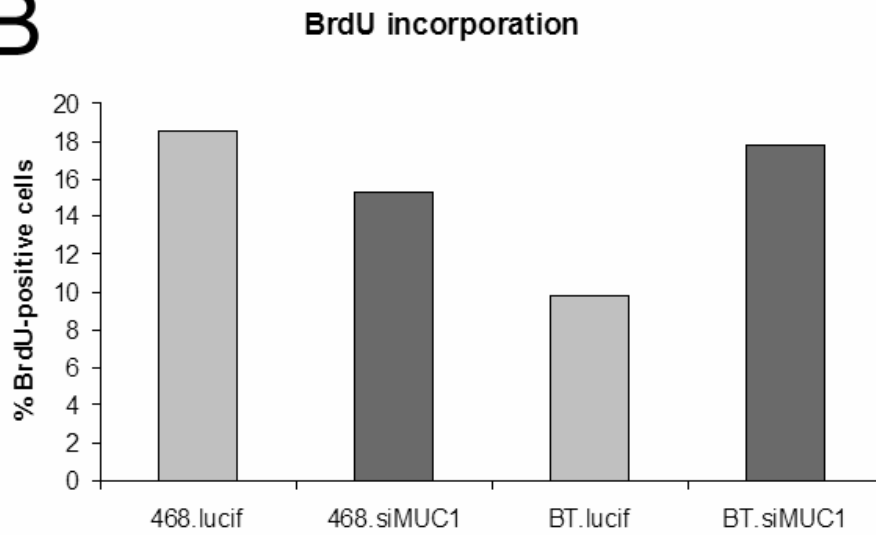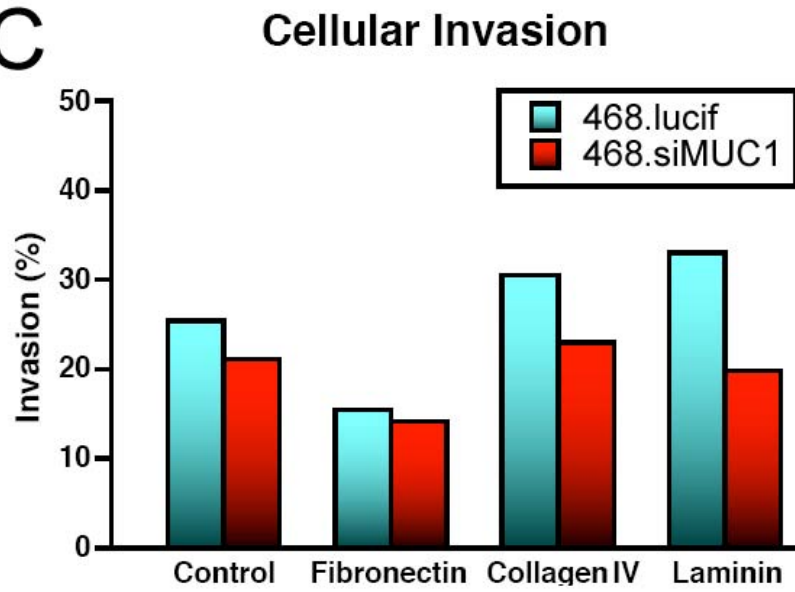
B

Figure 6 cont'd

C

D

APPENDIX II

TYROSINES IN THE MUC1 CYTOPLASMIC TAIL MODULATE TRANSCRIPTION VIA THE ERK1/2 AND NF-κB PATHWAYS

Eric J. Thompson[1, 2], Kandavel Shanmugam[1,3], Christine L. Hattrup[4], Kari L. Kotlarczyk[3], Albert Gutierrez[4], Judy M. Bradley[3], Pinku Mukherjee[3], Sandra J. Gendler[3,4].

From [3]Cancer Center Scottsdale and [4]Mayo Clinic College of Medicine, Mayo Clinic Arizona, Scottsdale, Arizona 85259

Running title: MUC1 tyrosines in transcription

[1] These authors contributed equally to this work. [2]Current address: AZ Biodesign Institute, Arizona State University, Tempe, AZ.

Address correspondence to Sandra J. Gendler, Johnson Research Building, Mayo Clinic Arizona, 13400 E. Shea Boulevard, Scottsdale, Arizona 85259, Tel. 480-301-7062, Fax 480-301-7017, E-mail gendler.sandra@mayo.edu

ABSTRACT

Much of the ability of the MUC1 oncoprotein to foster tumorigenesis and tumor progression likely originates from the interaction of its cytoplasmic tail with proteins involved in oncogenic signaling. Many of these interactions are regulated by phosphorylation, as the cytoplasmic tail contains seven highly conserved tyrosines as well as several serine/threonine phosphorylation sites. We have developed a cell line-based model system to study the effects of tyrosine phosphorylation on MUC1 signaling, with particular emphasis on its effects on gene transcription. COS-7 cells, which lack endogenous MUC1, were stably infected with wildtype MUC1 or a MUC1 construct lacking all seven tyrosines (MUC1 Y0) and analyzed for effects on transcription mediated by the extracellular signal regulated kinase (ERK1/2) and nuclear factor κB (NF-κB) pathways. COS.MUC1 Y0 cells showed heightened active ERK1/2 with increased AP-1 and Stat-3 transcriptional activity; there was also a simultaneous decrease in NF-κB transcriptional activity and nuclear localization. These changes altered the phenotype of COS.MUC1 Y0 cells, as this line displayed increased invasion and enhanced [^{3}H]thymidine incorporation. Analysis of the three lines also showed significant differences in their cell cycle profile and bromodeoxyuridine (BrdU) incorporation when the cells were serum-starved. These data support the growing evidence that MUC1 is involved in transcriptional regulation, and link MUC1 for the first time to the NF-κB pathway.

INTRODUCTION

MUC1 is a tumor antigen and oncoprotein that is overexpressed on a majority of tumors, including breast, pancreatic, ovarian, and colon cancers (1). MUC1 is a heterodimer consisting of a large, glycosylated extracellular domain, and a smaller subunit consisting of a short extracellular stem, the transmembrane sequence, and a 72-amino acid cytoplasmic tail (collectively called MUC1-CT)[2]. Though the reasons for its oncogenic activity remain unclear, much recent work has focused on the ability of this protein to interact with signaling molecules, primarily through the MUC1-CT. The MUC1-CT has multiple phosphorylation sites, including seven tyrosine residues, and associates with many kinases, including glycogen synthase kinase 3β (GSK 3β) (2), protein kinase Cδ (PKCδ) (3), c-Src (4, 5), and all four members of the ErbB family (6, 7). MUC1 interactions with other proteins can be regulated by phosphorylation: for example, MUC1-β-catenin binding is increased by c-Src, ErbB1 or PKCδ phosphorylation, but decreased by GSK 3β phosphorylation (4). Increased MUC1-β-catenin interaction after MUC1-CT phosphorylation led to decreased E-cadherin-β-catenin association and stimulated anchorage-independent growth, demonstrating a functional role for MUC1-CT phosphorylation. An additional argument for the importance of the MUC1-CT tyrosine residues is that six of the seven are 100% conserved in mammals (1, 8), likely reflecting an essential role for tyrosine phosphorylation in regulating MUC1-associated signaling. The overexpression, oncogenic activity, and phosphorylation-dependent interactions of MUC1 make the study of the role of MUC1 tyrosine phosphorylation of great importance.

Among the most interesting recent findings regarding MUC1 oncogenic activity are its presence in the nucleus and its ability to interact with and regulate transcription factors. MUC1 can interact with p53-responsive promoter elements, and can regulate transcription through binding to the p53 regulatory domain (9). In addition, the MUC1-CT can be found in the nucleus in association with β-catenin (10), and can alter transcription of a β-catenin-driven reporter construct in a manner depending on the presence of tyrosine 46 in the MUC1-CT (11). These studies support a role for MUC1 that was previously considered unlikely, if not impossible: involvement of a transmembrane glycoprotein—long thought to be involved only in steric modulation of adhesion—in transcriptional regulation in the nucleus.

These studies emphasize the importance of examining MUC1 in a new light: searching for novel signaling pathways that could be affected by MUC1, and seeking to clarify the role of MUC1 in pathways to which it has already been linked. One such signaling network is the extracellular signal regulated kinase (ERK1/2) pathway. Epidermal growth factor treatment of mouse mammary glands resulted in tyrosine phosphorylation of the MUC1-CT, which correlated with activation of ERK1/2 as seen by dual phosphorylation (dpERK1/2) (6). Cell culture studies show similar results, as both expression of a CD8/MUC1 chimera in MUC1 non-expressing cells (12) and binding of *Pseudomonas aeruginosa* to MUC1 on airway cells (13) increased dpERK1/2 levels. Interestingly, when the seven MUC1-CT tyrosine residues were mutated in this CD8/MUC1 chimera, endogenous dpERK1/2 levels decreased, and were not able to be stimulated by CD8 antibody treatment of the mutant chimera. Increased dpERK1/2 has been linked to enhanced proliferation and alterations in cell motility and invasive capacity, in part because it can alter gene expression via the signal transducer and activator of transcription 3 (Stat-3), the activator protein 1 (AP-1) complex, and other transcription factors (14). Stat-3 activity is increased in a wide variety of tumor types, including breast cancer, and is capable of stimulating proliferation while inhibiting apoptosis (15, 16). AP-1 is a heterodimeric transcription factor comprised of c-Fos, c-Jun, or other related proteins. Though the specific targets of AP-1 depend on the composition of the heterodimer, in general, AP-1 transcription is thought to signal for increased invasive capacity, proliferation and cellular survival (17).

The involvement of MUC1 in pro-survival signaling is not surprising, considering that MUC1 has long been thought to play a role in protecting epithelial layers and enhancing epithelial cell survival (1). Mice lacking Muc1 show little or no phenotype when housed in a pathogen-free environment, but develop chronic reproductive tract infections when housed in non-sterile conditions (18). Exposure of cultured cells to inflammatory cytokines can upregulate MUC1 expression, indicating that increased MUC1 levels

may be an important part of cellular stress responses (19). MUC1 has also been linked to decreased apoptosis in response to oxidative stress and genotoxic agents (20), for example by suppressing p53-responsive gene targets. An additional mechanism by which MUC1 could affect cellular stress response is through modulation of the NF-κB pathway. NF-κB is a heterodimeric transcription factor comprised of a variety of subunits from the Rel family of proteins (21). It is heavily involved in regulating response to cellular stress, typically through increased transcription of pro-inflammatory and anti-apoptotic targets. Classical regulation of NF-κB occurs largely through controlling its cellular localization: when inactive, NF-κB is sequestered in the cytoplasm by IκB (inhibitors of NF-κB) proteins. Phosphorylation of IκB by the IKK (IκB kinases) complex causes degradation of IκB, thus releasing NF-κB to enter the nucleus and affect transcription of a variety of gene targets. Given the importance of phosphorylation in this network, it is likely that other proteins involved in affecting NF-κB activity will also show phosphorylation-dependent regulation.

This report describes a model for studying the importance of MUC1-CT tyrosine-based signaling, using a non-tumor-derived cell line to clarify the regulation of MUC1 in cells lacking tumor-associated genetic and epigenetic changes. Expression of wildtype MUC1 (MUC1 WT) and a mutant lacking the seven cytoplasmic tail tyrosine residues (MUC1 Y0) in COS-7 cells showed striking differences in transcriptional regulation, leading to alterations in invasion and [^{3}H]thymidine incorporation. Our results confirm that MUC1 can modulate the activity of ERK1/2 and its downstream target, AP-1. Interestingly, the MUC1 Y0 mutant is far more potent than MUC1 WT in activating the ERK1/2 pathway, suggesting the presence of previously undetected, tyrosine-dependent interactions between MUC1 and negative regulators of this pathway. In addition, we describe for the first time the ability of MUC1 to alter NF-κB-responsive transcription, adding yet another important pathway to the growing list of signaling networks affected by the MUC1 oncoprotein.

RESULTS

Recent studies have shown that MUC1 is capable of regulating transcription, which may in part explain the effect of MUC1 on events involved in oncogenesis. In order to study the importance of MUC1-CT tyrosine phosphorylation in this setting, COS-7 cells were infected with constructs expressing MUC1 WT or the MUC1 Y0 mutant where all seven tyrosine residues in the MUC1-CT were changed to phenylalanine (Fig. 1*A*). Empty vector infection (COS.Neo) was used as a control. The COS-7 line was chosen because it does not express endogenous MUC1; it is important to note that though this line was immortalized with SV40 T antigen, it was derived from normal kidney cells and therefore lacks many of the genetic and epigenetic alterations that occur in tumor-derived cells. Expression of MUC1 was confirmed by western blots using an antibody directed against the MUC1-CT (Fig. 1*B*), while proper surface localization of both MUC1 constructs was seen by flow cytometry on non-permeabilized cells (Fig. 1*C*). Note that the cytoplasmic tail of MUC1 Y0 shows a shift in electrophoretic mobility relative to MUC1 WT; this likely reflects a decrease in phosphorylation due to mutation of the tyrosine residues. Several bands appear in the blot for the MUC1-CT, which are thought to represent differentially glycosylated forms of this subunit.

Given that the MUC1-CT can be tyrosine phosphorylated in cells expressing endogenous MUC1, we analyzed whether this is also true of the transfected protein. Immunoprecipitations for MUC1 from all three cell lines (Fig. 1*D*) were blotted for phosphotyrosine and the MUC1-CT. Only COS.MUC1 WT cells exhibit a phosphotyrosine band that overlaps with the MUC1-CT; as expected, COS.MUC1 Y0 cells show no phosphotyrosine while COS.Neo cells display neither MUC1 nor phosphotyrosine at this size. The faint phosphotyrosine band seen in all lanes is most likely immunoglobulin light chain, which runs slightly above the MUC1-CT. Immunoprecipitations with hamster pre-immune serum were used as controls.

Much work done in tumor-derived cell lines and in mouse tumor models points to a link between MUC1 and the ERK1/2 kinases. We therefore examined the consequences of MUC1 WT and MUC1 Y0 expression on these proteins and their downstream effectors. Western blots for dpERK1/2 (Fig. 2*A*) show

a mild increase in ERK1/2 activation in COS.MUC1 WT cells relative to COS.Neo, as is expected based on previous reports (6, 22). Surprisingly, COS.MUC1 Y0 cells display a substantial increase in dpERK1/2 levels compared to either of the other two cell lines. ERK 2 (p42) appears to be activated more strongly than ERK1 (p44) by expression of either MUC1 WT or MUC1 Y0. ERK1/2 total protein levels are consistent across all three cell lines. This increase in dpERK1/2 is serum-dependent, but not responsive to epidermal growth factor treatment, as these cell lines show identical dpERK1/2 levels with this treatment (data not shown). To confirm that the increase in dpERK1/2 corresponds to enhanced transcriptional activity of ERK1/2 effectors, COS.Neo, COS.MUC1 WT, and COS.MUC1 Y0 cells were transiently transfected with a reporter construct containing the luciferase gene driven by six tandem AP-1 consensus DNA binding sites. Though there is little difference in AP-1 activity between COS.Neo and COS.MUC1 WT, the COS.MUC1 Y0 line have a 4- to 5-fold increase in AP-1 activity (Fig. 2*B*), corroborating the striking increase in dpERK1/2 in these cells. A second factor which can mediate transcription downstream of ERK1/2 is Stat-3. Transcription of a Stat-3-responsive reporter was also increased in COS.MUC1 Y0 cells as compared to COS.MUC1 WT and COS.Neo (Fig. 2*C*).

Given the important role of the ERK1/2 pathway in cellular proliferation and survival, we examined the effect of MUC1 WT and MUC1 Y0 expression on other proteins involved in these events. No differences were seen in levels of p53, p21, or p27 in the COS-derived cell lines (data not shown), likely excluding MUC1 regulation of p53 as an important pathway in these cells. In contrast, a luciferase reporter responsive to NF-κB indicated that MUC1 Y0 expression may alter basal NF-κB transcription activity. COS.MUC1 WT cells show no significant change in NF-κB activity compared to COS.Neo (Fig. 3*A*). Activity of NF-κB in COS.MUC1 Y0 cells, however, is at approximately one-fifth the level seen in the other two cell lines, indicating that mutation of the MUC1-CT tyrosine residues has a negative influence on NF-κB-mediated transcription. Reverse transcriptase-PCR array analysis of an NF-κB target gene, interleukin-8, showed greatly reduced transcription in COS.MUC1 Y0 cells as compared to the other lines (data not shown). To corroborate these data, we analyzed nuclear localization of the p65 subunit of NF-κB under steady-state conditions. As expected, basal levels of nuclear p65 are relatively low in all three cell lines, but there is significantly less nuclear p65 in the COS.MUC1 Y0 cells as compared to COS.Neo or COS.MUC1 WT (Fig. 3*B*, *C*).

With the striking differences seen in AP-1 and NF-κB transcriptional activity, we wanted to examine cellular events tied to these pathways. Given that AP-1 transcription is capable of increasing the invasive potential of cells, and that a previous report showed that MUC1-derived peptides could stimulate invasion (23), this phenomenon was examined using a standard transwell assay. Serum-starved cells were plated on top of Matrigel, with medium containing 10% serum in the lower chamber as an attractant. Not surprisingly based on the transcriptional profile, there was little change seen in COS.MUC1 WT cells as compared to COS.Neo (Fig. 4). However, a striking increase in invasion was seen in COS.MUC1 Y0 cells relative to the other lines, with approximately 80% of COS.MUC1 Y0 cells successfully invading into the matrix.

We next studied the effect of MUC1 WT and MUC1 Y0 expression on proliferation and survival. [^{3}H]thymidine incorporation assays revealed a 10- to 20-fold increase in nucleotide incorporation in the COS.MUC1 Y0 line compared to COS.Neo and COS.MUC1 WT (Fig. 5*A*). This result would seem to reflect a substantial gain in proliferation in response to MUC1 Y0 expression. However, growth curves obtained for all three lines showed only slightly higher cell counts in the COS.MUC1 Y0 line, with no difference seen until the seventh day in culture (Fig. 5*B*). The disparity between these results is not due to increased cell death, as baseline apoptosis was not higher in the COS.MUC1 Y0 cells as compared to the other two lines (data not shown). Cell cycle analysis indicated a decrease in the percentage of COS.MUC1 Y0 cells in G0/G1 phase, with a simultaneous increase in the percentage of cells in G2/M (Fig. 5*C*). No significant differences in cell cycle profile exist between the COS.Neo and COS.MUC1 WT lines.

To examine these results, we studied bromodeoxyuridine (BrdU) incorporation in these cells, either in the presence of serum or after 24 hours serum starvation. BrdU is incorporated into DNA both during

DNA synthesis and in other processes such as DNA repair. COS.Neo, COS.MUC1 WT, and COS.MUC1 Y0 show little difference in BrdU incorporation when maintained in normal growth medium (data not shown). However, after 24 hours serum starvation, there is an approximately two-fold difference in BrdU incorporation in the COS.MUC1 Y0 cells as compared to the other cell lines (Fig. 6*A*). Quantification of BrdU-positive nuclei confirms statistical significance of these results (Fig. 6*B*).

DISCUSSION

Though it has long been known that MUC1 is highly overexpressed in a wide range of tumors, it is only very recently that some of the effects of MUC1 upregulation have come to be understood. MUC1 levels and MUC1-CT tyrosine phosphorylation have been linked to ERK1/2 activity in mice (6), while phopsphorylation of the MUC1-CT by Src, ErbB1 or PKCδ regulates its association with proteins such as β-catenin and GSK 3β in cell lines (3, 4, 7). PKCδ-mediated phosphorylation of MUC1 led to anchorage-independent cell growth, which likely resulted from decreased association of β-catenin with E-cadherin upon MUC1-CT phosphorylation. Despite these studies, however, it remains unclear what the functional consequences of MUC-CT tyrosine phosphorylation are. Similarly, it is unknown whether all seven MUC1-CT tyrosine residues are phosphorylated, or which of the residues is most important for MUC1-related signaling. These studies were designed to examine both transcriptional activity and cell behavior in response to exogenous expression of MUC1 WT, which shows constitutive tyrosine phosphorylation in this system, as compared to the tyrosine-lacking mutant MUC1 Y0.

Interestingly, the COS-7-derived cell lines appear to show differential regulation of MUC1 as compared to many other models. Given previous reports, we expected that MUC1 WT would result in increased ERK1/2 activity, leading to increased proliferation and invasion. We also expected that mutation of the MUC1-CT tyrosine residues would diminish or abrogate these effects. There are several possible reasons to explain why our data disagree with expectations. First, it is important to note that prior studies (e.g., (6, 12)) were performed largely in cancer-derived or embryonic cell lines, or in mouse tumor models. COS-7 cells are SV40-immortalized derivatives of normal adult kidney fibroblasts and would therefore lack many of the genetic and epigenetic alterations that accompany oncogenesis. COS-7 cells are not normal, but the results seen in this line may more accurately reflect the role of MUC1 in non-tumor-derived systems, although the possibility exists that SV40 T antigen may affect MUC1-related signaling. Second, COS-7 cells are derived from male green monkey kidney, so species- or cell type-specific regulation could be involved. Finally, our studies use the entire MUC1 molecule, in contrast to other reports examining chimeric MUC1 proteins. One such study in COS-7 cells noted that anti-CD8 stimulation of the CD8/MUC1 chimera activated ERK2 through the Ras pathway (22), supporting our finding that MUC1 is linked to this pathway in these cells. Though such chimerae are useful for studying alterations in the MUC1-CT after extracellular stimulation, it is not clear whether this accurately represents the behavior of intact MUC1, making study of the entire molecule very important.

Many of the interactions attributed to MUC1 involve phosphorylation of the MUC1-CT. The fact that mutation of the tyrosine residues in the MUC1 Y0 construct does not cause the expected decrease in survival or invasion likely reflects a unique advantage of the COS-7 model system that has been lost or masked in tumor-based models. Specifically, the MUC1-CT tyrosine residues may in fact be involved in one or more previously uncharacterized interactions with inhibitory factors that cannot associate with the MUC1 Y0 mutant. Examples of such factors could include phosphatases or proteins capable of mislocalizing MUC1 or its signaling partners. In normal or close-to-normal cells, these inhibitory factors could downregulate the potentially oncogenic signals associated with MUC1 expression, which would explain the failure of the COS.MUC1 WT cell line to show altered transcription via the ERK1/2 or NF-κB pathways. Lacking tyrosine residues, MUC1 Y0 would not face inhibition and could therefore stimulate survival and invasion using pathways that do not require MUC1 tyrosine phosphorylation. As tyrosine-dependent inhibition of MUC1 signaling has not been described in other models, the factor(s) responsible may be decreased in tumor-based systems, or may be prevented from interacting with the MUC1-CT due to altered signaling or competition with other MUC1-binding proteins.

In agreement with this idea, COS.MUC1 Y0 cells show a dramatic enhancement of ERK1/2 phosphorylation and activity of the Stat-3 and AP-1 transcription factors, which could contribute to the increased invasion seen in this cell line. ERK1/2 activity can alter several pathways capable of driving tumor progression, including transcription of invasion-stimulating molecules like matrix metalloproteinases (14). MUC1 expression has been linked to increased ERK activity before, though the mechanism by which this occurs remains unexplored. *P. aeruginosa* binding to MUC1 in airway cells (13) and antibody stimulation of a CD8-MUC1-CT chimera in embryonic cells (12) activated ERK1/2 downstream of MUC1. Similarly, we have shown that overexpression of human MUC1 in the mouse mammary gland results in increased dpErk1/2 as compared to wildtype or Muc1-null glands (6). Note that these studies saw the most striking increase in ERK1/2 activation after stimulation, whereas this report shows alteration only in baseline dpERK1/2. The identical responses of the COS-7-derived cell lines after epidermal growth factor stimulation supports the idea that these cells show regulation of MUC1 that was not characterized in previous studies, as several groups have shown that MUC1 tyrosine phosphorylation is important in this pathway (6, 7). The ability of MUC1 Y0, but not MUC1 WT, to stimulate ERK1/2 signaling in COS-7 cells could reflect a tyrosine-dependent interaction of MUC1 with proteins involved in inhibiting ERK1/2 activity, such as the dual-specificity phosphatases capable of inactivating dpERK1/2.

The increased ERK1/2 activity in COS.MUC1 Y0 cells would suggest that the sharp rise in [^{3}H]thymidine incorporation in this line should correspond to enhanced proliferation. It is intriguing that the growth curves do not reflect a significant increase in proliferation in COS.MUC1 Y0 cells as compared to the other two lines. Routine passaging in cell culture also indicates similar growth rates between the three cell lines. The [^{3}H]thymidine must therefore be involved in non-proliferative pathways, such as DNA repair or synthesis of DNA that is not associated with cell division (e.g., endoreduplication, telomere synthesis or incorporation into the mitochondrial genome). Some light is shed on this riddle by the results of the BrdU incorporation studies. Given that COS-7 cells cycle quite rapidly, the majority of BrdU incorporation in the presence of serum is likely due to DNA synthesis. It is therefore not surprising that the three lines showed little difference in BrdU incorporation in normal growth medium. However, as the rate of proliferation slows after serum removal, other causes for BrdU incorporation are more likely to be visible. The increased incorporation of both [^{3}H]thymidine and BrdU in COS.MUC1 Y0 may therefore reflect higher levels of DNA repair in these cells. This might explain the change in the cell cycle profile of the COS.MUC1 Y0 line: the apparent accumulation of cells in G2/M could reflect a repair-related checkpoint that prevents these cells from completing mitosis, which would therefore clarify the failure of this line to proliferate more rapidly than the other two. If so, this would be the first study to suggest a connection between MUC1 and genomic repair mechanisms. Studies are ongoing to confirm that the altered nucleotide incorporation does indeed reflect an involvement in DNA repair.

This is also the first report to correlate MUC1 expression with regulation of NF-κB activity. Though preliminary, it appears that MUC1 can alter NF-κB-responsive reporter activity, p65 nuclear localization, and transcription of an endogenous target gene, interleukin-8. It is not yet clear what role MUC1 plays in this pathway, but there are at least two mechanisms by which it could be proposed to affect NF-κB activity and localization. First, MUC1 could modulate association of proteins within this pathway, either by directly influencing NF-κB itself or its regulatory proteins. MUC1 could interact with members of the IKK or IκB families to alter their regulation of NF-κB localization, for example. Second, MUC1 could directly affect NF-κB localization by changing its rate of transport through the nuclear pore complex. Though the MUC1-CT lacks a nuclear localization signal (NLS), binding to NF-κB could allow it to alter the accessibility of the NF-κB NLS. If the MUC1-CT is not tyrosine phosphorylated, as is the case with MUC1 Y0, it could mask the NF-κB NLS directly or cause a conformational change in NF-κB that hides the NLS. Phosphorylation of the MUC1-CT could then release this masking effect or cause a different conformational change that reveals the NF-κB NLS, thus facilitating transport into the nucleus. Studies are ongoing to clarify the role of MUC1 in NF-κB signaling.

The finding that mutation of the MUC1-CT tyrosine residues affects basal NF-κB activity indicates for the first time that MUC1 can influence this important cellular pathway. In addition to this novel result, we confirm previous reports showing that MUC1 regulates the ERK1/2 pathway, and present evidence that MUC1 can alter AP-1 mediated transcription. These data suggest that MUC1 tyrosine phosphorylation may be involved in previously uncharacterized negative regulatory interactions that dampen ERK1/2 activity. Finally, our results also hint at a role for MUC1 in regulating DNA repair, though confirmation of this phenomenon is still in progress. The possible significance of the effect of MUC1 on the ERK1/2 and NF-κB pathways is apparent, as these networks are tied to a multitude of cellular events important for tumorigenesis and metastasis. Further study of the influence of tyrosine phosphorylation on the MUC1 oncoprotein will likely clarify its important role in tumor formation and progression.

MATERIALS AND METHODS

Cloning of MUC1 WT and MUC1 Y0 vectors - MUC1 Y0 was created using the QuickChange mutagenesis kit (Stratagene, La Jolla, CA). Briefly, primers based on the MUC1 sequence were designed containing single-base alterations resulting in mutation of the cytoplasmic tail tyrosine residues to phenylalanine. Successful mutation was confirmed with DNA sequencing. MUC1 Y0 and MUC1 WT were cloned into the pLNCX.1 vector for retroviral infection.

Cell culture and retroviral infection - COS-7 cells (American Type Culture Collection, Manassas, VA) were maintained in Dulbecco's Modified Eagle's Medium (Invitrogen, Carlsbad, CA) supplemented with 10% fetal calf serum, 1% Glutamax (Invitrogen, Carlsbad, CA) and 1% penicillin/streptomycin. Cell counts were performed every 24 hours after plating, with three wells of each line counted in triplicate (i.e., a total of nine counts per line each day). For retroviral infection, GP2-293 packaging cells (stably expressing the *gag* and *pol* proteins) were co-transfected with the appropriate MUC1 construct and a vector expressing the VSV-G envelope protein. After 48 hours, medium was removed from the transfected packaging cells and cleared of debris by centrifugation at 3000 rpm. Virus was pelleted from the cleared medium; this was resuspended in growth medium containing 8 μg/ml polybrene (hexadimethrine bromide) and incubated overnight with COS-7 cells that had been pre-treated for 2-3 hours with polybrene. COS-7 cells were selected with 0.5 mg/ml G418, beginning 48 hours post-infection. For phosphotyrosine analysis, cells were treated for 30 min prior to lysis with 200 nM sodium orthovanadate (24).

Western blots, immunoprecipitations, and antibodies - Briefly, cells were lysed in HEPES buffer (20 mM HEPES, 150 mM sodium chloride, 1% Triton X-100, 2 mM EDTA) containing protease (Complete inhibitor cocktail, Roche, Indianapolis, IN) and phosphatase inhibitors (10 mM sodium fluoride, 2 mM sodium vanadate, 50 μM ammonium molybdate). Protein concentration was determined by BCA assay (Pierce, Rockford, IL) and equal quantities of lysate were loaded on SDS-PAGE gels. For immunoprecipitation, 1 mg of protein was incubated with an antibody specific to MUC1 or pre-immune serum in TNEN buffer (50 mM Tris, 150 mM NaCl, 1 mM EDTA, 0.5% NP-40, pH 7.4). Antibody complexes were captured with rProtein G agarose beads (Pierce, Rockford, IL) and eluted in 2X reducing sample buffer for loading onto gels. The MUC1 cytoplasmic tail antibody, CT2, was made in-house by the Mayo Clinic Arizona Immunology Core (6). Antibodies to phosphotyrosine (BD Biosciences, San Jose, CA), ERK1/2 (Cell Signaling, Danvers, MA), NF-κB (Santa Cruz Biotechnology, Santa Cruz, CA) and dpERK1/2 (Sigma, St. Louis, MO) were used according to manufacturer's recommendations. FACS analysis of MUC1 was performed with a FITC-conjugated antibody (HMPV) that recognizes an epitope in the extracellular domain of MUC1 (Pharmingen, San Jose, CA).

Flow cytometry - Staining for MUC1 surface localization was performed on cells that were trypsinized, but not permeabilized. For cell cycle analysis, cells were serum starved 24 hours, then fixed in -20 °C ethanol, treated with RNase A to remove RNA, and stained with propidium iodide (1 mg/ml in 0.1% sodium citrate). Flow cytometry for all assays was done on a FACScan flow cytometer. Cell cycle data were analyzed using the ModFit software program.

Immunocytochemistry - Cells were plated on chamber slides and grown to the desired confluence for bromodeoxyuridine incorporation or p65 NF-κB staining. For BrdU incorporation, cells were either maintained in normal medium or serum-starved for 24 hours. After one hour incubation with BrdU (50 μM) cells were washed, fixed in -20 °C ethanol, permeabilized with 0.5% Tween-20, and stained with undiluted anti-BrdU antibody (a kind gift of Dr. R. Fonseca, Mayo Clinic Arizona) and anti-mouse-Alexa 488 secondary (Invitrogen, Carlsbad, CA). For p65 staining, cells maintained in complete growth medium were fixed and permeabilized in -20 °C methanol, and stained with anti-p65 primary (Santa Cruz) and anti-mouse-Alexa 488 secondary antibodies. Quantitation for both stains was performed by determining the FITC fluorescence intensity in 150 propidium iodide-positive nuclei (50 nuclei in each of three 200X fields).

Invasion assays - Transwell chambers (BD Biosciences, San Jose, CA) were coated with Matrigel (Fisher, Houston, TX). Cells were plated in serum-free medium over the Matrigel and cultured for 24 hours. Medium containing 10% serum was used in the bottom well as an attractant. After incubation, non-invaded cells and Matrigel were removed from half of the wells (samples, containing only invaded cells), and retained in the other half (controls, containing all cells). Membranes were stained with 0.5% crystal violet in 20% methanol, washed and destained in 10% acetic acid. Samples and controls were loaded in quadruplicate into 96-well plates, which were read at 570 nm. Percent invasion was determined as the average sample absorbance over the average control absorbance multiplied by 100.

[^{3}H]thymidine incorporation assays - Cells were plated in quadruplicate at low density (5 or 25 x 10^3 cells) in normal growth medium in 96-well plates. [^{3}H]thymidine was added in fresh medium (1 μCi/well) 24 hours after plating and cells were permitted to grow for another 24 hours. At this time, cells were washed to remove excess radioactivity, trypsinized, and harvested to a filter plate, which was then read on a TopCount plate reader.

Luciferase reporter assays - Cells were transiently transfected with constructs expressing the luciferase reporter gene under the control of consensus binding sites for the appropriate transcription factors. Co-transfection with β-galactosidase was used to control for transfection efficiency. Cells were lysed in reporter lysis buffer (Promega, Madison, WI) 48 hours after transfection, and equal volumes of lysate were added in triplicate to 96-well OptiPlates (Packard, Meriden, CT). Luciferase substrate (Promega, Madison, WI) was added to each well and plates were read on a luminometer. The Gal-Screen kit (Tropix, Foster City, CA) was used to determine β-galactosidase activity, and values were normalized by dividing the average luciferase activity for each sample by its average β-galactosidase activity. For each experiment, relative luciferase values for COS.Neo control cells were set to 1 and values for the other cell lines calculated as fold increase or decrease as compared to COS.Neo.

Statistical analysis - Statistics were analyzed with JMP 5.1.2 software (SAS Institute, Inc., Cary, NC). P-values were generated using the two-tailed student's t test, and significance was confirmed using the Wilcoxon rank sum and Pearson Chi-squared tests.

REFERENCES

1.   Gendler, S. J. MUC1, the renaissance molecule. J Mammary Gland Biol Neoplasia, *6:* 339-353., 2001.
2.   Li, Y., Bharti, A., Chen, D., Gong, J., and Kufe, D. Interaction of glycogen synthase kinase 3beta with the DF3/MUC1 carcinoma-associated antigen and beta-catenin. Mol Cell Biol, *18:* 7216-7224., 1998.
3.   Ren, J., Li, Y., and Kufe, D. Protein Kinase C delta Regulates Function of the DF3/MUC1 Carcinoma Antigen in beta -Catenin Signaling. J Biol Chem, *277:* 17616-17622., 2002.
4.   Li, Y., Kuwahara, H., Ren, J., Wen, G., and Kufe, D. The c-Src tyrosine kinase regulates signaling of the human DF3/MUC1 carcinoma-associated antigen with GSK3 beta and beta-catenin. J Biol Chem, *276:* 6061-6064., 2001.
5.   Al Masri, A. and Gendler, S. J. Muc1 affects c-Src signaling in PyV MT-induced mammary tumorigenesis. Oncogene, *24:* 5799-5808, 2005.
6.   Schroeder, J. A., Thompson, M. C., Gardner, M. M., and Gendler, S. J. Transgenic MUC1 interacts with epidermal growth factor receptor and correlates with mitogen-activated protein kinase activation in the mouse mammary gland. J Biol Chem, *276:* 13057-13064., 2001.
7.   Li, Y., Ren, J., Yu, W., Li, Q., Kuwahara, H., Yin, L., Carraway, K. L., 3rd, and Kufe, D. The epidermal growth factor receptor regulates interaction of the human DF3/MUC1 carcinoma antigen with c-Src and beta-catenin. J Biol Chem, *276:* 35239-35242, 2001.
8.   Spicer, A. P., Duhig, T., Chilton, B. S., and Gendler, S. J. Analysis of mammalian MUC1 genes reveals potential functionally important domains. Mamm Genome, *6:* 885-888., 1995.
9.   Wei, X., Xu, H., and Kufe, D. Human MUC1 oncoprotein regulates p53-responsive gene transcription in the genotoxic stress response. Cancer Cell, *7:* 167-178, 2005.
10.   Wen, Y., Caffrey, T. C., Wheelock, M. J., Johnson, K. R., and Hollingsworth, M. A. Nuclear association of the cytoplasmic tail of MUC1 and beta-catenin. J Biol Chem, *278:* 38029-38039, 2003.
11.   Huang, L., Ren, J., Chen, D., Li, Y., Kharbanda, S., and Kufe, D. MUC1 Cytoplasmic Domain Coactivates Wnt Target Gene Transcription and Confers Transformation. Cancer Biol Ther, *2:* 702-706, 2003.
12.   Wang, H., Lillehoj, E. P., and Kim, K. C. MUC1 tyrosine phosphorylation activates the extracellular signal-regulated kinase. Biochem Biophys Res Commun, *321:* 448-454, 2004.
13.   Lillehoj, E. P., Kim, H., Chun, E. Y., and Kim, K. C. Pseudomonas aeruginosa stimulates phosphorylation of the airway epithelial membrane glycoprotein Muc1 and activates MAP kinase. Am J Physiol Lung Cell Mol Physiol, *287:* L809-815, 2004.
14.   Viala, E. and Pouyssegur, J. Regulation of tumor cell motility by ERK mitogen-activated protein kinases. Ann N Y Acad Sci, *1030:* 208-218, 2004.
15.   Hodge, D. R., Hurt, E. M., and Farrar, W. L. The role of IL-6 and STAT3 in inflammation and cancer. Eur J Cancer, *41:* 2502-2512, 2005.
16.   McCubrey, J. A., May, W. S., Duronio, V., and Mufson, A. Serine/threonine phosphorylation in cytokine signal transduction. Leukemia, *14:* 9-21, 2000.
17.   Kundu, J. K. and Surh, Y. J. Molecular basis of chemoprevention by resveratrol: NF-kappaB and AP-1 as potential targets. Mutat Res, *555:* 65-80, 2004.

18.	DeSouza, M. M., Surveyor, G. A., Price, R. E., Julian, J., Kardon, R., Zhou, X., Gendler, S., Hilkens, J., and Carson, D. D. MUC1/episialin: a critical barrier in the female reproductive tract. J Reprod Immunol, *45:* 127-158, 1999.
19.	O'Connor, J. C., Julian, J., Lim, S. D., and Carson, D. D. MUC1 expression in human prostate cancer cell lines and primary tumors. Prostate Cancer Prostatic Dis, *8:* 36-44, 2005.
20.	Yin, L., Huang, L., and Kufe, D. MUC1 oncoprotein activates the FOXO3a transcription factor in a survival response to oxidative stress. J Biol Chem, *279:* 45721-45727, 2004.
21.	Pande, V. and Ramos, M. J. NF-kappaB in human disease: current inhibitors and prospects for de novo structure based design of inhibitors. Curr Med Chem, *12:* 357-374, 2005.
22.	Meerzaman, D., Shapiro, P. S., and Kim, K. C. Involvement of the MAP kinase ERK2 in MUC1 mucin signaling. Am J Physiol Lung Cell Mol Physiol, *281:* L86-91., 2001.
23.	Schroeder, J. A., Adriance, M. C., Thompson, M. C., Camenisch, T. D., and Gendler, S. J. MUC1 alters beta-catenin-dependent tumor formation and promotes cellular invasion. Oncogene, *22:* 1324-1332., 2003.
24.	Wang, H., Lillehoj, E. P., and Kim, K. C. Identification of four sites of stimulated tyrosine phosphorylation in the MUC1 cytoplasmic tail. Biochem Biophys Res Commun, *310:* 341-346, 2003.

FIGURE LEGENDS

Fig. 1. MUC1 WT and MUC1 Y0 can be expressed in COS-7 cells. *A*, the sequence of the MUC1 WT cytoplasmic tail and the MUC1 Y0 mutant, which has the seven tyrosine residues changed to phenylalanine (*highlighted*). *B*, COS-7 cells stably expressing Neo control, MUC1 WT, or MUC1 Y0 constructs. Whole-cell lysate was blotted for expression of the MUC1 cytoplasmic tail using the CT2 monoclonal antibody. *C*, cell-surface expression of MUC1 was confirmed by FACS. Non-permeabilized cells were stained with HMPV-FITC antibody, which is directed against the MUC1 extracellular domain: COS.Neo, COS MUC1 WT (*unshaded*), COS MUC1 Y0 (*shaded*). *D*, analysis of tyrosine phosphorylation in immunoprecipitations with a MUC1 antibody (*CT2*) or hamster pre-immune serum. Immunoprecipitations were blotted for phosphotyrosine (*top panel*) or MUC1-CT (*bottom panel*). Results shown are representative of three independent experiments.

Fig. 2. ERK1/2 phosphohrylation and activity of AP-1 and Stat-3 are increased in COS.MUC1 Y0. *A*, whole cell lysates were blotted for dpERK1/2 and total ERK1/2 (*arrows*). *B*, AP-1 transcriptional activity was measured in COS.Neo, COS.MUC1 WT and COS.MUC1 Y0 cells by transfection of a luciferase reporter driven by AP-1 consensus sites. Relative luciferase units for COS.Neo were set to 1; data for the other lines are shown as fold change relative to COS.Neo. *C*, transcriptional activity of Stat-3 was measured as described in *B*. *p < 0.001 compared to COS.Neo.

Fig. 3. NF-κB activity and nuclear localization are decreased in COS.MUC1 Y0. *A*, transcription of a luciferase reporter driven by NF-κB consensus sites was assessed in COS.Neo, COS.MUC1 WT and COS.MUC1 Y0 cells. Relative luciferase units for COS.Neo were set to 1; data for the other lines are shown as fold change relative to COS.Neo. *B*, immunocytochemical staining of the p65 subunit of NF-κB. Areas of co-localization of propidium iodide (*PI*) and anti-p65-FITC were colored white for clarity (*Overlay*). *C*, quantitation of nuclear p65, shown as box plots. Staining was quantitated using the FITC fluorescence intensity of 150 propidium iodide-positive nuclei. The central line for each cell type denotes the mean relative fluorescence units (*RFU*) from 150 nuclei; the upper and lower boundaries of the box reflect the range of data from the 25th to 75th percentile RFU scores. *p < 0.001 compared to COS.Neo.

Fig. 4. COS.MUC1 Y0 cells display increased invasive potential. Serum-starved cells were plated in transwell chambers coated with Matrigel, with serum-containing medium in the lower chamber as an attractant. Invasion was determined as the percentage of cells that successfully entered the Matrigel; data represent averages from three independent experiments. *p < 0.001 compared to COS.Neo.

Fig. 5. [³H]thymidine incorporation and cell cycle profile are altered in COS.MUC1 Y0. *A*, cells plated at two different densities (5,000 or 25,000 cells per well) were incubated with [³H]thymidine and harvested 24 hours later. Uptake of radiolabel is shown in cpm. *B*, COS.Neo, COS.MUC1 WT and COS.MUC1 Y0 cells were plated in triplicate and counted at 24-hour intervals for seven days. *C*, cells were stained with propidium iodide and analyzed by FACS for cell cycle distribution. Results are shown as the percentage of cells in G0/G1, S, or G2/M phases. *p < 0.01 compared to COS.Neo.

Fig. 6. COS.MUC1 Y0 show increased BrdU incorporation. *A*, immunocytochemical staining of BrdU incorporation. Serum-starved cells were treated with BrdU one hour prior to fixation. Areas of co-localization of propidium iodide (*red*) and anti-BrdU (*green*) are shown in yellow. Confocal settings were determined using the COS.Neo line and maintained for all three cell lines to ensure comparability. *B*, quantitation of BrdU incorporation, shown as box plots. Staining was quantitated using the FITC fluorescence intensity of 150 propidium iodide-positive nuclei. The central line for each cell type denotes the mean relative fluorescence units (*RFU*) from 150 nuclei; the upper and lower boundaries of the box reflect the range of data from the 25th to 75th percentile RFU scores. *p < 0.001 compared to COS.Neo.
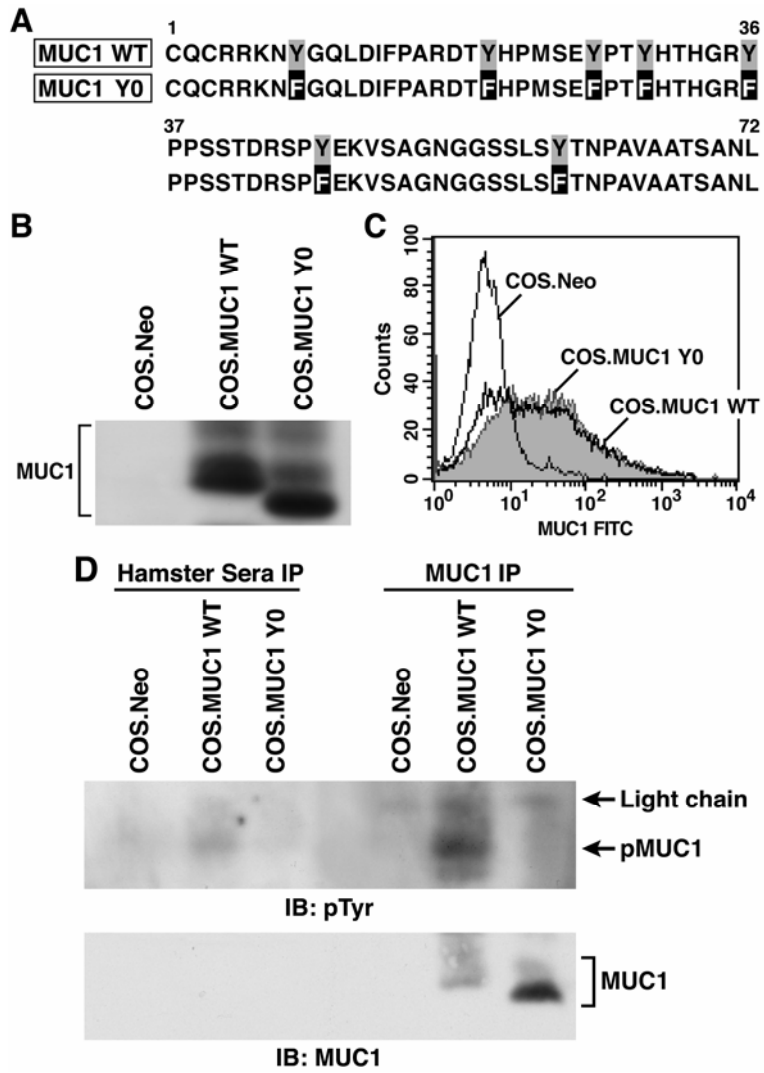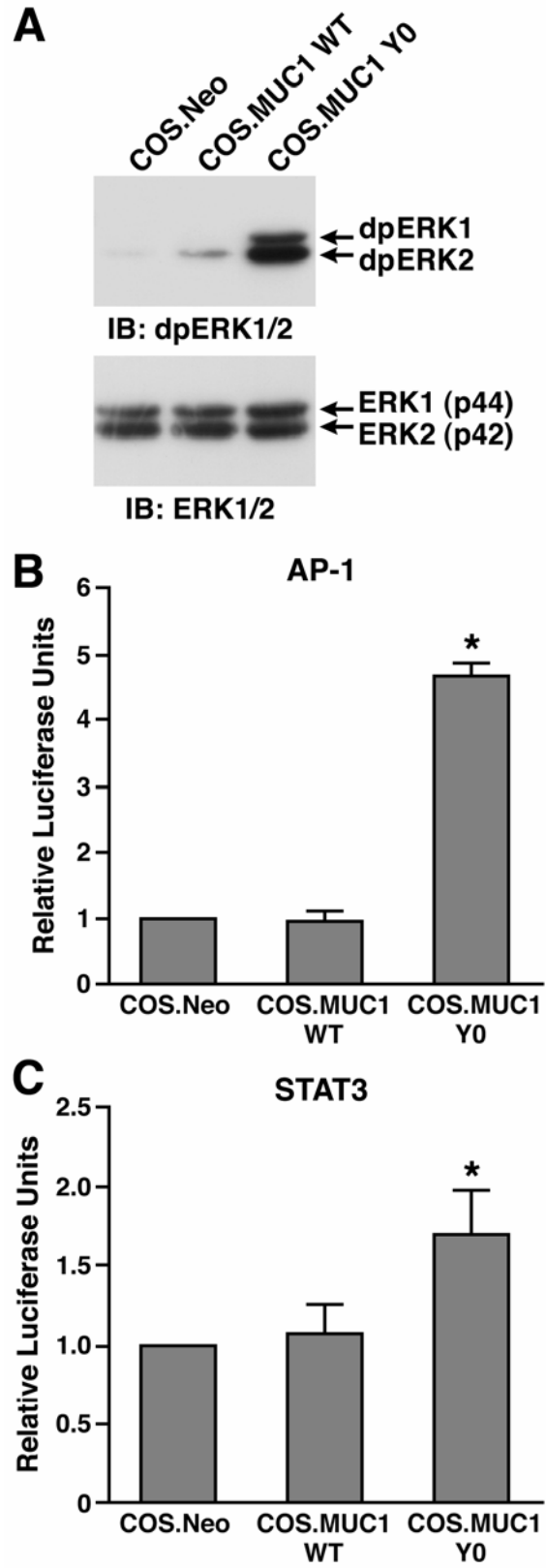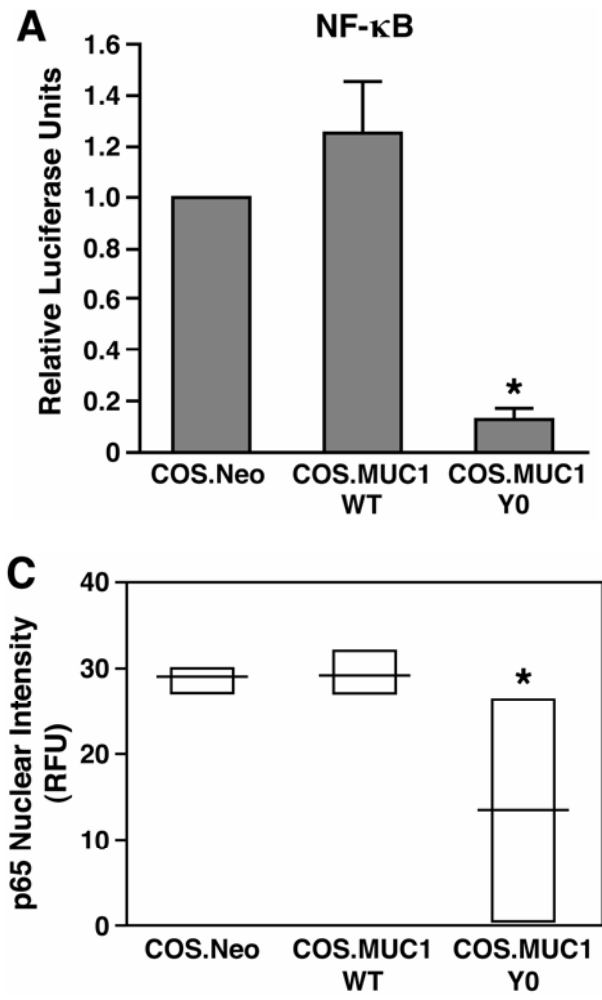
FIGURE 1

A

MUC1 WT	1		36

MUC1 WT   CQCRRKNYGQLDIFPARDTYHPMSEYPTYHTHGRY
MUC1 Y0   CQCRRKNFGQLDIFPARDTFHPMSEFPTFHTHGRF

37   72
PPSSTDRSPYEKVSAGNGGSSLSYTNPAVAATSANL
PPSSTDRSPFEKVSAGNGGSSLSFTNPAVAATSANL

B

MUC1

COS.Neo
COS.MUC1 WT
COS.MUC1 Y0

C

Counts
100
80
60
40
20
0
10⁰ 10¹ 10² 10³ 10⁴
MUC1 FITC

COS.Neo
COS.MUC1 Y0
COS.MUC1 WT

D

Hamster Sera IP   MUC1 IP

COS.Neo
COS.MUC1 WT
COS.MUC1 Y0
COS.Neo
COS.MUC1 WT
COS.MUC1 Y0

← Light chain
← pMUC1

IB: pTyr
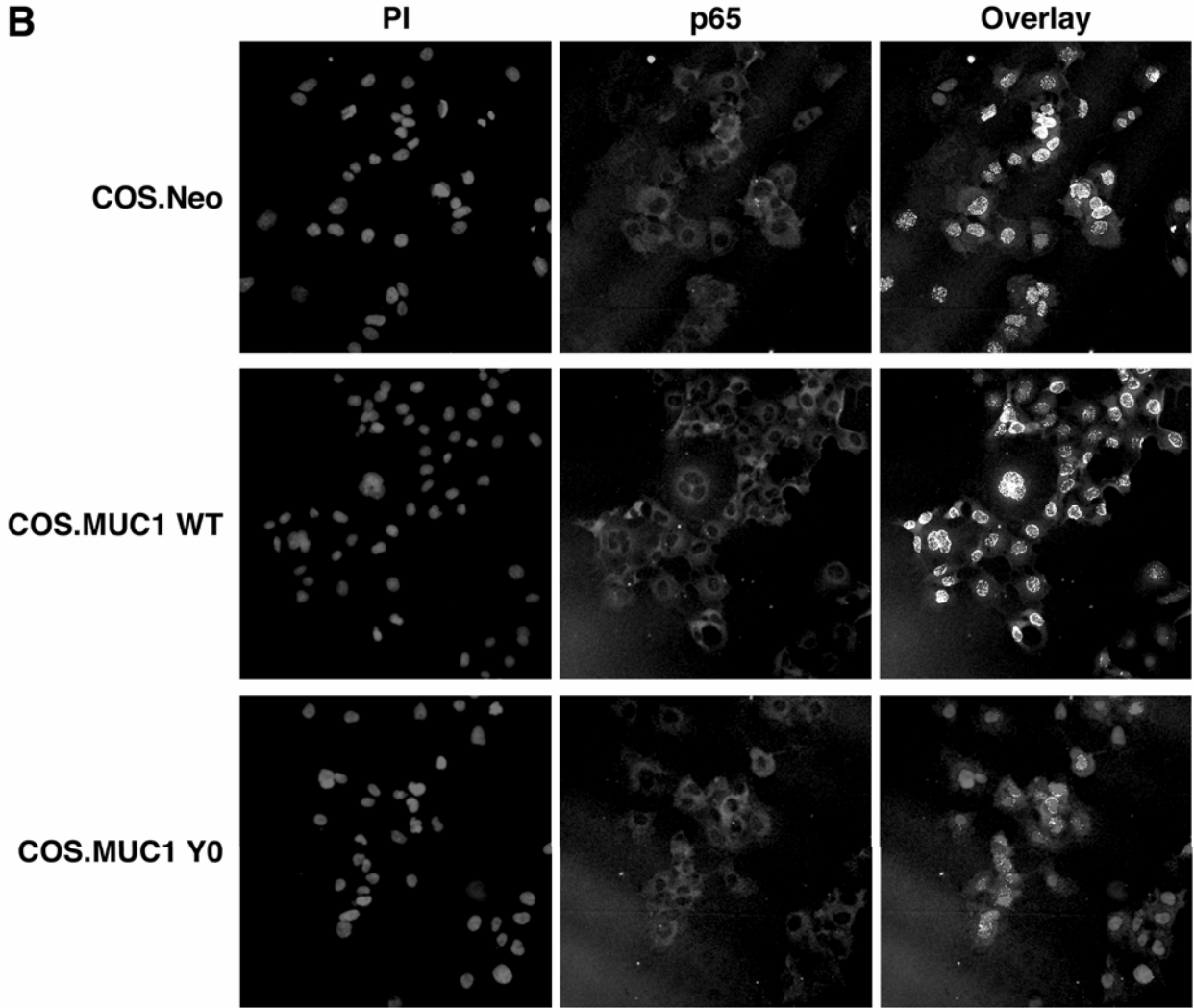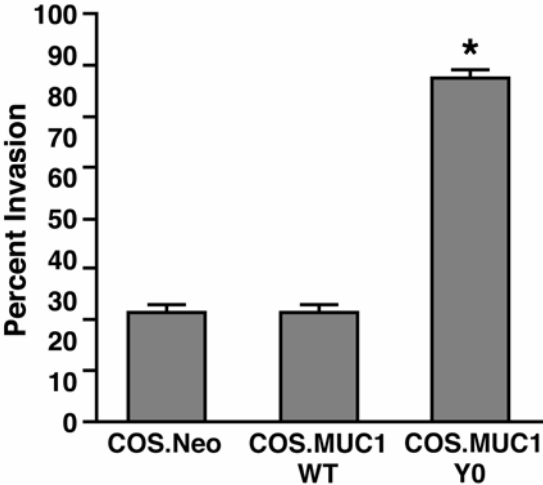
MUC1

IB: MUC1

FIGURE 2

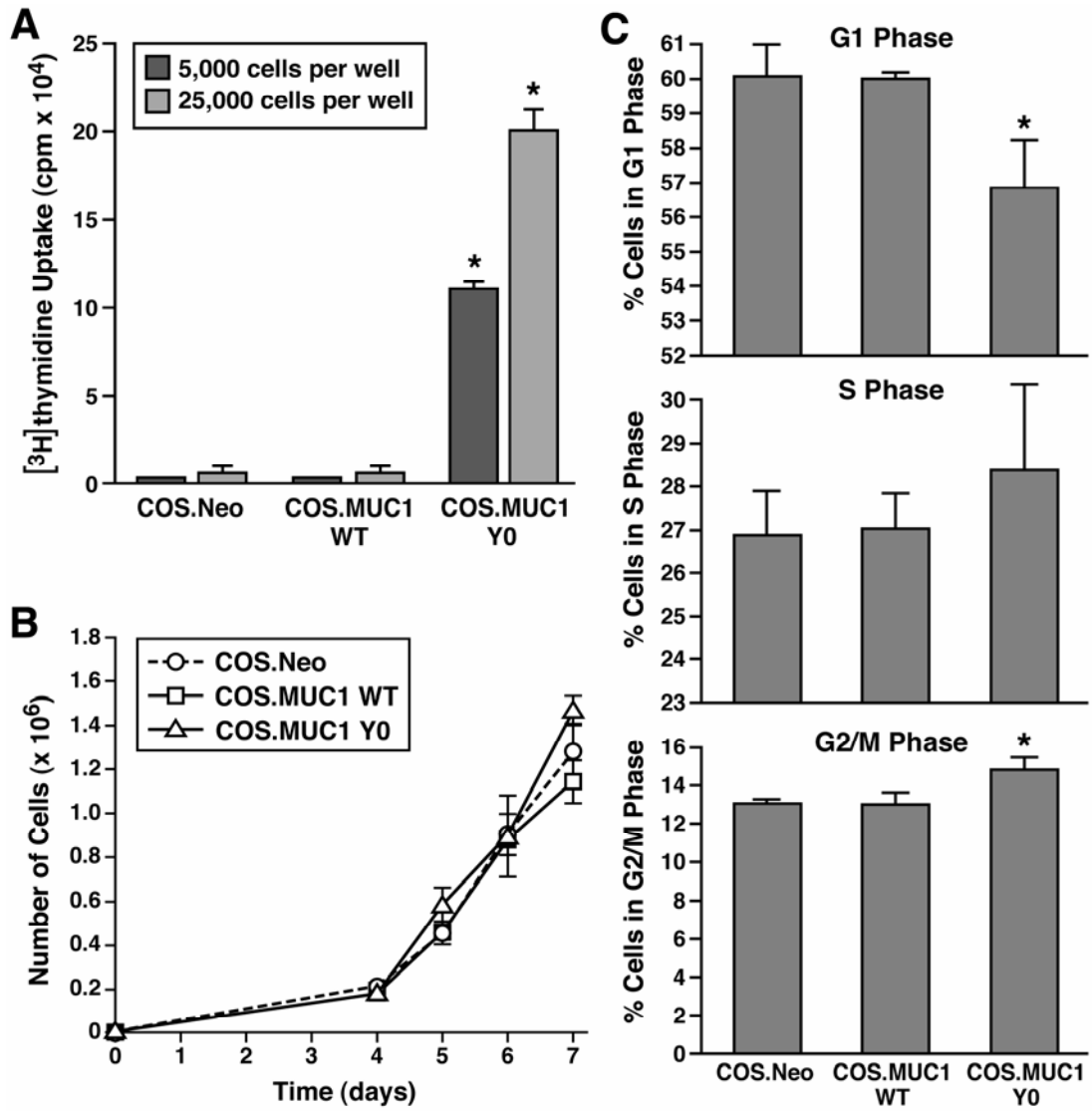FIGURE 3A AND C
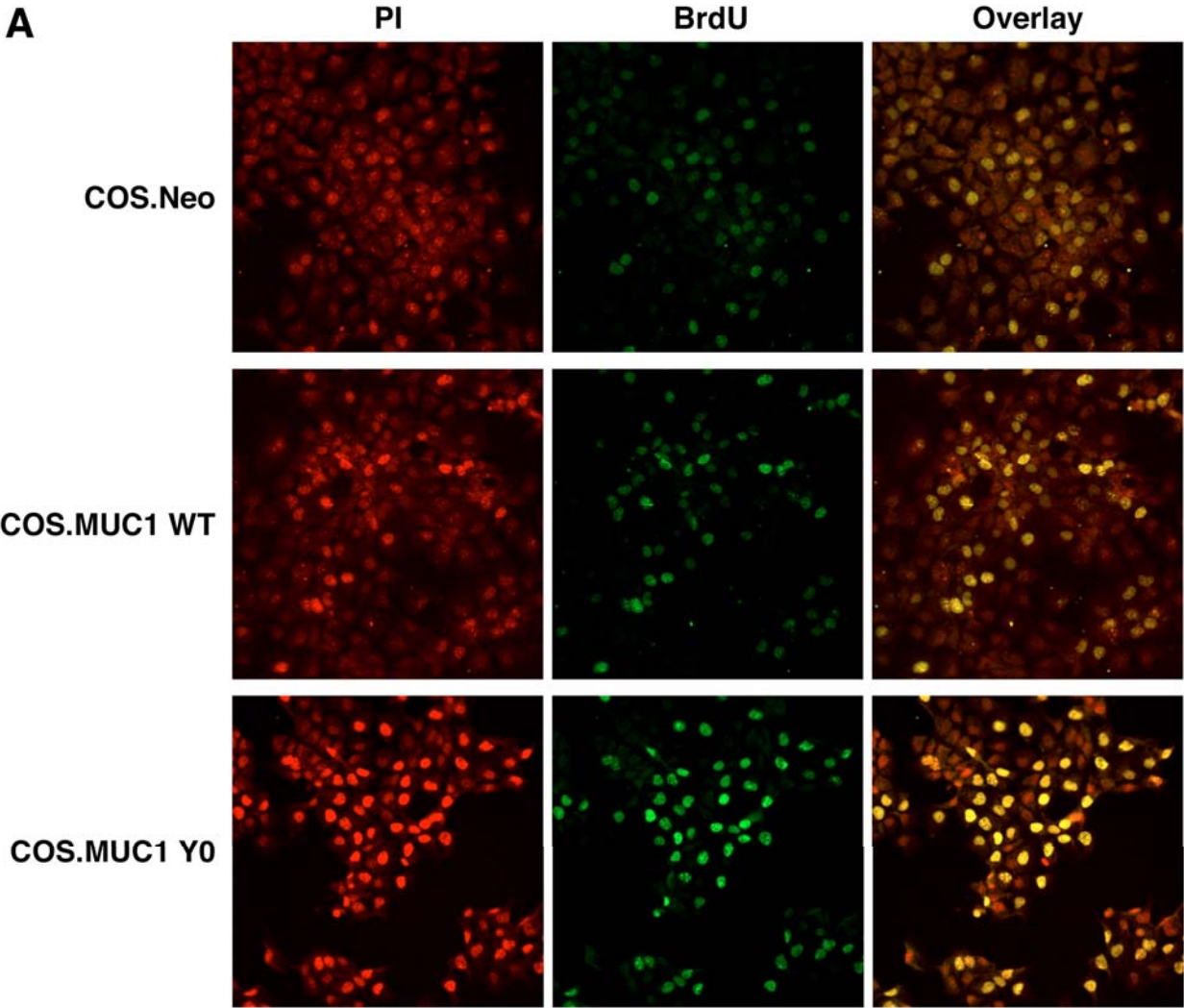
FIGURE 3B, color
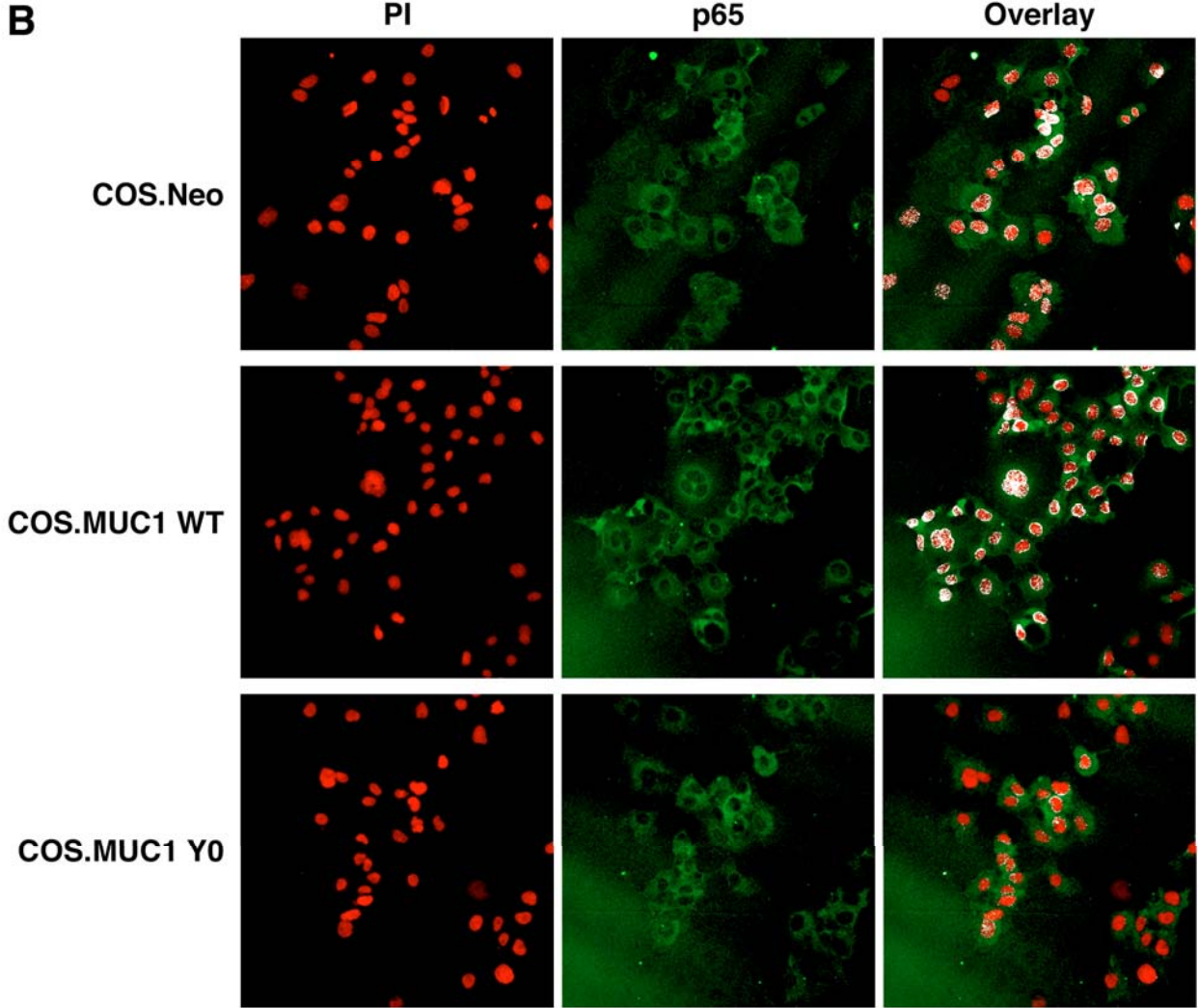
FIGURE 3B, black and white

FIGURE 4

FIGURE 5

FIGURE 6A

FIGURE 6B